Faculteit Wetenschappen
Vakgroep Wiskundige Natuurkunde en Sterrenkunde

Academiejaar 2002-2003

Low frequency waves and instabilities in self-gravitating dusty plasmas

Laagfrequente golven en instabiliteiten in zelfgraviterende stofplasma's

Gerald Jacobs

Promotor : Prof. dr. Frank Verheest
Co-Promotor: dr. Victoria V. Yaroshenko

Proefschrift ingediend tot het behalen van de graad van doctor in de wetenschappen: natuurkunde.

Dankwoord

In de eerste plaats stel ik er prijs op mijn promotor Prof. dr. Frank Verheest oprecht te bedanken voor zijn steun en toewijding. Hij heeft mij uitstekend en vakkundig begeleid vanaf het prille begin van mijn doctoraat tot en met de laatste details van deze thesis. Zijn ervaring en inzicht zijn onmiskenbaar van onschatbare waarde geweest bij de uitvoering van dit onderzoek. Zijn niet aflatend enthousiasme heeft mij sterk beïnvloed en was mijn belangrijkste stimulans.

Daarnaast wil ik ook mijn co-promotor dr. Victoria Yaroshenko bedanken voor haar bijdrage tot dit onderzoek. Tijdens haar verblijf aan de Universiteit Gent hadden wij de gelegenheid om met haar talrijke vruchtbare en leerrijke discussies te voeren. Dit betekende voor mij een bijkomende motivatie en een extra impuls op wetenschappelijk vlak.

Verder dank ik graag dr. Vladimir Čadež, die te gast was aan de Universiteit Gent tijdens het eerste jaar van dit doctoraat, voor de geduldige uitleg en de interessante discussies.

Prof. Frank Verheest heeft steeds het belang benadrukt van deelname aan het internationale forum van fysici, gespecialiseerd op het vlak van stofplasma's. Dank zij hem heb ik dan ook in ruime mate kunnen deelnemen aan internationale conferenties, die niet alleen een overzicht gaven van de recente ontwikkelingen op het vlak van het wetenschappelijk onderzoek, maar tevens de gelegenheid boden tot leerrijke contacten in internationaal verband.

Dat de plasmafysica geen grenzen kent kwam ook tot uiting in de intense samenwerking met de universiteiten van Natal en Durban-Westville uit Zuid-Afrika. Een deel van mijn onderzoek heb ik verricht in Durban, waar ik steeds kon rekenen op een grote gastvrijheid. Ik dank hierbij vooral dr. Sadhasivan Pillay voor zijn oprechte zorg en zijn warme vriendschap. Ook Prof. dr. Manfred Hellberg zorgde ervoor dat ik me perfect thuisvoelde in Durban, zijn enthousiasme en expertise werden erg gewaardeerd. Verder hebben dr. Richard Mace, Prof. dr. Ramesh Bharuthram, dr. Juggy Govender, Logis Pillai, Shimul Maharaj en vooral de hele familie Pillay ervoor gezorgd dat Zuid-Afrika haast een tweede thuis geworden is, waar men wetenschap kan bedrijven in een fascinerend natuurlijk decor.

Ik denk ook met veel genoegen terug aan de talrijke wetenschappelijke discussies met dr. Sadha Pillay en de betreurde dr. Nagesha Rao, die voornamelijk plaatsvonden tijdens het nuttigen van een verrukkelijke, traditioneel Indische curry.

Tot slot, bedank ik ook mijn ouders en mijn broer voor hun niet aflatende steun op alle gebied.

Contents

Samenvatting

Geïoniseerde gassen werden voor het eerst gekarakteriseerd door de naam plasma's door Nobelprijswinnaar (1932) Irving Langmuir in 1927. De term plasma werd een eeuw eerder reeds gebruikt in de geneeskunde en verwijst ook daar naar een typisch dynamisch karakter. Net zoals het bloedplasma rode en witte bloedcellen vervoert, worden energetische elektronen, ionen en onzuiverheden getransporteerd in het elektrisch geleidende gas. Het taalkundig verwante adjectief "plastisch" benadert misschien nog het meest het veranderlijk karakter van plasma's in vorm, volume en ionisatiegraad. De verzamelnaam plastic heeft trouwens dezelfde origine als plasma, de polymeren in kwestie kunnen tijdens de productiefase namelijk in haast eender welke vorm gegoten worden.

In de natuur- en scheikunde staat een plasma effectief voor een vierde aggregatietoestand, naast de traditionele vaste, vloeibare en gas-aggregatietoestanden. Het voornaamste onderscheidende kenmerk tussen de verschillende aggregatietoestanden is de sterkte van de bindingen tussen de samenstellende deeltjes. Het verhitten van een substantie verstoort het bestaande evenwicht tussen de thermische energie en de bindingen van de deeltjes en kan leiden tot een overgang naar een andere aggregatietoestand. Zo zal de voldoende verhitting van een vaste stof leiden tot een vloeibare fase en verdere verhitting op analoge wijze tot een gasfase. Als de temperatuur nog verder wordt opgevoerd zal een moleculair gas geleidelijk dissociëren in atomen en vervolgens zullen deze atomen geïonizeerd worden, de elektronen in de buitenste schil worden uiteindelijk voldoende energetisch zodat zij kunnen ontsnappen. Nochtans zijn er ook verschillen met de traditionele aggregatietoestanden, zo vindt de overgang van bijvoorbeeld de vloeistof- naar de gasfase plaats bij constante temperatuur en druk en vereist deze overgang energie (latente warmte). Dit in tegenstelling tot de vorming van een plasma waar geen warmte wordt geabsorbeerd en de overgang geleidelijk gebeurt met de toename van de temperatuur.

Een plasma is dus een verzameling van energetische ionen en elektronen, die niet langer aan elkaar gebonden zijn. De term plasma wordt in het algemeen slechts toegekend aan geïonizeerde gassen met een voldoende groot aantal geladen deeltjes opdat de deeltjes zich collectief zouden gedragen. Dit betekent in de praktijk dat de dimensies van het plasma deze van de Debyelengte vele malen overtreffen.

De plasmatoestand is in feite de standaard in de kosmos, waar meer dan 99% zich in deze toestand bevindt. Door de aanwezigheid van een atmosfeer op aarde echter vereist de aanwezigheid van een plasma zodanig hoge temperaturen dat ze eerder uitzonderlijk in de natuur voorkomen. De natuurlijke fenomenen op aarde die plasma's creëren zijn

onder andere bosbranden, vulkaanerupties en bliksem. De bliksemschichten bestaan uit een lint van luchtmoleculen, waarvan ongeveer 20% geïonizeerd is. Ook de poollichten zijn niets anders dan grootschalige elektrische ontladingsprocessen, veroorzaakt door de zonnewind, met een typisch wit-groene kleur voornamelijk veroorzaakt door de geëxciteerde zuurstofatomen. Terwijl op het aardoppervlak plasma's nog relatief weinig voorkomen, verandert dit snel als we het aardoppervlak verlaten. Vanaf 80 km hoogte reeds neemt het aandeel van de geladen deeltjes gestaag toe en op een hoogte van 400 km is het grootste gedeelte van de aanwezige materie geïonizeerd. Verlaten we alzo de flinterdunne schil die onze atmosfeer is, dan bereiken we een universum waarin waarlijk de heerschappij van de plasma's heerst, met als meest bekende exponent de zon waarin de warmte gegenereerd via nucleaire fusie enkel de plasmatoestand toelaat.

Naast het gebruik van plasma's in TL-lampen en ook steeds meer in plasmatelevisies zijn plasma's in onze moderne technologie gemeengoed, zo worden ze onder andere intensief gebruikt bij de fabricage van chips door middel van het plasma-etsen. Ook tekende de wisselwerking tussen technologie en natuurkunde vaak voor een sprong in kennis. Zo leidde de transistor en de daaruit voortvloeiende studie van radiogolven tot de beschrijving van de ionosfeer. De ionosfeer vormt een reflecterend schild voor radiogolven van lange golflengte, de meervoudige weerkaatsingen op de ionosfeer verklaren het zeer grote ontvangstbereik van deze golven. Verder is een groot deel van het onderzoek gericht op het realizeren van kernfusie, een concept dat een haast onbeperkte energieproduktie mogelijk zou maken en bovendien enkel relatief ongevaarlijke afvalprodukten zou opleveren. Dit ambitieuze projekt vereist dat men het plasma in de fusiereaktor voldoende kan verhitten en daarenboven moet men het extreem verhitte plasma volledig kunnen opsluiten en afschermen van de reaktorwanden.

Zoals reeds vermeld, gedragen plasmadeeltjes zich collectief in voldoend grote volumes. Dit feit brengt ons haast op natuurlijk wijze tot golfbewegingen in plasma's, daar golven niets anders zijn dan collectieve bewegingen van deeltjes, zoals bijvoorbeeld de geluidsgolven, die lokale ophopingen van deeltjes laten afwisselen met lokale gebieden van lage deeltjesdichtheid. Golven zijn inderdaad in ruime mate aanwezig in plasma's en kunnen een diagnostisch waardevol instrument zijn voor astrofysische objecten en de beschrijving ervan brengt ons tot de grondlegger van de moderne plasmafysica namelijk Hannes Alfvén (Nobelprijs 1970). Alfvén's creativiteit opende een nieuwe wereld, vooral door zijn theorieën over magnetohydrodynamica (MHD), de studie van de beweging van een elektrisch geleidend fluïdum, interagerend met magnetische velden. In MHD-modellen is het fluïdum een sterk geïonizeerd gas, bestaande uit haast gelijke aantallen van negatief en positief geladen deeltjes. Alfvén paste zijn plasmamodellen toe op o.a. geomagnetische stormen, de aurora, de Van Allen stralingsgordels, zonnevlekken en de evolutie van het zonnestelsel. Hoewel zeker niet zonder belang, vormde de plasmafysica voorheen een eerder beperkte tak van de natuurkunde die zich beperkte tot theorieën over gasontladingen. Het is grotendeels Alfvén's verdienste dat de plasmafysica heden ten dage zulk een waaier van toepassingen behelst.

In de productie van wafers van steeds meer geminiaturiseerde chips wordt de aanwezigheid van minuscule stofdeeltjes in de productieruimtes een cruciaal en groeiend probleem. De

aanwezigheid van stof zorgt evenzeer voor praktische problemen in de huidige experimentele fusiereaktoren, die haast onvermijdelijk als een vergaarbak voor ongewenste stofdeeltjes fungeren. Deze technologische problemen onderstrepen het groeiende belang dat men hecht aan de invloed van stofdeeltjes. Dit besef betreffende het belang van stof, is voornamelijk in het begin van de twintigste eeuw gegroeid. Daarvoor werd stof namelijk enkel beschouwd als een ongemak voor telescopische waarnemingen. Het werd toen echter steeds duidelijker dat stof een belangrijke rol speelt in verschillende fysische processen. Een mooi voorbeeld van een fenomeen te wijten aan de aanwezigheid van stof is het zodiakale licht. Het zodiakale licht is een diffuse lichtvlek die in het schemerdonker af en toe kan waargenomen worden in het eclipticavlak of tijdens een zonsverduistering en is het gevolg van de diffractie en reflectie van zonlicht op de stofdeeltjes die zich bevinden in de buurt van de aardbaan.

Onder de noemer stof wordt doorgaans een indrukwekkend scala van deeltjes gecatalogiseerd. De chemische samenstelling van stofdeeltjes kan enorm variëren en is sterk afhankelijk van hun omgeving. Zo zijn stofdeeltjes geassocieerd met meteorieten meestal silicaten, zijnde mineraalstrukturen gebaseerd op SiO_4-viervlakken. Vele stofdeeltjes zijn ijzer- en/of koolstofhoudend, maar ook makromoleculen, "vuile" ijsdeeltjes en met ijs bedekte deeltjes worden tot de familie van de stofdeeltjes gerekend. Niet alleen de samenstelling van de stofdeeltjes is verschillend, zij komen ook in vele maten en vormen voor. De grootte kan daarbij variëren van de orde van grootte van makromoleculen tot zelfs deze van een rotsblok. We kunnen zonder overdrijven stellen dat stofdeeltjes alomtegenwoordig zijn, meer zelfs, het zou quasi-onmogelijk zijn een traject uit te stippelen dat geen stof-bevattende omgeving passeert.

Zowel de plasmatoestand als stofdeeltjes zijn overvloedig aanwezig in het universum en het is dus ook vanzelfsprekend dat stofdeeltjes in een plasma-omgeving voorkomen. Zulke plasma's die een voldoende hoeveelheid stofpartikels bevatten worden doorgaans stofplasma's genoemd. Ook in ons zonnestelsel komen stofplasma's royaal voor, bijvoorbeeld in de heliocentrische stofringen, de ringen rond Jupiter, in de staart en coma van kometen alsook in de zogenaamde lichtende nachtwolken in onze atmosfeer. Exemplarisch voor toepassingen buiten ons zonnestelsel zijn interstellaire stofwolken. Op aarde zijn de lichtende nachtwolken misschien wel het meest voor de hand liggende voorbeeld van een stofplasma. Het zijn ijle wolken met een witte of wit-blauwe kleur die zich op erg grote hoogte bevinden (in de mesopause op 75 tot 90 km hoogte) en bij erg lage temperaturen ($\simeq -80°$C). Deze lichtende nachtwolken kunnen waargenomen worden in het schemerdonker en dit gedurende de zomermaanden op breedtegraden van 45° tot 70°, doordat ze nog verlicht zijn door de zon wanneer deze laatste zich al beneden de horizon van de waarnemer bevindt.

Stofkorrels zijn doorgaans elektrostatisch geladen waarbij de lading verkregen kan worden door middel van verschillende processen. De belangrijkste manier van opladen gebeurt door de zogenaamde primaire absorptie van ladingen. In dit ladingsmodel wordt beschreven hoe een fractie van de elektronen en ionen, die de stofkorrels continu bombarderen, blijft "kleven" aan het stofoppervlak. Bovendien is dit ladingsproces veranderlijk in de tijd, de ladingen van de stofdeeltjes kunnen hoogst variabel zijn. De lading van de stofdeel-

tjes zorgt ervoor dat de stofdeeltjes elektrostatisch met het plasma alsmede met andere stofdeeltjes kunnen interageren. Aldus zullen ook de golfverschijnselen mogelijk beïnvloed worden door de aanwezigheid van het stof. Laten we de ladingsfluctuaties even buiten beschouwing, dan kunnen we stellen dat de invloed van stof op golven zich voornamelijk op twee manieren kan laten gevoelen. Enerzijds zal het aantal beschikbare elektronen en ionen voor golfprocessen niet constant zijn, vermits de stofdeeltjes de elektronen en ionen kunnen adsorberen. Anderzijds kunnen de stofdeeltjes zelf deelnemen aan de golfbeweging met dien verstande dat dit fenomeen zich enkel zal voordoen voor voldoend lage frequenties. Inderdaad, vergeleken met ionen zijn de stofdeeltjes werkelijk massief en kunnen ze enkel voldoend trage frequenties gehoorzamen.

De relatief enorme massa van de aanwezige stofdeeltjes is slechts één van de afwijkende eigenschappen ten opzichte van de traditionele plasma's, die enkel elektronen en ionen bevatten. Het is echter vooral de ongewoon kleine verhouding van lading tot massa van stofdeeltjes die verantwoordelijk zullen blijken voor nieuwe golfverschijnselen, alsook voor de aanpassing van reeds bekende golfmodes. Doordat de verhouding van lading tot massa zodanig drastisch verschilt van deze van de traditionele plasma-ingrediënten zullen de karakteristieke frequenties van het stof aanzienlijk kleiner zijn. Dit levert een bijzonder interessant frequentiedomein op, namelijk datgene dat frequenties behelst die groter zijn dan de karakteristieke frequenties van het stof, maar kleiner dan de karakteristieke ionfrequenties. In deze tak van ultralage frequenties demonstreren de lichte plasmadeeltjes nauwelijks inertie en zijn het de logge stofdeeltjes die een golfbeweging kunnen ontplooien. Ook profileren stofplasma's zich ook door de verscheidenheid in grootte, samenstelling en vorm van de stofdeeltjes. Dit maakt dat haast ieder stofdeeltje anders zal reageren ten opzichte van de grootte en richting van de heersende elektrische en magnetische velden, wat meteen de complexiteit van stofplasma's illustreert.

De aanwezigheid van zware stofdeeltjes heeft ook tot gevolg dat de zelf-gravitationele krachten dikwijls niet verwaarloosd mogen worden in de beschrijving van omvangrijke astrofysische stofplasma's met voldoend hoge stofconcentraties. Reeds voor stofdeeltjes van een orde van grootte van millimeters zullen de elektrostatische en gravitationele krachten elkaar ongeveer balanceren en kunnen deze laatste dus onmogelijk genegeerd worden. De gecombineerde massa van de stofdeeltjes kan zelfs een gravitationele implosie van een astrofysische stofwolk veroorzaken.

Voor de studie van stofplasma's is het noodzakelijk enkele begrippen uit de traditionele electron-ion plasma's uit te breiden of aan te vullen, zoals verduidelijkt in hoofdstuk 2. Bovendien zullen ook elementaire noties uit de sondetheorieën die noodzakelijk zijn voor de ladingsbeschrijving van de stofdeeltjes worden herhaald.

Vervolgens worden in hoofdstuk 3 de basisvergelijkingen voor golven in stofplasma's geformuleerd, dit zowel in het kader van een kinetisch model als in het kader van een fluïdum model. Meteen wordt de algemene dispersiewet voor golven afgeleid en dit in het algemeen voor schuine voortplanting, deze zal natuurlijk vereenvoudigd kunnen worden in de specifieke gevallen van parallelle of loodrechte voortplanting. Ook worden de specifieke moeilijkheden voor de verwezenlijking van een bevredigend kinetisch model geduid. Voor de meeste hoofdstukken zal gebruik worden gemaakt van het meer transparante

en makkelijker hanteerbaar fluïdum model. Toch zal in de hoofdstukken 8 en 9 worden teruggegrepen naar een kinetisch model teneinde de fenomenen die teloor gegaan zijn ten gevolge van de vereenvoudigingen in een fluïdumbeschrijving, te herwinnen.

In hoofdstuk 4 recapituleren we de meest fundamentele, elektrostatische golfmodes in stofplasma's. De initiële beschrijving van deze laagfrequente golfmodes door Rao, Shukla en anderen hebben een ware doorbraak betekend voor het onderzoek in stofplasma's. Heden ten dage is de nomenclatuur, geïntroduceerd door deze pioniers, een standaard geworden met als voornaamste voorbeeld de "stof-akoestische golf" (dust-acoustic wave), die voor het eerst beschreven werd door Rao, Shukla en Yu in 1990. Deze thesis bouwt verder op deze fundamenten, de stof-akoestische golf en de aanpassingen ervan ten gevolge van zelf-gravitatie zullen merkbaar de rode draad door deze thesis vormen.

Hoofdstuk 5 behandelt het delicate onderwerp van de "Jeans swindle". De "Jeans swindle" is een creatieve vereenvoudiging ingevoerd door Sir James Jeans om de criteria voor een zelfgravitationele instabiliteit te bepalen. De vereenvoudiging in kwestie impliceert een krachtige techniek voor de analyse van zelf-graviterende systemen maar is tegelijk ook de zwakke plek in het hele betoog. Deze Achilleshiel werd door Jeans' tegenstanders dan ook weinig flatterende "Jeans swindle" gedoopt waarvan de letterlijke vertaling "Jeans' zwendel" ongeveer dezelfde connotatie oproept. Dit heikele punt noopt de meeste onderzoekers tot het hinken op twee gedachten. Enerzijds kan men consistent weigeren de vereenvoudiging toe te passen met alle wiskundige, dikwijls zelfs onoverbrugbare, complicaties vandien. Anderzijds kan men ervoor kiezen de "Jeans swindle" toe te passen, zoals in de grote meerderheid van toepassingen in de literatuur. Deze werkwijze eist echter een strikte controle *a posteriori* van de gedane veronderstelling, een vereiste waaraan zelden gevolg wordt gegeven met het gevolg dat vele resultaten mogelijk gebreken vertonen. Desalniettemin betekent dit niet dat deze onderzoeken waardeloos of weinig informatief zouden zijn. Integendeel, het zal blijken dat een gedegen traditionele studie van zelf-graviterende systemen waardevolle informatie zal opleveren in verband met typische lengteschalen. Het is dan ook makkelijk te rechtvaardigen dat in de hierop volgende hoofdstukken de "Jeans swindle" zal toegepast worden.

Vervolgens wordt in hoofdstuk 6 de koppeling tussen elektrostatische en zelf-gravitationele effecten bestudeerd. Terzelfdertijd wordt de invloed van de massaverdeling van de stofdeeltjes op elektrostatische golven in zelf-graviterende stofplasma's onder de loupe genomen. Er wordt onderzocht hoe een discrete massaverdeling de Jeanslengte beïnvloedt, waarbij de Jeanslengte de typische lengtedimensie is voor dewelke een gravitationele instabiliteit dreigt. In de analyse van een stofplasma dat meerdere stofcomponenten bevat zal de al dan niet aanwezigheid van neutrale deeltjes van cruciale invloed blijken te zijn op de bekomen Jeanslengte. Voor stofplasma's met exclusief geladen stofdeeltjes zullen de bekomen Jeanslengtes veel groter zijn dan voor gelijkaardige plasma's met enkel neutrale deeltjes, wat betekent dat zulke stofwolken op een veel grotere schaal kunnen stabiel blijven. Evenwel, voor stofplasma's die naast geladen stofdeeltjes zelfs maar een gering aantal neutrale stofdeeltjes bevat wordt die stabiliserende invloed totaal teniet gedaan.

In hoofdstuk 7 wordt dan de invloed van de massaverdeling op elektromagnetische modes getest, eerst voor loodrechte en vervolgens voor schuine voortplanting. Enigszins ver-

rassend zal blijken dat het instabiliteitscriterium voor schuine voortplanting haast identiek is aan dat voor parallelle voortplanting, met uitzondering van quasi-loodrechte voortplanting. Bovendien komen we tot de algemene conclusie dat voor de studie van laagfrequente golven in zelf-graviterende stofplasma's de invloed van een discrete massaverdeling redelijk klein is. Deze gevolgtrekking betekent dat men in verder onderzoek een stofplasma best kan modelleren door middel van één enkele stofsoort met gemiddelde eigenschappen, vermits deze vereenvoudiging de realiteit haast evengoed benadert. Ook voor elektromagnetische golven zal de aanwezigheid van neutrale deeltjes een verwoestende invloed op de stabiliserende eigenschappen van geladen stofdeeltjes tot gevolg hebben.

Zoals reeds eerder vermeld wordt in hoofdstuk 8 teruggegrepen naar een kinetisch model. Dit is het meest algemene model, dat toelaat de invloed van de thermische agitatie van de deeltjes ten volle te bestuderen. Immers, het fluïdummodel is strikt gesproken niet meer geldig voor fasesnelheden kleiner dan de thermische snelheden van de deeltjes. Als we de resultaten uit beide beschrijvingen vergelijken, blijkt dat de bekomen voorwaarde voor stabiliteit erg vergelijkbaar is. Daarentegen zal de aangroeisnelheid van een instabiliteit erg verschillend zijn in beide beschrijvingen. Dit is te wijten aan de "Landau demping", een botsingsloos mechanisme dat de golven verzwakt en enkel kan beschreven worden in het raam van een kinetisch model. Dit mechanisme zorgt ervoor dat de stof-akoestische golf in de realiteit nauwelijks zal kunnen geëxciteerd worden in een bepaald bereik van golflengten, ook al levert een fluïdumbeschrijving geen enkele indicatie hiervan.

Daaropvolgend wordt in hoofdstuk 9 een massaverdeling geïntroduceerd in de kinetische beschrijving van zelfgraviterende stofplasma's. De gebruikte massadistributie is continu en is gemodelleerd volgens een dalende machtwet, wat een goede benadering van de werkelijkheid betekent voor vele astrofysische toepassingen. De mate van koppeling tussen plasma en gravitationele effecten zal sterk afhankelijk zijn van de parameters van de massadistributie. De vooropgestelde parameters zullen uiteindelijk bepalen welke stofdeeltjes de grootste invloed hebben op de zelf-gravitatie, de overvloedig aanwezige maar kleine stofdeeltjes of de minder frequente maar grotere stofdeeltjes.

Tenslotte wordt in hoofdstuk 10 de invloed van onderlinge botsingen in het stofplasma onderzocht. In stofplasma's zijn de meest significante botsingen deze tussen enerzijds de neutrale stofdeeltjes en anderzijds de geladen stofdeeltjes. In plasma's die enkele geladen stofdeeltjes bevatten daarentegen, zullen de meest invloedrijke botsingen deze tussen de ionen en de geladen stofdeeltjes zijn. Het is dit laatste geval dat nader onderzocht zal worden. In dit hoofdstuk wordt gebruik gemaakt van een semi-analytische methode, namelijk de poolbaanmethode, die toelaat de invloeden van de ion-stof botsingen te onderzoeken op de gravitationele stabiliteit met een minimum aan rekenwerk en bovendien grafisch de invloed van de botsingsfrequentie op de laagfrequente golfmodes weergeeft op een kwalitatieve manier.

Deze thesis steunt voornamelijk op de volgende publicaties:

Publications in refereed journals

F. Verheest, G. Jacobs and M.A. Hellberg, Transition from Langmuir-Jeans modes to Alfvén-Jeans modes in dusty plasmas, *Phys. Scripta* **84**, 171-174 (1999).

F. Verheest, G. Jacobs and V. V. Yaroshenko, Gravitational collapse in dusty plasmas with mass distributions and neutral gas, *Phys. Plasmas* **7**, 3004-3008 (2000).

G. Jacobs, F. Verheest, M.A. Hellberg and S.R. Pillay, Magnetosonic modes with dust mass distributions, *Phys. Plasmas* **7**, 4390-4395 (2000).

V.V. Yaroshenko, G. Jacobs and F. Verheest, Kinetic approach to low-frequency waves in dusty self-gravitating plasmas, *Phys. Rev. E* **63**, 066406 (2001).

V.V. Yaroshenko, G. Jacobs and F. Verheest, Dust-acoustic modes in self-gravitating plasmas with dust-size distributions, *Phys. Rev. E* **64**, 036401 (2001).

F. Verheest, V.V. Yaroshenko, G. Jacobs and P. Meuris, Charge and mass fluctuations in dusty plasmas revisited, *Phys. Scripta* **64**, 494-500 (2001).

G. Jacobs and S.R. Pillay, Effect of dust charge inhomogeneities on electrostatic waves over arbitrary fugacity range, *Phys. Scripta*, **66**, 159-164 (2002).

G. Jacobs, V.V.Yaroshenko and F. Verheest, Low-frequency electrostatic waves in self-gravitating dusty plasmas with dust-ion collisions, *Phys. Rev. E*, **66**, 026407 (2002).

Publications in conference proceedings

G. Jacobs, F. Verheest, M.A. Hellberg, S.R. Pillay and V.V. Yaroshenko, Jeans modes in dusty plasmas with dust mass distributions, *AIP Conference Proceedings* **537**, $53-60$ (2000).

F. Verheest, V.M. Čadež and G. Jacobs, Janus faces of Jeans instabilities, *AIP Conference Proceedings* **537**, $91-98$ (2000).

G. Jacobs, V.V. Yaroshenko and F. Verheest, Influence of dust-ion collisions on waves in self-gravitating dusty plasmas, Conference proceedings *ICPDP* 2002, Durban, South Africa (2002), *accepted*.

Chapter 1

Introduction

Ionized gases were referred to as plasmas for the first time by Nobel Laureate (1932) Irving Langmuir in 1927, inspired by the observation that certain phenomena displayed by the heated gases in gas discharge tubes display a similar dynamic behaviour as that of plasma in blood. Indeed, the energetic electrons, ions and impurities are transported in the electrically conducting, ionized gases just like the red and white blood cells are carried through the bloodstream. *Au fait*, the generic term plastic is of the same origin as the term plasma and also expresses a variable nature. During the production steps, plastics can be moulded into virtually any shape, size and color.

Plasmas actually represent the fourth state of matter, thus complementing the solid, liquid and gaseous state. The addition of sufficient thermal energy to a solid matter disturbs the existing equilibrium between the thermal mobility of the particles and the strength of the inter-particle bonds and causes a phase transition towards a liquid state. If the liquid is heated even more, it will go over to the gaseous state and finally for even higher temperatures the plasma state is reached, as the electrons in the outer layer of the atoms become sufficiently energetic to escape. However, the transition towards a plasma state is not completely analogous with respect to the other phase transitions. For instance, the transition from liquid to gas occurs at a constant temperature and pressure and requires energy in the form of latent heat, whereas the formation of a plasma does not absorb energy and occurs gradually for increasing temperatures.

Generally the term plasmas is preserved for those ionized gases that are composed of sufficiently large numbers of electrically charged particles in order that these particles can display a collective behaviour. In effect, this means that the dimensions of a plasma exceed the Debye length considerably.

Here on Earth, the plasma state is quite unusual and exotic and only occurs in extreme conditions, like in lightning bolts, fires, volcano eruptions and auroras. But what we see on Earth is the exception, plasma is the most common state of matter in the universe, in fact more than 99 % of all observable matter is plasma. As soon as we move away from the Earth, plasmas immediately become very common. In the upper atmosphere, the radiation of the Sun, being nothing more than a huge ball of glowing hot hydrogen plasma itself, is able to dislodge electrons from neutral gas atoms or molecules. This ionization process is

responsible for the plasma state of the upper layers of the atmosphere, aptly named the ionosphere. In fact, when we look at the night sky with a telescope, just about everything we see is a plasma. Also in everyday life plasmas and their applications are more and more present. Nowadays fluorescent light bulbs and plasma televisions are the most encountered plasmas, whereas the most common application of plasmas is probably plasma etching in the manufacturing processes of optical and electronic components. Furthermore, plasma physics is the key for realizing nuclear fusion, an ambitious project that would provide mankind with a virtually endless source of energy and this without producing dangerous or difficultly disposable waste products. The main focus in this branch of plasma physics aims at being able to heat the plasma sufficiently and to shield the extremely hot plasma from the reactor walls.

As mentioned before, the particles in plasmas can display a collective behaviour, because each particle affects many other particles in the plasma. This interdependence automatically leads to the concept of wave motion in plasmas, as waves are nothing else than collective motions of particles. The foundations of wave theory in plasmas were laid in 1942 by Nobel laureate Hannes Alfvén and his insights extended plasma theory from a highly specialized branch of physics, mainly limited to the study of gas discharges, to an interdisciplinary theory with innumerable applications. Especially in astrophysics, the knowledge of plasma theory is invaluable as the plasma state is predominating in the universe. The epoch-making research of Alfvén resulted in the development of the so called magnetohydrodynamic model, which describes the motion of an electrically conducting fluid interacting with magnetic fields. Alfvén applied the magnetohydrodynamic model to *e.g.* the study of geomagnetic storms, the aurora, the Van Allen radiation belts, solar spots and the evolution of our solar system.

In the beginning of the 20th century it also became clear that dust is omnipresent in the universe and ever since the notion of its importance has been growing. At first, there hardly was intrinsic interest for the dust itself, dust just seemed a passive agent that regrettably obscured the skies and hindered proper photometric observations. But times have changed, nowadays dust represents a vital ingredient for many models and in general a major influence on several fields in modern astronomy. A beautiful example of a phenomenon due to the presence of dust is the zodiacal light. The zodiacal light is a diffuse band of light that can be observed occasionally in the ecliptic during twilight and is caused by the diffraction and reflection of sunlight on dust particles within and outside the orbit of the Earth. The study of dust and its properties also becomes more and more important in laboratory plasmas, plasma reactors and electronics. In the latter domains, dust is usually very undesirable and in particular is it posing increasing problems in the production of electronic components, as miniaturization keeps advancing.

The ubiquitousness of the dust particles brings about that many space plasmas contain substantial amounts of dust grains. However, there was no crossover in the respective models of plasmas and dust conglomerations until the 1980's. Since then, mixtures of traditional plasma components and dust grains are aptly referred to as dusty plasmas. The presence of dust grains in plasmas allows for new and exciting phenomena that set dusty plasmas apart from traditional plasmas, the description of which requires the use

of a proper dusty plasma model. For instance, a dusty plasma model is called upon in order to explain the occurrence of spokes and braids in the rings of Jupiter. On Earth, noctilucent clouds are probably the most obvious example of dusty plasmas. Noctilucent clouds are tenuous clouds on very high altitudes (in the mesopause at altitudes of 75 to 90 km) and with very low temperatures ($\simeq -80°$C). During twilight, they appear as white or blue-white clouds on latitudes of 45° to 70°, because they are still illuminated by the Sun, when the latter is already below the horizon of the observer. Other examples of dusty plasmas in our solar system are the circumsolar dust rings and cometary comae and tails, whereas interstellar dust clouds usually serve as the prototype for dusty plasma models applied outside our solar system.

In this thesis, the focus is primarily on waves and instabilities in dusty space plasmas. The study of waves is very important for various reasons, the most obvious being that waves can be observed relatively easy and thus reveal information about the events within the plasma. It will become clear that the study of dusty plasmas extends the existing zoo of waves as studied in plasmas with only traditional constituents. Instabilities are concomitant with the study of waves since waves can grow as they propagate, eventuating in amplitudes so large that they can disrupt the plasma.

The influence of the dust particles can be distinguished in a twofold manner. On the one hand, dust grains are highly charged and extremely massive, when compared to ions and electrons, and so introduce new time and lengthscales. This is translated into a wealth of new wave modes, with very low frequencies in comparison with wave phenomena in electron-ion plasmas. On the other hand, the peculiarities of dust grains also cause important additions to the existing range of waves. Whereas the electrons and ions are monomorphic and have fixed charges, the dust grains display a rich diversity in shape and size and can have fluctuating charges. The variable charge of a dust grain is influenced through different charging mechanisms like primary charging (electron/ion capture by the dust grains) and photoemission (if there is a radiation source), where both mechanisms are obviously dependent on parameters of the surrounding environment. The fluctuations in the charges of dust grains influence the local electric fields. Hence, the fluctuating charges couple with the wave mechanism and increase the complexity of the wave description tremendously.

Due to the presence of heavy dust particles, self-gravitational interactions cannot be neglected in any model that aims at an accurate description of large, astrophysical dusty plasmas like giant dust clouds. In such self-gravitational dusty plasmas there is a competition between electrostatic and self-gravitational forces and the model for such a plasma can be seen as a bridge between plasma and celestial mechanics.

The combined mass of all the dust particles can even cause a gravitational collapse of a large dust cloud and the introduction of self-gravitational interactions allows the study of gravitational stability in dusty plasmas. In this way, the pioneering theories of Sir James Jeans about gravitational stability can be extended from neutral clouds to clouds of charged dust particles.

Outline

In the introductory chapter 2, the nomenclature of traditional plasma physics is generalized to the use in dusty plasma physics. Moreover, the most common charging mechanisms for dust grains are recalled.

In chapter 3, the basic equations for waves in dusty plasmas are formulated, both in a fluid and in a kinetic description. Consequently the general dispersion law for waves is derived and interpreted in the specific cases of parallel and perpendicular propagation. Furthermore, the specific difficulties for realizing a satisfying kinetic model are summarized. In the following chapters, the fluid model will be applied, for the sake of simplicity. However, in the chapters 8 and 9, the kinetic description is called upon in order to retrieve the information that is lost due to the simplifications in a hydrodynamic model.

Subsequently, the most relevant electrostatic low-frequency modes in dusty plasmas are summarized. The initial description of these basic modes was the impetus for the majority of the present investigations, especially in the case of the dust-acoustic mode, first described by Rao, Shukla and Yu in 1990. This dust-acoustic wave and the modifications due to self-gravitation will clearly run through this thesis like a continuous thread.

In chapter 5, the delicate topic of the "Jeans swindle" is introduced and discussed in a one dimensional model. The Jeans swindle is a simplification procedure, introduced by Sir James Jeans, for determining the criterion for gravitational stability more easily. This procedure represents a powerful tool since the stability analysis becomes much simpler, but on the other hand the Jeans swindle disregards a part of the problem. This double-edged nature of the Jeans swindle provides two distinct possibilities for approaching the stability analysis of self-gravitating systems. One can choose to reject the Jeans swindle, which poses serious, possibly unbridgeable mathematical problems. Conversely, one can invoke the Jeans swindle, being by and large the preferred approach in the relevant literature. The latter operating procedure requires however that the conditions for applying justifiably the Jeans swindle are checked *a posteriori*, which is often neglected and as a consequence, some of the results are possibly flawed. Nevertheless, applying the Jeans swindle yields valuable information, because it provides information about important lengthscales. In the remainder of the thesis, the mainstream of investigations is followed and the Jeans swindle is consistently applied.

The influence of self-gravitational effects is obviously intertwined with the mass distribution of the dust grains and this interdependence is studied in chapter 6. In this chapter, the influence of discrete mass distributions on the coupling between electrostatic and gravitational disturbances is investigated. The study of continuous distributions is relegated to chapter 9, for this requires a kinetic framework.

Next, in chapter 7 the modifications due to a mass distribution are studied in dusty plasmas which are pervaded by a magnetic field. First, the gravitational stability is studied in directions perpendicular to the magnetic field. Later on, the stability analysis is extended to all directions.

In chapter 8, a kinetic framework is called upon. In a kinetic description, the implications of the thermal motion of the particles can be fully investigated. Indeed, strictly speaking,

a fluid model is not valid anymore for phase velocities smaller than the thermal velocities of the particles. This approach allows for investigating the Landau damping, which is a collisionless damping mechanism, in self-gravitating dusty plasmas. Later on, in chapter 9, the Landau damping is investigated in a dusty plasma model that comprises a continuous mass distribution.

Finally, in chapter 10, the influence of collisions in self-gravitating plasmas is analyzed. In dusty plasmas, the most significant collisions occur between neutral and charged dust particles. However, in dusty plasmas with exclusively charged dust, the dominating collisional mechanism describes the dust-ion collisions. The latter case is investigated closely to show the influence of the dust-ion collision frequency on the low frequency wave modes.

Chapter 2

Synergy between plasmas and dust

Here on Earth the plasma state is quite unusual and exotic. In effect, the Earth's atmosphere is inhospitable for low temperature plasmas, so that in nature plasmas only occur in extreme or artificial conditions like for extremely high temperatures or man-made vacuums. Even so, one does not need to go far from the surface of the Earth to encounter already the dominion of the plasma state, from altitudes above circa 80 km the fraction of charged particles is steadily increasing and the neutral component is already negligible above an altitude of 400 km. Outside the safe shell of Earth-like environments, evading plasmas is well-nigh impossible, indeed, one can justifiably state that the plasma state is entirely dominating the universe.

Plasmas are generally defined as a fully, or at least significantly, ionized gas with free electrons and ions. Often plasmas, both in space and in laboratories, contain dust particles the presence of which influences the plasma characteristics significantly. These mixtures of dust particles and plasma species are named dusty plasmas and occur frequently in space. It is not a surprise that many space plasmas contain substantial amounts of dust particles, after all dust particles are so omnipresent that "dust free" environments hardly exist. Even industrial *clean rooms*, used for plasma etching, do not succeed in creating a perfectly dust free environment.

In this chapter several elementary properties of dust and dusty plasmas are introduced and discussed. While some of the peculiarities and remarkable properties of dust grains are portrayed, the analogies and differences between standard electron-ion plasmas and dusty plasmas will become clear. The emphasis in this introductory chapter predominantly lies on those properties that exert a prominent influence on wave phenomena in astrophysical plasmas, therefore some basic concepts of wave theory in plasmas are repeated. Immediately, these concepts are adapted to the formalism of dusty plasmas. Afterwards, a concise overview of the major charging mechanisms is given, because the possibility of fluctuating dust charges is one of the key features of dusty plasmas. Lastly, the role of gravitation, or more precise self-gravitation in a sizeable dusty plasma is accounted for.

2.1 What is dust?

Traditionally, the term dust is anything but discriminative and extends over a vast range of sizes and compositions. Interplanetary dust and meteorites are often of a silicate nature, *i.e.* with a mineral structure based on SiO_4 tetrahedra. In space, there are also substantial amounts of dust grains of a ferriferous (ferruginous) or carbonaceous nature, Carbonaceous dust can occur in different chemical forms as graphite, amorphous carbon and organic compounds, for example in organic refractory mantles. Furthermore, macromolecules, dirty ice particles and ice coated particles are also catalogued as dust particles. These ice coated particles are often found in molecular clouds, where the dust particles can prove to be successful nucleation centers for the growth of ices. However, making a rigorous classification is impracticable as in many occasions the constitution of dust grains will be an amalgamate of some of the mentioned components and even exhibit a myriad of other possible compositions.

In comparison with the electrons and ions, dust particles are orders of magnitudes larger and display a size spectrum as impressive as the gamut of possible compositions, varying from the just mentioned organic macromolecules and microscopic ice particles to even boulders and rocks. However, in order to grasp a qualitative notion of a certain phenomenon, often the dust grains are assumed to be typically micron sized.

This century it became clear that dust is ubiquitous in space and dust has been studied intensively ever since, but in the last decades a renewed impetus was generated thanks to the yield of data provided by the multiple spacecrafts that visited other planets in our solar system. Several of these successful space missions within our solar system have provided us with a profusion of data concerning the composition and size spectra of dust particles for many solar environments. Unfortunately, detailed data for dust agglomerations outside our solar system are less available, even scarce. In fact, as yet many issues about dust are hotly debated and still a matter of intense speculation, despite the imposing record of remote and in situ observations. Nevertheless, the existing models and assumptions prove to be reliable and ever improving.

2.2 Dusty plasmas

As a matter of course we can turn now to the interplay between dust particles and the omnipresent ionized gases and so enter the world of dusty plasmas. Prime examples of dusty plasmas in our solar system are circumsolar dust rings, rings of the Jovian planets, cometary comae and tails and noctilucent clouds. Outside our solar system, interstellar dust clouds are among the most obvious astrophysical applications.

Due to various processes, explored more in detail in some of the subsequent sections, dust grains, immersed in plasmas, can become electrically charged. The charged dust particles can electrostatically interact with each other as well as with plasma species, thus providing a new means for dust particles to play a part in wave mechanisms. Evidently, the presence of charged dust particles results in a more complex description but, in order to be able to explain certain phenomena, often proves to be necessary.

2.3 Concepts

Some basic concepts and quantities of plasmas can easily be adapted and/or extended in order to be of use in the scene of dusty plasmas. In wave theory, one of the most primal quantities is the Debye length and this characteristic must be adapted for the use in a dusty plasma theory, because of the changed screening mechanisms. Whereas the electron screening of the ions is the only screening effect in standard two component plasmas, in dusty plasmas both the electrons and ions will be screening the charged dust particles and the combination of these screening effects can be adequately described by a global Debye length. The response time of the heavy dust particles for local perturbations of the electric neutrality will naturally be much larger than for the electrons and ions. Therefore, the plasma frequencies and gyrofrequencies for the dust species will be much smaller than their respective values for the lighter plasma species and so introduce new timescales in the wave description of a dusty plasma. These dust plasma frequencies and dust gyrofrequencies are straightforward generalizations of their counterparts for the ionic species.

2.3.1 Charge neutrality

In the absence of particle sources and external forces, a dusty plasma in equilibrium will be macroscopically quasi-neutral, which can be translated mathematically into

$$n_{e0}e = q_i n_{i0} + \sum_d q_{d0} n_{d0}, \tag{2.1}$$

where $n_{\alpha 0}$ is the unperturbed number density per species α, q_{d0} is the equilibrium dust charge per dust species and the summation index d runs over all dust species. A premise for the previous expression is the existence of an equilibrium dust charge, a presupposition which might be unwarranted. Indeed, dust grain charges are variable and one could think of a dynamic equilibrium wherein the dust grains never attain an equilibrium charge. We will revert to this issue later when discussing the different dust grain charging mechanisms.

If we presume the dust to be negatively charged, which by and large applies to astrophysical plasmas, the condition for charge neutrality becomes

$$n_e + \sum_d Z_d n_d = Z_i n_i. \tag{2.2}$$

As, for astrophysical applications, the dust grains often devour most of the electrons, a dusty plasma frequently displays a large electron depletion and then equation (2.2) implies $n_e \ll n_i$. This has an interesting repercussion for the comparison of electron and ion plasma frequencies. Whereas the ion plasma frequency always is much smaller than the electron plasma frequency in electron-ion plasmas, the magnitude of both plasma frequencies can become comparable in dusty plasmas. Due to this phenomenon, wave modes in dusty plasmas may deviate considerably from their analogues in electron-ion plasmas.

2.3.2 Introduction of new frequency scales

Dust grains can achieve charges much higher than electrons and ions, and dust masses are even more staggeringly high in comparison with these standard plasma ingredients. This extremely low charge-to-mass ratio of the dust is translated into the common assumptions,

$$\begin{aligned} Z_d m_e &\ll m_d, \\ Z_d m_i &\ll Z_i m_d, \end{aligned} \tag{2.3}$$

with $Z_\alpha = |q_\alpha|/e$ being the number of unit (electron) charges per species α. Therefore, characteristic dust frequencies will be considerably lower than the corresponding electron and ion frequencies. Further on, these characteristic frequencies are defined and there the notations n_α, q_α and m_α will be used, standing respectively for the density, charge and mass of species α. Capital letters will be used to denote equilibrium values of the aforementioned quantities.

Pursuing the analogy with electrons and the ions, a dust plasma frequency can be introduced for every dust species α as

$$\omega_{p\alpha}^2 = \frac{N_\alpha q_{\alpha 0}^2}{\varepsilon_0 m_\alpha}, \tag{2.4}$$

where N_α is the equilibrium density of the respective fluid species. Expression (2.4) is a trivial generalization of the standard definition for plasma species and here too, the dust plasma frequency typifies the oscillatory behaviour of a dust particle around its equilibrium position, when being disturbed electrostatically. For simplicity, we can consider a single dust species and presume the dust to be negatively charged, as by and large applies to astrophysical plasmas. If we then presume a state of complete charge neutrality

$$Z_i N_i = N_e + N_d Z_d, \tag{2.5}$$

the dust plasma frequency can be expressed as

$$\omega_{pd}^2 = \frac{N_d q_{d0}^2}{\varepsilon_0 m_d} = \frac{Z_d m_i}{Z_i m_d}\omega_{pi}^2 - \frac{Z_d m_e}{m_d}\omega_{pe}^2, \tag{2.6}$$

being evidently much smaller than the ion and electron plasma frequencies.

Similarly, per dust species a dust gyrofrequency Ω_d can be defined and compared to the electron and ion gyrofrequencies as follows

$$|\Omega_d| = \frac{|q_{d0}|B_0}{m_d} = \frac{Z_d e B_0}{m_d} = \frac{Z_d m_i}{Z_i m_d}\Omega_i, \tag{2.7}$$

where B_0 stands for the static magnetic field. It is clear that the magnitudes of the gyrofrequencies follow the same ordering per species as for the plasma frequencies, namely $|\Omega_d| \ll \Omega_i \ll |\Omega_e|$.

These small characteristic frequencies for the dust species launch new very low-frequency wave modes and thus extend the attainable frequency range in a dusty plasma to extremely low frequencies, compared to the frequency range covered by possible wave modes in an electron-ion plasma. Precisely this extremely low frequency regime will be further explored in detail in this thesis.

2.3.3 Global Debye length

As mentioned before, the standard definition of Debye lengths can be refined for utilization in dusty plasmas and becomes, per species

$$\lambda_{D\alpha}^2 = \frac{\varepsilon_0 k_B T_\alpha}{N_\alpha q_\alpha^2}. \tag{2.8}$$

We now consider a dusty plasma for which macroscopic charge neutrality applies and where the dust particle have constant charges and are treated as point charges. Additionally, the electrons and ions are assumed to be in local thermodynamic equilibrium, so that they can be considered as being Boltzmann distributed,

$$\begin{aligned} n_e &= N_e \exp\left(\frac{e\phi}{k_B T_e}\right), \\ n_i &= N_i \exp\left(-\frac{e\phi}{k_B T_i}\right), \end{aligned} \tag{2.9}$$

where k_B is the Boltzmann constant. The charge neutrality is expressed as

$$eN_e = eN_i + q_d N_d \tag{2.10}$$

and the electrostatic Poisson's equation

$$\nabla^2\phi = -\frac{1}{\varepsilon_0}\sum_\alpha n_\alpha q_\alpha, \tag{2.11}$$

now becomes

$$\begin{aligned} \varepsilon_0\nabla^2\phi &= en_e - en_i - \sum_d q_d(\mathbf{r})\delta(\mathbf{r}-\mathbf{r}_d) \\ &= eN_e \exp\left(\frac{e\phi}{k_B T_e}\right) - eN_i \exp\left(-\frac{e\phi}{k_B T_i}\right) - \sum_d q_d(\mathbf{r})\delta(\mathbf{r}-\mathbf{r}_d). \end{aligned} \tag{2.12}$$

In the vicinity of a single, spherical dust particle but with $\mathbf{r} \neq \mathbf{r}_d$ and assuming $|e\phi| \ll k_B T_\alpha$, the latter equation yields the Green's function $G(r|r_d)$, being the solution of

$$\nabla^2 G(r|r_d) = \frac{q_d N_d}{\varepsilon_0} + \frac{G(r|r_d)}{\lambda_D^2}. \tag{2.13}$$

The definition for the global Debye length λ_D is in general

$$\frac{1}{\lambda_D^2} = \sum_{\text{lighter species}} \frac{1}{\lambda_{D\alpha}^2}, \tag{2.14}$$

and reduces here to

$$\frac{1}{\lambda_D^2} = \frac{1}{\lambda_{De}^2} + \frac{1}{\lambda_{Di}^2}. \tag{2.15}$$

Because of the spherical symmetry and for $G(r) = G(r|0)$, the latter equation can be rewritten as

$$\frac{1}{r^2}\frac{d}{dr}\left[r^2\frac{dG(r)}{dr}\right] = \frac{q_d N_d}{\varepsilon_0} + \frac{G(r)}{\lambda_D^2} \tag{2.16}$$

and becomes with the substitution $G'(r) = rG(r)$

$$\frac{d^2G'(r)}{dr^2} = \frac{q_d N_d}{\varepsilon_0} r + \frac{G'(r)}{\lambda_D^2}, \tag{2.17}$$

with solutions

$$G(r) = \frac{G'(r)}{r} = \frac{A}{r}\exp\left(\frac{r}{\lambda_D}\right) + \frac{B}{r}\exp\left(-\frac{r}{\lambda_D}\right) - \frac{q_d N_d \lambda_D^2}{\varepsilon_0}. \tag{2.18}$$

The integration constant A is zero because for $r \to \infty$, the potential ϕ must also go to zero, on the other hand the integration constant B can be determined as being $B = q_d/4\pi\varepsilon_0$, because for $N_e = 0 = N_i$ the Coulomb potential for a point charge q_d should be recovered. Thus, we arrive at

$$\begin{aligned} G(r|r_d) &= -\frac{q_d N_d \lambda_D^2}{\varepsilon_0} + \frac{q_d}{4\pi\varepsilon_0|r-r_d|}\exp\left(-\frac{|r-r_d|}{\lambda_D}\right) \\ &= \frac{q_d}{4\pi\varepsilon_0}\left[\frac{1}{|r-r_d|}\exp\left(-\frac{|r-r_d|}{\lambda_D}\right) - \frac{f}{a}\right] \\ \phi &= \sum_d \frac{q_d}{4\pi\varepsilon_0}\left[\frac{1}{|r-r_d|}\exp\left(-\frac{|r-r_d|}{\lambda_D}\right) - \frac{f}{a}\right], \end{aligned} \tag{2.19}$$

where a is the grain size, $f = 4\pi a N_d \lambda_D^2$ the fugacity parameter which will be introduced and discussed in chapter 4. In expression (2.19) the quantity $f/a \sim N_d\lambda_D^2$ is the influence of "grain packing".

2.4 Dusty plasmas vs multispecies plasmas

Often dusty plasmas are treated as multispecies plasmas although, strictly speaking, there are distinct differences between dusty plasmas and multispecies plasmas. Dusty plasmas set themselves apart from multi-ion descriptions as the dust particles can have fluctuating charges and display ample variety in shape, size and composition, unheard-of characteristics for mere ionic species. That is why dusty plasmas, in their true denotation, require a formalism that self-consistently includes the effects of grain charge fluctuations and also deals with the intrinsic heterogeneity of dust species. Such a blueprint for the description of dusty plasmas is regrettably not yet available, although efforts are currently being made, so that one is forced to use more naive descriptions.

Despite of its limitations however, a multispecies formalism can be an invaluable tool that is able to mimic accurately many important features of a dusty plasma and has the advantage of providing an elegantly structured and manageable framework.

2.5 Charging of dust grains

The charging of the dust grains in a dusty plasma is a very fundamental aspect in dusty plasma physics, yet the issue of dust charging provides several difficulties and intricacies. The description of the charging of a single dust grain, surrounded by plasma, is almost identical with the main theme of probe theory, developed by Mott-Smith and Langmuir [1926], at the dawn of plasma theory investigations. Indeed, a dust grain can be considered as a probe with a probe current $I = I_e + I_i$ due to the fluxes of electrons and ions that reach or leave the grain, where the positive direction for the current is from the plasma towards the probe. The probe current will exist as long as there is a difference in potential between the surrounding unperturbed plasma and the grain surface, both being separated by a screening layer of the order of a few Debye lengths that is not electrically neutral. Here it is advantageous to define a characteristic charging time t_{ch}, being the time needed for a neutral grain to reach 90% of its equilibrium value. This parameter may be considered constant, although the charging process can be highly nonlinear. When the dust grain has reached its equilibrium potential V_0, the grain potential can be recognized as a floating potential, continuing the analogy with probe theory. This steady state is described by the charging equation

$$\frac{dQ_d}{dt} = \sum_\beta I_\beta(V_0, \ldots) = 0, \tag{2.20}$$

where the index β stands for all charging mechanisms present and Q_d is the equilibrium charge of the dust grain. The charging equation (2.20) is nonlinear and might exhibit hysteresis, in the latter case the equilibrium potential will be dependent on the grain history. Different charging mechanisms account for the fluctuating charges of the dust particles, yet primary charging usually is the most important mechanism for astrophysical applications, and generally the only mechanism that is retained in treatments of waves and instabilities. Therefore, in this section the focus will be chiefly on the primary charging process.

2.5.1 Capacitance model

For calculating the grain charge, the dust grain can be considered as a spherical capacitator with concentrical shells formed by the grain and its Debye shield. Since the grain radius a is usually much smaller than the Debye length, the capacitance C is practically that of an isolated sphere with radius a, namely

$$C = 4\pi\varepsilon_0 a, \tag{2.21}$$

so that the grain charge q_d and the equilibrium grain potential V_{d0} are related as [Houpis and Whipple Jr. 1987]

$$q_d = 4\pi\varepsilon_0 a V_{d0}. \tag{2.22}$$

2.5.2 Primary charging

A single dust grain in a plasma endures a continuous bombardment of the plasma species, of which some can get stuck onto the grain surface or end up being captured by the grain, thereby changing the dust grain charge. This type of grain charging is called primary charging and in many dusty plasmas the main grain charging mechanism. Indeed, physical adsorption to the surface requires no activation energy and a particle colliding with the dust particle is thus likely to give up enough kinetic energy so that it will become bound. Obviously, the probabilities for catching plasma particles are different for electrons and ions and depend on the instantaneous grain potential. The primary charging theory starts from a number of assumptions and simplifications, namely

- The grains are considered to be in a dynamic equilibrium, meaning that in this ideal situation a single dust grain catches oppositely charged particles almost simultaneously so as to keep the grain potential and charge constant.
- Primary charging theory ignores the presence of other charging mechanisms and also the existence of external magnetic fields.
- The dust grains are identical spheres, perfectly sticky and conducting.
- Plasma particles have Maxwellian velocity distributions at infinity, ideally, far from the grain considered.
- Currents are orbital motion limited, based on the assumption that some particles of every energy range can graze the grain surface. Implicitly this assumption excludes trapped orbits for the plasma particles.

In the absence of equilibrium drifts the primary charging theory yields the following charging current per species,

$$I_\alpha = n_\alpha q_\alpha \int_{v_0}^{|v|=\infty} v \sigma_\alpha f_\alpha(\mathbf{v}) d^3\mathbf{v}, \tag{2.23}$$

here σ_α is the charging cross section per species and v_0 the smallest particle velocity required to hit the grain. For an attractive potential ($q_\alpha V < 0$), respectively repulsive potential ($q_\alpha V > 0$), the latter equation yields

$$I_\alpha = \pi a^2 n_\alpha q_\alpha \sqrt{\frac{8 k_B T_\alpha}{\pi m_\alpha}} \left(1 - \frac{q_\alpha V_d}{k_B T_\alpha}\right), \tag{2.24}$$

$$I_\alpha = \pi a^2 n_\alpha q_\alpha \sqrt{\frac{8 k_B T_\alpha}{\pi m_\alpha}} \exp\left[-\frac{q_\alpha V_d}{k_B T_\alpha}\right], \tag{2.25}$$

where V_d is the grain potential relative to the plasma potential V_p, the latter being arbitrarily set equal to zero for the rest of this section. For a negatively charged grain these

expressions can be rewritten as,

$$I_i = \pi a^2 n_i e \sqrt{\frac{8k_B T_i}{\pi m_i}} \left(1 - \frac{eV_d}{k_B T_i}\right), \tag{2.26}$$

$$I_e = -\pi a^2 n_e e \sqrt{\frac{8k_B T_e}{\pi m_e}} \exp\left[\frac{eV_d}{k_B T_e}\right], \tag{2.27}$$

A grain will initially collect more electrons than ions, because the electrons are more mobile, so building up a negative potential. As a result the electron flux decreases and the ion flux increases until both fluxes are balanced. The equilibrium grain potential can then be found from the nonlinear equation

$$n_i c_{si} \left(1 - \frac{eV_d}{k_B T_i}\right) = n_e c_{se} \exp\left[\frac{eV_d}{k_B T_e}\right], \tag{2.28}$$

and the thermal speeds $c_{s\alpha}^2 = k_B T_\alpha / m_\alpha$ have been introduced.

2.5.3 Other charging mechanisms

Depending on the parameters of the plasma and the surrounding environment, other charging mechanisms may be of considerable importance too, of which the most important are

- *Tunnelling*
  Electrons with energies higher than $E_{min} = \sqrt{K_W a}$, with K_W the constant of Whiddington are capable to tunnel through the grain. The threshold E_{min} is usually of the order of $10^4 eV \sqrt{a_{\{\mu m\}}}$ for insulators as well as for conductors. This tunnelling effect is only of importance for extremely small grains, as the number of electrons that attain an energy E_{min} is usually negligible.

- *Secondary emission*
  The impact on a dust grain of plasma particles, if sufficiently energetic, may release secondary electrons. For space applications, electrons are usually the most energetic plasma particles and therefore it is mostly electron driven secondary emission that is taken into account. The yield of secondary electrons then represents a positive grain current. On the other hand, ion induced secondary electron emission has been extensively studied in laboratory plasmas (sputtering), due to its use in the production for semiconductor based devices as integrated circuits and optoelectronic components. Secondary emission is evidently strongly dependent on the surface properties and the material of the dust grain. Moreover it has been shown [Chow et al. 1993] that two grains with the same history but with different sizes can have charges of the opposite sign. This is the case when besides the primary currents, the secondary electron and tunnelling currents are taken into account. The effects of tunnelling and secondary electron current are therefore strongly related to the grain size distribution.

- *Photo-emission*
  The absorption of photons can release photoelectrons and these then contribute to a positive grain charging current. The absorption characteristics of electromagnetic radiation are strongly dependent on the radiation wavelength as well as the grain size and type [Havnes 1984]. Upon absorption of solar photons, a grain surface with negative potential will emit a constant photo-electric current

$$I_p = e\pi a^2 \Gamma, \tag{2.29}$$

  where Γ stands for the number of photo-electrons per square meter, per second [Horányi 1996],

$$\Gamma \simeq \frac{2.5 \cdot 10^1 4\kappa}{d^2_{\{AU\}}} \frac{1}{\mathrm{m}^2\,\mathrm{s}}, \tag{2.30}$$

  with d the distance from the Sun and the efficiency factor κ close to unity for conductors and close to 0.1 for dielectric materials [Whipple Jr. 1981]. On the other hand, for a positive grain potential, only the most energetic electrons can escape the grain, without being pulled back to the surface. Positively charged grains contribute a net current

$$I_p = e\pi a^2 \Gamma \exp\left[-\frac{eV}{k_B T_p}\right], \tag{2.31}$$

  with $k_B T_p \simeq 1 - 3$ eV, the average energy of the assumed Maxwellian distribution of the photo-electrons. The ratio between the photo-electron flux and the electron flux [Havnes et al. 1990]

$$R_{p/e} = \eta \frac{40 \cdot 10^9}{r^2_{h\{A.U.\}} N_{e\{m^{-3}\}} \sqrt{T_{e\{K\}}}}, \tag{2.32}$$

  determines the importance of the photo-emission.

- *Grain destruction and grain growth*
  Electrostatic tension in a dust grain builds up dramatically if a dust grain acquires a very high potential. A charged spherical and conducting grain will pulverize if its tensile strength F_t is exceeded by the electrostatic repulsive force at a surface potential V_0 [Öpik 1956],

$$F_t \leqslant \varepsilon_0 \frac{V_0^2}{a^2}, \tag{2.33}$$

  this expression underestimates the importance of the breaking up process as capricious geometries or surface conditions facilitate the electrostatic disruption of the grain.

  Conversely, coagulation of colliding dust grains can produce larger particles. For neutral particles, this condensation process can be described via the Smoluchowsky kinetic equation [Bliokh et al. 1995], which describes the formation of a mass spectrum, out of an initially monodisperse plasma, due to the coagulation processes. Another mechanism that can also be responsible for grain growth is mantle growth,

due to the continuous adsorption of gas phase atoms and molecules onto the dust surface. Both mechanisms have a different influence on the size distribution curve, whereas coagulation modifies the form of the distribution mantle growth primarily shifts the distribution to larger sizes, for the greater part conserving the functional form.

- *Field-emission*
  Some micron- and submicron-sized particles composed of silicates, glass or metal can be mono crystals. These microcrystalline dust particles have extremely high tensile strengths and are able to support high electric fields. For these particles the maximum electric field attainable is limited by ion field emission for positively charged grains and electron field emission for negatively charged grains.

2.5.4 Charging model for grain ensembles

In this section several charging mechanisms were mentioned. However, all of them reasoned on a single dust grain embedded in a plasma whilst a description in terms of dust grain ensembles actually is much more appropriate for dusty plasma theory. If we treat a dusty plasma as a closed system, assumed to be created with the injection of dust particles in a neutral plasma, the equilibrium dust charge on the dust grains will decrease dramatically when the dust density increases [Goertz and Ip 1984, Whipple et al. 1985, Havnes et al. 1984, 1987, 1990] as experimentally verified by Xu et al. [1993]. As the dust density increases, the average distance between grains decreases and the Debye spheres around the particles become compressed, when the average grain distance has been reduced to the order of a Debye length. As mentioned before, the grain and its Debye shield act like a spherical capacitator, having a capacitance inversely proportional to the Debye length. Consequently, one would expect the dust charges to increase. However, this potential behaviour of the dust particles comes to nought due to another phenomenon. As the plasma is thought of as being created with the injection of dust grains into a neutral plasma, the dust grains will become negatively charged thus creating an electron depletion in the plasma. Therefore grains cannot achieve higher charges, notwithstanding their increased capacitance. In fact, in the case of sufficient electron depletion in the plasma so that $\lambda_D = d \sim n_d^{-1/3}$, the aforementioned charging equations for a single dust particle are no longer valid because a dust particle then can no longer be treated as an individual test particle [Mendis and Rosenberg 1994].

2.6 Self-gravitation

Self-gravitational forces, or in other words gravitational grain-grain interactions, inevitably become significant for large clusters of dust particles, hence also for dusty plasmas with large dimensions, for instance dust clouds or large molecular clouds. Self-gravitational forces are attractive forces, directed radially towards the center of mass of the cluster and consequently such a cluster contracts unless the self-gravitational forces are counteracted

by pressure forces from within. The nature of these pressure forces can be manifold, *e.g.* radiation pressure, magnetic pressure and thermal pressure may all enter into the stability analysis. Here, an important distinction has to be made between neutral and charged dust grains. Whereas neutral dust grains are mainly affected by gravity forces and possibly also collisional forces, the charged dust grains also interact via the Lorentz forces and are thus highly susceptible to the electron and ion pressure. Provided the lion's share of the dust grains is charged and in the absence of radiation sources and strong magnetic fields, the electron and ion pressure turn out to be sufficient for stabilizing the plasma against gravitational collapse, if the plasma does not exceed a certain critical lengthscale. This critical lengthscale is known as the Jeans length.

2.7 Forces on dust grains

In this introduction, the discussion of the acting forces on dust grains was restricted to the electromagnetic forces and the gravitational forces. It almost goes without saying that these are not the only possible forces on a dust particle.

Other possible forces include the drag forces, often introduced into the description through collisional frequencies between the different species. The most important drag forces in a dusty plasma are those between charged dust particles and neutral dust particles. If neutral particles are absent, the dust ion collisions prove to be the major collision mechanism, and this situation is discussed in chapter 10.

Evidently, near the Sun or in the presence of other radiation sources, the radiation pressure will be of considerable importance and will have to be included as well. The radiation pressure can be expressed as $p = W/c = \hbar\omega_0/c$, with W the energy of the wave and ω_0 the radiation frequency.

And the list does not end here, thermophoretic forces and the Poynting-Robertson effect may also be important. The thermophoretic forces are associated with a momentum transfer from the surrounding neutral gas to the dust particle due to a temperature gradient in the gas. On the other hand, the Poynting-Robertson effect is a braking force due to reradiation of the absorbed solar energy, ensuing from the Poynting-Robertson effect the particles loose orbital energy and their orbit radius is decreased. The importance and influence of the thermophoretic forces and the Poynting-Robertson effect is reviewed in the books of Shukla and Mamun [2002] and Bliokh et al. [1995] respectively.

2.8 Reviews and books

Over the years, many state of the art reviews and excellent books appeared, providing a valuable summary for the recent developments in the field of dusty plasmas and lowering the threshold for people new to this exciting field.

In order of chronology and restricting the list of reviews to those that mostly deal with space applications, the following eminent reviews are among the most instructive, namely

Goertz [1989], De Angelis [1992], Mendis and Rosenberg [1994], Horányi [1996], Verheest [1996] and Shukla [2001].

Recently, several detailed books have rejoiced the dusty plasma community. The first monograph dealing with dusty plasmas was that of Bliokh et al. [1995], and emphasized on self-gravitational effects in dusty space plasmas. On the other hand, the recent technological developments in laboratory applications of dusty plasmas were summarized by Bouchoule [1999]. Both the monograph of Verheest [2000] and that of Shukla and Mamun [2002] cover a very wide base and provide excellent companions for dusty plasma researchers. Moreover, the books of Verheest [2000] and Shukla and Mamun [2002] provide typical parameters of astrophysical plasmas. However, because the data related to dusty plasmas are scarce and often disputed, estimations for orders of magnitude of relevant parameters are by and large avoided in this thesis.

Chapter 3

Basic equations and waves

The very low frequency modes under study in this thesis are mainly wave phenomena the description of which resembles that of acoustic modes in ordinary plasmas. These sound waves are intertwined with the thermal effects within a plasma and when taking into account these thermal effects then, apart from the acoustic wave phenomena, there also arise kinetic phenomena due to the fact that in a thermal or near thermal distribution, there are some particles moving at or near the phase velocity. These particles have resonant interactions with the wave, which can lead to either collisionless wave damping or to instabilities and wave growth.

In order to study the latter effects, the framework of a kinetic theory is required. Unfortunately in the derivation of dusty plasma kinetic theories, there are specific and as yet unresolved problems due to *e.g.* the possible charging and diversity of the dust grains. The diversity in size and composition of the dust particles undermines certain steps in the traditional derivation of a kinetic theory and requires for a careful reexamination. Incorporating the charging mechanisms within a kinetic framework is not straightforward and complicates the calculations considerably, for instance some theories [Varma 2000] include charging mechanisms at the cost of extra phase variables, namely the dust charge and the dust mass. Despite the weaknesses and unresolved issues in current dusty plasma kinetic theories, they represent the most comprehensive and accurate description available. On the other hand, the fluid approach has the advantages of being mathematically more manageable and straightforward, but is not accurate at small phase velocities.

In this chapter, the difficulties regarding kinetic theories are sketched, before advancing to a multifluid model. In this multifluid model, the dispersion law for obliquely propagating linear waves in magnetized, self-gravitating dusty plasmas is derived. In chapters 8 and 9, we will revert in more detail to a dusty plasma kinetic theory in order to recover some of the generality that is lost due to the use of a fluid description.

3.1 Kinetic model

3.1.1 Microscopic description

A microscopic theory for a many body system aims at the complete knowledge of the coordinates and velocities of every single particle. However, a complete microscopic description requires solving a system of coupled differential equations, where the number of equations may exceed 10^{23}! Clearly such an approach is neither practicable nor desirable, even a priori impossible as we are ignorant of the exact initial conditions, but the microscopic study of a plasma provides an excellent starting point for statistical plasma theories.

When switching over to a statistical method, the exact position in phase space of each particle is not necessary, instead probability functions are introduced. For the introduction of the probability functions we reason on a system of N_0 particles and associate a six dimensional coordinate system with each particle. As the individual particles of the system shift in a six-dimensional phase space, the system moves along continuously in a $6N_0$-dimensional phase space. The assumption of having a Gibbs ensemble of such systems, then links each system with a point in the $6N_0$-dimensional phase space and we can define a continuous function f_{N_0} so that

$$f_{N_0}(\mathbf{x}_1, \mathbf{v}_1, \mathbf{x}_2, \mathbf{v}_2, \ldots, \mathbf{x}_{N_0}, \mathbf{v}_{N_0}, t)\, d\mathbf{x}_1 d\mathbf{v}_1 d\mathbf{x}_2 d\mathbf{v}_2 \ldots d\mathbf{x}_{N_0} d\mathbf{v}_{N_0}, \tag{3.1}$$

represents the probability of retrieving a system in a volume $d\mathbf{x}_1 d\mathbf{v}_1 d\mathbf{x}_2 d\mathbf{v}_2 \ldots d\mathbf{x}_{N_0} d\mathbf{v}_{N_0}$, around the phase space point $(\mathbf{x}_1, \mathbf{v}_1, \mathbf{x}_2, \mathbf{v}_2, \ldots, \mathbf{x}_{N_0}, \mathbf{v}_{N_0})$ at time t. The probability function satisfies the Liouville equation

$$\frac{\partial f_{N_0}}{\partial t} + \sum_{i=1}^{N_0} \mathbf{v}_i \cdot \frac{\partial f_{N_0}}{\partial \mathbf{x}_i} + \sum_{i=1}^{N_0} \mathbf{a}_i \cdot \frac{\partial f_{N_0}}{\partial \mathbf{v}_i} = 0, \tag{3.2}$$

as the total probability is a conserved quantity. The probability function basically contains the same information as microscopic distributions with the exception that it is rather regarded as a continuous function, whereas the microscopic distribution functions are thought of as discontinuous in actual positions and velocities. Consequently, a complete description for a many body system, using probability functions is just about as unattainable as a microscopic theory, since the distribution functions carry essentially the same amount of information and complexity. For reducing the complexity, reduced functions are introduced and as these contain less information they offer a feasible approach. The description of the reduced probability functions leads to the so called BBGKY hierarchy, a set of equations named after respectively Bogoliubov, Born, Green, Kirkwood, and Yvon.

3.1.2 BBGKY hierarchy

Another way of describing the function f_{N_0} is the joint probability of locating every particle i between the coordinates $(\mathbf{x}_i, \mathbf{v}_i)$ and $(\mathbf{x}_i + d\mathbf{x}_i, \mathbf{v}_i + d\mathbf{v}_i)$. On the other hand, the so called reduced probability functions

$$f_k(\mathbf{x}_1, \mathbf{v}_1, \mathbf{x}_2, \mathbf{v}_2, \ldots, \mathbf{x}_k, \mathbf{v}_k, t) = V^k \int d\mathbf{x}_{k+1} d\mathbf{v}_{k+1} \ldots d\mathbf{x}_{N_0} d\mathbf{v}_{N_0} F_{N_0} \tag{3.3}$$

with V^k a normalization factor, denote the probability of finding k particles in an elementary 6-dimensional phase space volume encompassing the coordinates $(\mathbf{x}_i, \mathbf{v}_i)$ for $i = 1 \ldots k$, irrespective of the coordinates of the other $N_0 - k$ particles. The reduced probabilities evidently contain less information than the probability density f_{N_0} and are thus easier to manipulate. The Liouville equation yields a differential equation for every f_k so producing a chain of equations, where each equation for f_k is coupled to the next higher equation through an f_{k+1} term. This chain of equations forms the famous BBGKY hierarchy, where the acronym conjoins the pioneering authors Bogoliubov [1946], Born and Green [1949], Kirkwood [1946, 1947] and Yvon [1935], each of which developed similar theories but often in different contexts.

The underlying assumption for the previous derivations is a symmetry of particle labels for f_{N_0} *i.e.* a full interchangeability of all particles, which is clearly an idealization of astrophysical dusty environments. Obviously, the simplest type of reduced functions are the one particle distribution functions, they depend only on six coordinates and time and obey the collisionless Boltzmann equation

$$\frac{\partial f_1}{\partial t} + \mathbf{v} \cdot \frac{\partial f_1}{\partial \mathbf{x}} + \mathbf{a}_{ext} \cdot \frac{\partial f_1}{\partial \mathbf{v}} = 0, \tag{3.4}$$

where $\mathbf{a}_{ext}$ stands for the acceleration due to external sources only. The two particle reduced distribution functions include interactions between particles and when the particles are thought of to be completely independent, correlation factors can be neglected, yielding the famous Vlasov equation [Vlasov 1945]

$$\frac{\partial f_1}{\partial t} + \mathbf{v} \cdot \frac{\partial f_1}{\partial \mathbf{x}} + (\mathbf{a}_{\text{ext}} + \mathbf{a}_{\text{self}}) \cdot \frac{\partial f_1}{\partial \mathbf{v}} = 0, \tag{3.5}$$

with $\mathbf{a}_{\text{self}}$ being the mean acceleration due to all particles. The latter equation indicates that differences between the collisionless Boltzmann equation and the Vlasov equation are hidden in the precise interpretation of the acceleration terms.

3.1.3 Difficulties in kinetic dusty plasma theory

As mentioned before, the assumption of a full interchangeability of all particles is generally not justifiable in astrophysical dusty environments, due to the incredible diversity of the dust and their ability to adsorb the lighter plasma constituents. Indeed the charging, and possibly also creation/destruction processes, of dust particles poses serious problems in the derivations of kinetic theories, when applied to dusty plasmas in the true sense of their meaning. This because the identity of the dust particles can change continuously and, to make things even more complicated, intimately depends on the surroundings. Moreover, the considerable size of the dust grains forces a serious reconsideration of the derivations necessary to obtain the Liouville equation.

The aforementioned difficulties for obtaining a "proper" dusty plasma kinetic theory are hitherto still unresolved and are for the moment being investigated intensively [Tsytovich and De Angelis 1999, 2000, 2001, 2002, Varma 2000]. Nowadays, the use of extra phase

space variables for the dust charge and dust mass seems a viable approach for wave mode analysis in dusty plasmas [Varma 2000, Verheest et al. 2002].

Despite the open problems, kinetic plasma theories applied to multispecies plasmas can be a valuable tool for the exploration of waves in dusty plasmas and provide a framework for studying the effects associated with the thermal motion of particles.

3.1.4 Kinetic dispersion relation for electrostatic waves

Having outlined the principles, but also the restrictions, of extending the use of kinetic plasma theory to dusty plasmas, we can now turn to the study of low-frequency waves in dusty plasmas. Because of the very low frequencies, the intricacies arising due to the charging processes do not necessitate a serious reconsideration. Indeed, as in general the charging frequencies are situated way out of the window of the considered wave frequencies, the charges can safely be assumed constant. For simplicity we consider plasma waves in unmagnetized and collisionless self-gravitating plasmas, where for the moment only one dust species is included. All particle species α (with $\alpha = e, i, d$) can be described by a distribution function f_α , which obeys the ordinary Vlasov equation

$$\frac{\partial f_\alpha}{\partial t} + \boldsymbol{\nabla} \cdot (\mathbf{v} f_\alpha) + \boldsymbol{\nabla}_v \cdot \left[f_\alpha \left\{ \frac{q_\alpha}{m_\alpha} (\mathbf{E} + \mathbf{v} \times \mathbf{B}) - \boldsymbol{\nabla} \psi \right\} \right] = 0. \tag{3.6}$$

Here $\mathbf{v}$ is the velocity in phase space and the nabla operator $\boldsymbol{\nabla}_v$ stands for

$$\boldsymbol{\nabla}_v \equiv \left(\frac{\partial}{\partial v_x}, \frac{\partial}{\partial v_y}, \frac{\partial}{\partial v_z} \right). \tag{3.7}$$

In the absence of a magnetic field, the self-consistent electric field $\mathbf{E} = -\boldsymbol{\nabla}\phi$ and gravitational field ψ can be found from the Poisson equations

$$\nabla^2 \phi = -\frac{1}{\varepsilon_0} \sum_\alpha q_\alpha n_\alpha, \tag{3.8}$$

$$\nabla^2 \psi = 4\pi G \sum_\alpha m_\alpha n_\alpha, \tag{3.9}$$

where ϕ is the electric potential, G the gravitational constant and densities are introduced as

$$n_\alpha = \int f_\alpha d^3\mathbf{v}. \tag{3.10}$$

For the description of plasma waves, all the external fields and average velocities of the particles are assumed to be zero in the unperturbed (equilibrium) state. Applying the standard linearization procedure then yields the perturbed distribution functions

$$f_{\alpha 1} = -\frac{\mathbf{k} \cdot \boldsymbol{\nabla}_v f_{\alpha 0}}{\omega - \mathbf{k} \cdot \mathbf{v}} \left[\frac{q_\alpha}{m_\alpha} \phi + \psi \right], \tag{3.11}$$

where values with subscript 0 refer to the zeroth-order state, and first-order terms are indicated by a subscript 1, the latter are assumed to vary as $\exp[i\mathbf{k} \cdot \mathbf{r} - i\omega t]$.

The substitution of the perturbed distribution function (3.11) into the Poisson equations (3.8) and (3.9) gives two coupled equations with respect to the electric and gravitational potentials, namely

$$\begin{aligned} \phi\varepsilon_p + \psi\frac{K}{\sqrt{G}} &= 0, \\ -\phi K\sqrt{G} + \psi\varepsilon_G &= 0. \end{aligned} \tag{3.12}$$

These equations involve a plasma dielectric constant ε_p and its analogue for a self-gravitating neutral medium, here represented by ε_G

$$\varepsilon_p = 1 + \frac{1}{\varepsilon_0 k^2}\sum_\alpha \frac{q_\alpha^2}{m_\alpha} I_\alpha, \tag{3.13}$$

$$\varepsilon_G = 1 - \frac{4\pi G}{k^2}\sum_\alpha m_\alpha I_\alpha, \tag{3.14}$$

and a coupling factor

$$K = \sqrt{\frac{4\pi G}{\varepsilon_0}}\frac{1}{k^2}\sum_\alpha q_\alpha I_\alpha, \tag{3.15}$$

where the abbreviation

$$I_\alpha = \int \frac{\mathbf{k}\cdot\boldsymbol{\nabla}_v f_{\alpha 0}}{\omega - \mathbf{k}\cdot\mathbf{v}} d^3\mathbf{v}. \tag{3.16}$$

has been used.

The dispersion relation for electrostatic waves in a kinetic model of self-gravitating plasmas is the eliminant of the system formed by equations (3.12) and simply becomes

$$\varepsilon(\omega, k) = \varepsilon_p + \frac{K^2}{\varepsilon_G} = 0, \tag{3.17}$$

which clearly indicates the coupling between electrostatic and gravitational disturbances.

3.2 Multifluid model

Whereas the kinetic theory treatment of plasma waves is the most comprehensive description, it is also the most complex. For this reason, a fluid description is usually the preferred tool for the description of wave modes, as it provides a more wieldable and transparent model. A fluid description requires the phase velocities under study to be large compared to the thermal velocities and so disregards the effects on wave propagation/damping caused by particles travelling at or near the phase velocity of the wave.

The fluid equations encompass the continuity equations, which express the conservation of number densities per species

$$\frac{\partial n_\alpha}{\partial t} + \boldsymbol{\nabla}\cdot(n_\alpha \mathbf{u}_\alpha) = S_\alpha, \tag{3.18}$$

here labeled per species with the index α and with the fluid velocities are denoted by $\mathbf{u}_\alpha$. The sink/source terms S_α on the right hand side of the continuity equation remain unspecified here and have to be invoked when dealing with dust charging. We continue with the equations of motion per species

$$\left(\frac{\partial}{\partial t} + \mathbf{u}_\alpha \cdot \boldsymbol{\nabla}\right) \mathbf{u}_\alpha + \frac{1}{n_\alpha m_\alpha} \boldsymbol{\nabla} \cdot \mathbf{P}_\alpha = \frac{q_\alpha}{m_\alpha} (\mathbf{E} + \mathbf{u}_\alpha \times \mathbf{B}) - \boldsymbol{\nabla}\psi + \mathbf{M}_\alpha, \tag{3.19}$$

where $\mathbf{E}$ and $\mathbf{B}$ denote the electric and magnetic fields, and ψ the gravitational potential. The equation of state is curtailed to changes of state where the pressure of a species exclusively depends on its density and is isotropic in nature,

$$\mathbf{P}_\alpha = p_\alpha(n_\alpha)\, \mathbf{1}. \tag{3.20}$$

This assumption of barotropic pressures is not a severe restriction and also allows the traditional isentropic changes of state. For the plasma in its totality, there is conservation of charge and this can be expressed as

$$\frac{\partial}{\partial t} \sum_\alpha n_\alpha q_\alpha + \boldsymbol{\nabla} \cdot \sum_\alpha n_\alpha q_\alpha \mathbf{u}_\alpha = 0. \tag{3.21}$$

With the help of the continuity equations (3.18), the charge conservation equation can easily be rewritten as

$$\sum_{\alpha=e,i} q_\alpha S_\alpha + \sum_d n_d \left(\frac{\partial}{\partial t} + \mathbf{u}_d \cdot \boldsymbol{\nabla}\right) q_d = 0. \tag{3.22}$$

Similarly as for the charges, we can write down an equation that expresses the conservation of mass for the plasma as a whole

$$\frac{\partial}{\partial t} \sum_\alpha n_\alpha m_\alpha + \boldsymbol{\nabla} \cdot \sum_\alpha n_\alpha m_\alpha \mathbf{u}_\alpha = 0, \tag{3.23}$$

or equivalently

$$\sum_{\alpha=e,i} m_\alpha S_\alpha + \sum_d n_d \left(\frac{\partial}{\partial t} + \mathbf{u}_d \cdot \boldsymbol{\nabla}\right) m_d = 0. \tag{3.24}$$

In this multifluid formalism the equations of Maxwell are

$$\begin{aligned}
&\boldsymbol{\nabla} \times \mathbf{E} + \frac{\partial}{\partial t}\mathbf{B} = \mathbf{0}, \\
&c^2 \boldsymbol{\nabla} \times \mathbf{B} = \frac{\partial}{\partial t}\mathbf{E} + \frac{1}{\varepsilon_0} \sum_\alpha n_\alpha q_\alpha \mathbf{u}_\alpha, \\
&\boldsymbol{\nabla} \cdot \mathbf{E} = \frac{1}{\varepsilon_0} \sum_\alpha n_\alpha q_\alpha, \\
&\boldsymbol{\nabla} \cdot \mathbf{B} = 0.
\end{aligned} \tag{3.25}$$

Finally, the gravitational Poisson equation

$$\nabla^2\psi = 4\pi G \sum_\alpha n_\alpha m_\alpha, \tag{3.26}$$

allows the calculation of the gravitational potential.

Phenomena that require the possibility of fluctuating grain charges, are dealt by using a current equation per dust species

$$\frac{dq_d}{dt} = \frac{\partial q_d}{\partial t} + \mathbf{u}_d \cdot \boldsymbol{\nabla} q_d = I_e + I_i, \tag{3.27}$$

the right hand side of the current equation for a negatively charged dust grain involves the charging currents towards or away from the dust grain. These charging currents for the electrons respectively ions are, provided that equilibrium drifts are small compared to the thermal velocities, and following the OML theory [Allen 1992]

$$\begin{aligned} I_e &= -\pi a^2 e n_e \sqrt{\frac{8k_B T_e}{\pi m_e}} \exp\left(\frac{eV_d}{k_B T_e}\right), \\ I_i &= \pi a^2 e n_i \sqrt{\frac{8k_B T_i}{\pi m_i}} \left(1 - \frac{eV_d}{k_B T_i}\right), \end{aligned} \tag{3.28}$$

where $V_d \equiv q_d/4\pi\varepsilon_0 a$ denotes the dust grain surface potential relative to the plasma potential.

3.3 Waves in magnetized plasmas

When dealing with magnetized plasmas, a unique direction is present in the description, namely the direction of the static, magnetic field $\mathbf{B}_0$. It is convenient to refresh the existing nomenclature for waves in magnetized plasmas, here $\mathbf{k}$ and $\mathbf{E}_1$ will represent respectively the wave vector and the first order electric field. The angle between the direction of the static, magnetic field and that of the wave propagation allows two special choices, waves are called *parallel propagating waves* if $\mathbf{k} \times \mathbf{B}_0 = 0$ and *perpendicularly propagating waves* if $\mathbf{k} \cdot \mathbf{B}_0 = 0$.

The direction of the wave electric field relative to the wave vector also marks waves, for $\mathbf{k} \times \mathbf{E}_1 = 0$ waves are named *longitudinal*, in contrast with *transverse* waves for which $\mathbf{k} \cdot \mathbf{E}_1 = 0$.

Finally, the absence of a magnetic field perturbation ($\mathbf{B}_1 = 0$), distinguishes the *electrostatic waves* from those with $\mathbf{B}_1 \neq 0$, namely the *electromagnetic waves*. From Faraday's law we learn that longitudinal waves are electrostatic and vice versa. Indeed from $\mathbf{k} \times \mathbf{E}_1 = 0$ (longitudinal waves) follows $\partial\mathbf{B}/\partial t = 0$, hence in a linear description $\mathbf{B}_1 = 0$ (electrostatic waves).

3.4 Space and time scales

The different forces and mechanisms in a dusty plasma act on different space and time scales. These are summarized here briefly and are compared to each other. Regarding the spatial scales, the smallest dimension under consideration is the typical dust grain size a. As Debye shielding is a prime example of plasma collective behaviour, the Debye length λ_D sets apart what is termed a "dusty plasma" from a so called "dust in plasma" environment. Here, we denote the average distance between grains as d and note that $a \ll \lambda_D$ in virtually every dusty plasma environment. For $a \ll \lambda_D < d$, the screened dust grains can be considered as isolated entities or impurities in the plasma and in this case one speaks of a dust-in-plasma. On the other hand, for $a \ll d < \lambda_D$ the Debye spheres of the dust grains overlap and so allow a conjoint motion of the dust particles. Making a leap in orders of magnitude we can now look at the lengthscales involved with the self-gravitational forces, which work on a much longer range than electrostatic forces. The relative magnitude of the parameter L, standing for a typical dimension of the total plasma under consideration and the Jeans length L_J, determines whether the plasma is stable against gravitational collapse. The plasma is gravitationally unstable if $L > L_J$ and vice versa the plasma is stable for $L < L_J$.

There are also different time scales in play [Verheest et al. 2001] in a dusty plasma wave description. If a dusty plasma is described as a closed system then there are four relevant timescales. The Saha equation supplies the shortest timescale, namely the thermal relaxation time needed for being able to consider a dynamic equilibrium, regarding the ionization and recombination processes in the plasma. Tacitly this timescale is mostly considered zero, as usually the global conservation of charge and mass is supposed. Another important timescale quantifies the typical charging time of the dust particles and is usually defined as

$$\tau_{\text{charge}} = \left[\frac{1}{\sigma_{d0}} \frac{d\sigma_{d0}}{dt} \right]^{-1}, \tag{3.29}$$

with σ_{d0} the total charge density in the plasma. Naturally, the wave period ω^{-1} also is an important timescale. Finally, there is the longest of all timescales, namely the timescale characterizing the mass loading

$$\tau_{\text{mass}} = \left[\frac{1}{\rho_{d0}} \frac{d\rho_{d0}}{dt} \right]^{-1}. \tag{3.30}$$

In fact it can often safely considered to be infinite, for instance when treating the electrons and ions as being Boltzmann distributed.

In analytical models, the typical charging time and the wave period are mostly assumed to differ considerably from each other. If this assumption is not justified, a numerical treatment is requisite.

3.5 Linear waves in multispecies plasmas

A sensible choice for a reference frame wherein wave phenomena for arbitrary propagation angles can be described, is a frame where one of the axes is aligned with either the direction of the static, external magnetic field or the direction of wave propagation. I choose for the latter possibility, aligning the z-axis with the direction of wave propagation, ergo $\boldsymbol{\nabla} = \mathbf{e}_z \partial/\partial z$. There is one more degree of freedom for the choice of the reference frame and this is used to assure that the static magnetic field vector $\mathbf{B}_0$ lies in the x, z-plane and thus $\mathbf{B}_0 = B_0(\sin\vartheta \mathbf{e}_x + \cos\vartheta \mathbf{e}_z)$, with ϑ being the angle between the directions of wave propagation and the external magnetic field.

Using this convention for the reference frame, the basic equations can be simplified, starting with the continuity equations

$$\frac{\partial n_\alpha}{\partial t} + \frac{\partial}{\partial z}(n_\alpha u_{\alpha z}) = 0, \tag{3.31}$$

and the equations of motion,

$$\frac{\partial \mathbf{u}_\alpha}{\partial t} + u_{\alpha z}\frac{\partial \mathbf{u}_\alpha}{\partial z} = \frac{q_\alpha}{m_\alpha}(\mathbf{E} + \mathbf{u}_\alpha \times \mathbf{B}) - \frac{1}{n_\alpha m_\alpha}\frac{\partial p_\alpha}{\partial z}\mathbf{e}_z - \frac{\partial \psi}{\partial z}\mathbf{e}_z. \tag{3.32}$$

The barotropic law is isotropic and thus becomes

$$p_\alpha = \mathcal{P}_\alpha(n_\alpha), \tag{3.33}$$

while Maxwell's equations simplify to

$$\mathbf{e}_z \times \frac{\partial \mathbf{E}}{\partial z} + \frac{\partial \mathbf{B}}{\partial t} = \mathbf{0}, \tag{3.34}$$

$$c^2 \mathbf{e}_z \times \frac{\partial \mathbf{B}}{\partial z} = \frac{\partial \mathbf{E}}{\partial t} + \frac{1}{\varepsilon_0}\sum_\alpha n_\alpha q_\alpha \mathbf{u}_\alpha, \tag{3.35}$$

$$\varepsilon_0 \frac{\partial E_z}{\partial z} = \sum_\alpha n_\alpha q_\alpha, \tag{3.36}$$

$$\frac{\partial B_z}{\partial z} = 0, \tag{3.37}$$

and finally, the gravitational Poisson equation becomes

$$\frac{\partial^2 \psi}{\partial z^2} = 4\pi G \sum_\alpha n_\alpha m_\alpha. \tag{3.38}$$

Linearizing and Fourier transforming the equations (3.31)–(3.34) allows us to express the fluid velocity for each species separately as linear functions of the components of the wave

electric field and of the self-gravitational potential

$$\begin{aligned}
u_{\alpha x} &= \frac{q_\alpha}{m_\alpha \mathcal{L}_\alpha}\left\{i\omega(\omega^2 - k^2c_{s\alpha}^2 - \Omega_\alpha^2\sin^2\vartheta)E_x - \Omega_\alpha(\omega^2 - k^2c_{s\alpha}^2)E_y\cos\vartheta\right. \\
&\quad \left. - i\omega\Omega_\alpha^2 E_z\sin\vartheta\cos\vartheta\right\} - \frac{\omega k\Omega_\alpha^2}{\mathcal{L}_\alpha}\psi\sin\vartheta\cos\vartheta, \\
u_{\alpha y} &= \frac{q_\alpha}{m_\alpha \mathcal{L}_\alpha}\left\{\Omega_\alpha(\omega^2 - k^2c_{s\alpha}^2)E_x\cos\vartheta + i\omega(\omega^2 - k^2c_{s\alpha}^2)\,E_y\right. \\
&\quad \left. - \omega^2\Omega_\alpha E_z\sin\vartheta\right\} + i\frac{k\omega^2\Omega_\alpha}{\mathcal{L}_\alpha}\psi\sin\vartheta, \\
u_{\alpha z} &= \frac{q_\alpha}{m_\alpha \mathcal{L}_\alpha}\left\{-i\omega\Omega_\alpha^2 E_x\sin\vartheta\cos\vartheta + \omega^2\Omega_\alpha E_y\sin\vartheta\right. \\
&\quad \left. + i\omega(\omega^2 - \Omega_\alpha^2\cos^2\vartheta)E_z\right\} + \frac{\omega k(\omega^2 - \Omega_\alpha^2\cos^2\vartheta)}{\mathcal{L}_\alpha}\psi,
\end{aligned} \tag{3.39}$$

where $\mathcal{L}_\alpha$ is shorthand for

$$\mathcal{L}_\alpha = \omega^2(\omega^2 - \Omega_\alpha^2) - k^2c_{s\alpha}^2(\omega^2 - \Omega_\alpha^2\cos^2\vartheta). \tag{3.40}$$

Here streaming effects have been omitted and different sound velocities $c_{s\alpha}$ have been defined through $m_\alpha c_{s\alpha}^2 = [d\mathcal{P}_\alpha/dn_\alpha]_{N_\alpha}$ and it is worth noting that the gyrofrequencies $\Omega_\alpha = q_\alpha B_0/m_\alpha$ include the sign of the charges. Substituting the fluid velocities (3.39) in the linearized forms of equations (3.35) and (3.38) then yields the following set of equations

$$\begin{bmatrix} D_{xx} & D_{xy} & D_{xz} & D_{x\psi} \\ D_{yx} & D_{yy} & D_{yz} & D_{y\psi} \\ D_{zx} & D_{zy} & D_{zz} & D_{z\psi} \\ D_{\psi x} & D_{\psi y} & D_{\psi z} & D_{\psi\psi} \end{bmatrix} \cdot \begin{bmatrix} E_x \\ -iE_y \\ \omega E_z \\ i(\omega k/\sqrt{4\pi\varepsilon_0 G})\psi \end{bmatrix} = 0, \tag{3.41}$$

with the elements of the symmetric dispersion tensor being given by

$$\begin{aligned}
D_{xx} &= \omega^2 - c^2k^2 - \omega^2\sum_\alpha \frac{\omega_{p\alpha}^2(\omega^2 - k^2c_{s\alpha}^2 - \Omega_\alpha^2\sin^2\vartheta)}{\omega^2(\omega^2 - \Omega_\alpha^2) - k^2c_{s\alpha}^2(\omega^2 - \Omega_\alpha^2\cos^2\vartheta)}, \\
D_{xy} &= D_{yx} = \omega\sum_\alpha \frac{\omega_{p\alpha}^2\Omega_\alpha(\omega^2 - k^2c_{s\alpha}^2)\cos\vartheta}{\omega^2(\omega^2 - \Omega_\alpha^2) - k^2c_{s\alpha}^2(\omega^2 - \Omega_\alpha^2\cos^2\vartheta)}, \\
D_{xz} &= D_{zx} = \omega\sum_\alpha \frac{\omega_{p\alpha}^2\Omega_\alpha^2\sin\vartheta\cos\vartheta}{\omega^2(\omega^2 - \Omega_\alpha^2) - k^2c_{s\alpha}^2(\omega^2 - \Omega_\alpha^2\cos^2\vartheta)}, \\
D_{x\psi} &= D_{\psi x} = -\omega\sum_\alpha \frac{\omega_{p\alpha}\omega_{J\alpha}\Omega_\alpha^2\sin\vartheta\cos\vartheta}{\omega^2(\omega^2 - \Omega_\alpha^2) - k^2c_{s\alpha}^2(\omega^2 - \Omega_\alpha^2\cos^2\vartheta)}, \\
D_{yy} &= \omega^2 - c^2k^2 - \omega^2\sum_\alpha \frac{\omega_{p\alpha}^2(\omega^2 - k^2c_{s\alpha}^2)}{\omega^2(\omega^2 - \Omega_\alpha^2) - k^2c_{s\alpha}^2(\omega^2 - \Omega_\alpha^2\cos^2\vartheta)},
\end{aligned}$$

$$
\begin{aligned}
D_{yz} &= D_{zy} = -\omega^2 \sum_\alpha \frac{\omega_{p\alpha}^2 \Omega_\alpha \sin\vartheta}{\omega^2(\omega^2-\Omega_\alpha^2) - k^2 c_{s\alpha}^2(\omega^2 - \Omega_\alpha^2\cos^2\vartheta)}, \\
D_{y\psi} &= D_{\psi y} = \omega^2 \sum_\alpha \frac{\omega_{p\alpha}\omega_{J\alpha}\Omega_\alpha \sin\vartheta}{\omega^2(\omega^2-\Omega_\alpha^2) - k^2 c_{s\alpha}^2(\omega^2 - \Omega_\alpha^2\cos^2\vartheta)}, \\
D_{zz} &= 1 - \sum_\alpha \frac{\omega_{p\alpha}^2(\omega^2 - \Omega_\alpha^2\cos^2\vartheta)}{\omega^2(\omega^2-\Omega_\alpha^2) - k^2 c_{s\alpha}^2(\omega^2 - \Omega_\alpha^2\cos^2\vartheta)}, \\
D_{z\psi} &= D_{\psi z} = \sum_\alpha \frac{\omega_{p\alpha}\omega_{J\alpha}(\omega^2 - \Omega_\alpha^2\cos^2\vartheta)}{\omega^2(\omega^2-\Omega_\alpha^2) - k^2 c_{s\alpha}^2(\omega^2 - \Omega_\alpha^2\cos^2\vartheta)}, \\
D_{\psi\psi} &= -1 - \sum_\alpha \frac{\omega_{J\alpha}^2(\omega^2 - \Omega_\alpha^2\cos^2\vartheta)}{\omega^2(\omega^2-\Omega_\alpha^2) - k^2 c_{s\alpha}^2(\omega^2 - \Omega_\alpha^2\cos^2\vartheta)},
\end{aligned}
\tag{3.42}
$$

from which the general dispersion law follows as

$$\det[D_{ij}] = 0. \tag{3.43}$$

The different plasma frequencies are defined through $\omega_{p\alpha}^2 = N_\alpha q_\alpha^2/\varepsilon_0 m_\alpha$, and the Jeans frequencies through $\omega_{J\alpha}^2 = 4\pi G N_\alpha m_\alpha$. Capital letters denote equilibrium values. As $\omega_{p\alpha}\omega_{J\alpha}$ is a convenient way to rewrite $N_\alpha q_\alpha$, up to normalizing constants, a single $\omega_{p\alpha}$ includes the sign of the charge.

3.6 Parallel propagation

At parallel propagation ($\vartheta = 0°$), there is a decomposition of the dispersion law. Indeed since $D_{xz} = D_{x\psi} = D_{yz} = D_{y\psi} = 0$, the matrix $[D_{ij}]$ has a blockdiagonal structure and its determinant can be written as

$$\det[D_{ij}] = \begin{vmatrix} D_{xx} & D_{xy} \\ D_{xy} & D_{yy} \end{vmatrix} \cdot \begin{vmatrix} D_{zz} & D_{z\psi} \\ D_{z\psi} & D_{\psi\psi} \end{vmatrix} = 0. \tag{3.44}$$

The dispersion law for parallel modes clearly decouples and, since in this case $D_{xx} = D_{yy}$, yields

$$D_{xx} \pm D_{xy} = 0, \tag{3.45}$$

$$D_{zz}D_{\psi\psi} - D_{z\psi}^2 = 0. \tag{3.46}$$

Equation (3.45) amounts to

$$\omega^2 = c^2k^2 + \omega \sum_\alpha \frac{\omega_{p\alpha}^2}{\omega \pm \Omega_\alpha}, \tag{3.47}$$

as E_x and E_y are out of phase with each other, the electric field vector performs a circular rotation in time. Thus the latter equation represents the ordinary right and left hand circularly polarized modes, respectively. These are transverse, electromagnetic modes and

therefore, within a fluid description, unaffected by the self-gravitational forces, or any gradient force for that matter.

On the other hand, equation (3.46) yields the longitudinal Langmuir-Jeans modes [Bliokh et al. 1995]

$$\left(1-\sum_\alpha \frac{\omega_{p\alpha}^2}{\omega^2-k^2c_{s\alpha}^2}\right)\left(1+\sum_\alpha \frac{\omega_{J\alpha}^2}{\omega^2-k^2c_{s\alpha}^2}\right)+\left(\sum_\alpha \frac{\omega_{p\alpha}\omega_{J\alpha}}{\omega^2-k^2c_{s\alpha}^2}\right)^2=0. \tag{3.48}$$

The Langmuir-Jeans modes are longitudinal and therefore have no magnetic field perturbation *i.e.* these modes are electrostatic. The dispersion law (3.48) will be fully described in the chapters dealing with electrostatic modes and self-gravitation.

3.7 Perpendicular propagation

On the other hand, at strictly perpendicular propagation ($\vartheta = 90^o$), the dispersion law (3.43) factorizes in the one for the ordinary mode, with dispersion law $D_{xx} = 0$ or

$$\omega^2 = c^2k^2 + \sum_\alpha \omega_{p\alpha}^2, \tag{3.49}$$

the remainder then giving the extraordinary mode [Verheest 2000]. Again, the ordinary mode is unaffected by self-gravitation or pressure effects. Conversely, the low-frequency part of the extraordinary mode undergoes notable changes due to self-gravitation [Verheest et al. 1999].

3.8 Instabilities

Linear plasma waves are nothing else than small perturbations about the equilibrium state, some of these perturbations however can continuously grow in time, leading to an unstable configuration [Chandrasekhar 1961]. Instabilities in plasmas are in fact common phenomena, being imputable to the intrinsic complexity of plasmas. Indeed, plasmas allow all kinds of possible perturbations, any of which can prove to be unstable. The mathematical translation of the stability criterion is quite simple, whenever we obtain a dispersion relation $D(\omega, k) = 0$, the corresponding wave is considered unstable if for some real wavenumber k_{cr} the frequency ω has a positive imaginary part. That is, if the dimensions of the system under consideration exceed a minimum length $L = 2\pi/k_{cr}$.

Unfortunately there are some pitfalls in a rigorous stability analysis. For instance, stabilities are studied within a linear theory, while there could be nonlinear limiting effects which are hardly amenable to a theoretical framework. Furthermore, the equilibrium state itself has to be stable and this is merely a premise in the existing theories of self-gravitating systems! This inconsistency and its consequences are discussed later.

Chapter 4

Basic modes

The addition of dust species to a plasma does not only modify the existing modes but also introduces new very low frequency wave modes. The first to recognize the new frequency scales introduced by the heavy dust particles were Rao et al. [1990], they included the dynamics of the dust and their investigations ultimately resulted in the prediction of the dust-acoustic wave. The poignant physics that described the dust dynamics in effect acted as a catalyst for many other dusty plasma investigations and turned the dust-acoustic mode into a precursor for a multitude of other low frequency modes. The dust-acoustic mode has been repeatedly observed, in an astonishing agreement with theoretical predictions [Barkan et al. 1995].

The very low frequency modes under study in this thesis are mainly wave phenomena resembling acoustic oscillations, and in this chapter the most relevant electrostatic modes are recalled. These basic modes delineate the different frequency regimes, wherein the charged dust particles play a role.

In order to extricate these very basic modes, relatively simple models are employed and these are inherently restricted to a certain frequency window. In doing so, the main physical mechanisms are exposed clearly, while keeping the mathematics manageable. In the following chapters, the initial restrictions on the frequency range are relaxed and then the coupling between the different wave modes hosted by a dusty plasma will be revealed. The reason for this strong coupling is manifold, due to the many possible interaction mechanisms between the particles. The interlacing between the different modes can not only be induced by the usual collisional and streaming effects between species, but the charged, heavy dust particles can also communicate by means of charge exchanges and gravitational interplay.

Firstly, the general dispersion law for electrostatic modes will be repeated, afterwards the different frequency regimes are separated and catalogued in order of diminishing frequencies. The discussed modes have ultra low frequencies and for these modes the grains generally charge so rapidly that they have ample time to achieve an equilibrium charge within a wave period. For this reason the dust charges can be treated as effectively constant, except for the description of the dust-Coulomb wave, where the dust charge fluctuations play a crucial and indispensable role.

To set the standards uncomplicatedly, the following descriptions only deal with collisionless plasmas, which may give imprecise results particularly in case of a strong presence of neutral dust grains. If collisions are important, the picture has to be refined and this problem is relegated to chapter 10. Furthermore, the described basic modes are usually portrayed in a monodisperse dusty plasma and the complications due to mass distributions will also be tackled further on.

4.1 Linear electrostatic waves

When dealing with linear electrostatic waves, Faraday's equation reduces to $\boldsymbol{\nabla} \times \mathbf{E} = \mathbf{0}$ and consequently the waves are exclusively longitudinal.

We can revert to the general dispersion law (3.48) for electrostatic waves, propagating parallel to an external magnetic field, namely

$$\left(1 - \sum_{\alpha} \frac{\omega_{p\alpha}^2}{\omega^2 - k^2 c_{s\alpha}^2}\right)\left(1 + \sum_{\alpha} \frac{\omega_{J\alpha}^2}{\omega^2 - k^2 c_{s\alpha}^2}\right) + \left(\sum_{\alpha} \frac{\omega_{p\alpha}\omega_{J\alpha}}{\omega^2 - k^2 c_{s\alpha}^2}\right)^2 = 0, \tag{4.1}$$

and this dispersion law illustrates clearly the coupling between the electrostatic and self-gravitational modes. After all, the first factor arises solely from electric interactions between particles. On the other hand, for neutral particles only the second factor remains, representing the dispersion law for waves in a self-gravitating, electrically neutral medium. Evidently, the last term is the coupling factor that denotes the degree of coupling between electric and gravitational processes, it disappears in neutral gases.

For simplicity the influence of self-gravitational effects is relegated to a later section, in effect this simplification boils down to setting a lower limit for the investigated frequencies. Without self-gravitation the dispersion law (4.1) now reduces to its purely electrostatic part

$$\sum_{\alpha} \frac{\omega_{p\alpha}^2}{\omega^2 - k^2 c_{s\alpha}^2} = 1. \tag{4.2}$$

Only the very low frequencies will allow the heavy dust grains to respond to the electrostatic perturbations, and in this frequency range the presence of the dust grains not only modifies existing wave modes but even brings about a habitat for wave modes that are nonexistent in "dust free" plasmas. In order to isolate the different wave mechanisms in dusty plasmas and situate the different frequency regimes, some of the most basic and celebrated wave modes are recalled now. The different wave modes are catalogued in a diminishing order and in doing so the influence of the dust will show to be increasingly elemental in the wave description.

As the dust particles are too sluggish to follow the highest frequencies, the outcome of their presence is negligible in that part of the frequency spectrum. For intermediate frequencies however, the dust particles commence to participate in wave motion, albeit that they act as it were in a supporting part and merely modify wave modes that occur in ordinary plasmas too. Finally for the lowest frequencies, corresponding with the characteristic time

scales of the dust dynamics, the plasma particles desist completely partaking in the wave motion and only provide pressure. The latter branch of the frequency spectrum wets most of our appetite for knowledge, as it is here that new wave modes emerge. Moreover, only this branch can be significantly influenced by self-gravitational effects, as will become clear later on.

4.2 Langmuir modes

Langmuir waves were among the first discovered plasma waves due to the fact that they can be studied in a very simple model. Basically, Langmuir waves [Langmuir 1926] are simple plasma oscillations in which only the electrons take part, with a mechanism closely connected to the charge screening processes in a plasma. The traditional model treats an electron-ion plasma, consisting of a fixed background of immobile ions, wherein initially a one-dimensional local perturbation of the electrons is created. Subsequently, the perturbation creates a positive charge density that pulls back the electrons to their original position. Yet the extremely mobile electrons overshoot their equilibrium position, which underlines the dynamic character of the electron screening, and the result is an ongoing harmonic oscillation with the electron plasma frequency ω_{pe} as the oscillation frequency.

Dust particles are *a fortiori* much heavier than ions and it would be futile to include them in the description of Langmuir waves. The regime of Langmuir waves is obtained when assuming all species but electrons to be infinitely massive or, equivalently, supposing frequencies high enough so that the heavier species cannot participate in the wave motion. In a dusty plasma with $m_i, m_d \to \infty$ ($\omega_{pi} = 0 = \omega_{pd}$), equation (4.2) then yields

$$\omega^2 = \omega_{pe}^2 + k^2 c_{se}^2 = \omega_{pe}^2 (1 + k^2 \lambda_{De}^2), \tag{4.3}$$

where the last term represents a relatively small thermal correction. The ions cannot keep pace with the high frequency electron oscillations and are therefore hardly influencing the physics of Langmuir oscillations. The presence of dust particles brings about electron depletion and therefore the Langmuir waves have a lowered plasma frequency in dusty plasmas.

If we take the ion motion into account, but still neglect all dust motion as dust particles are so much heavier than ions, the result can be adapted by formally replacing the electron mass by the reduced mass $(1/m_e + 1/m_i)^{-1}$, yielding [Akhiezer et al. 1975]

$$\omega^2 = \omega_{pe}^2 \left(1 + \frac{m_e}{m_i}\right) + k^2 c_{se}^2, \tag{4.4}$$

which is, as expected, a small correction.

4.3 Dust-ion-acoustic mode

For lower frequencies the ions too are involved in the wave motion whereas the electrons are displaced simultaneously with the electrostatic and pressure perturbations. Including

the ion motion, we now encounter the frequency domain of the dust-ion-acoustic waves, firstly described by Shukla and Silin [1992]. These can only be excited in a strongly non-isothermal plasma ($T_i \ll T_e$) and therefore I will suppose the ions to be practically cold. The cold ion approximation and the quasi-inertialess nature of the electrons in this frequency range restricts the phase velocities to the range $c_{sd}, c_{si} \ll \omega/k \ll c_{se}$, which clearly corresponds to the notion of an electron pressure that coerces the more massive ions and, to a much lesser extent, the dust grains into a collective motion. The dispersion law for the dust-ion-acoustic waves is easily derived from (4.2) and reads

$$\frac{\omega^2}{k^2} = \frac{\lambda_{De}^2(\omega_{pi}^2 + \omega_{pd}^2)}{1 + k^2\lambda_{De}^2}. \tag{4.5}$$

Since in dusty plasmas the ion plasma frequency ω_{pi} is much larger than the dust plasma frequency ω_{pd}, the latter can be safely neglected in equation (4.5). In the long wavelength limit $k^2\lambda_{De}^2 \ll 1$, the dispersion relation (4.5) then simplifies to

$$\frac{\omega}{k} = c_{dia} = \lambda_{De}\omega_{pi} \simeq kc_{ia}\sqrt{\frac{N_i}{N_e}}, \tag{4.6}$$

wherein the dust-acoustic velocity c_{dia} is defined and $c_{ia}^2 = k_B T_e/m_i$ is the usual ion-acoustic speed. Expression (4.6) implies the virtual immobility of the dust grains in this phase regime. In other words, the dust grains only influence the wave mode through electron depletion. However, due to the constraints on the phase velocities, the electron depletion is not allowed to be extremely small and must satisfy $m_e/m_i \ll N_e/N_i$ [Whipple et al. 1985].

4.4 Intricacies of the used fluid model

There is a note of caution that must be emphasize here, in the discussed phase speed regime the ions can be described hydrodynamically but, strictly speaking, the electrons cannot! A careful examination of the dynamic behaviour of the electrons requires a kinetic model and so we start with the Vlasov equation for the electrons

$$\frac{\partial f_e}{\partial t} + \mathbf{v}\cdot\frac{\partial f_e}{\partial \mathbf{r}} - \left[e\left(\mathbf{E} + \mathbf{v}\times\mathbf{B}\right) + m_e\boldsymbol{\nabla}\psi\right]\cdot\frac{\partial f_e}{\partial \mathbf{p}} = 0.$$

Since we assume phase velocities $\omega/k \ll c_{se}$, the Vlasov equation can be considered to be time independent ($\partial f_e/\partial t = 0$) and for electrostatic waves becomes

$$\mathbf{v}\cdot\frac{\partial f_e}{\partial \mathbf{r}} + \left(e\frac{\partial\phi}{\partial \mathbf{r}} - m_e\frac{\partial\psi}{\partial \mathbf{r}}\right)\cdot\frac{\partial f_e}{\partial \mathbf{p}} = 0.$$

Possible solutions of the latter equation are

$$f_e = f_e\left[-\frac{m\mathbf{v}^2}{2k_BT_e} + \frac{e\phi}{k_BT_e} - \frac{m_e\psi}{k_BT_e}\right],$$

where the right hand side denotes any arbitrary function of the argument residing between the square brackets. This implies that the Boltzmann distribution is also a solution

$$f_e \sim \exp\left[-\frac{m\mathbf{v}^2}{2k_BT_e} + \frac{e\phi}{k_BT_e} - \frac{m_e\psi}{k_BT_e}\right],$$

and so, with the use of

$$n_e = \int f_e d^3\mathbf{v}, \tag{4.7}$$

the following density distribution for the electrons is obtained,

$$n_e = N_e \exp\left(\frac{e\phi}{k_BT_e} - \frac{m_e\psi}{k_BT_e}\right).$$

To summarize, for the electrons, we can assume that they are in equilibrium under the conditions of low-frequency oscillations and that their density is Boltzmann distributed. After linearization of the Boltzmann equation, we finally obtain for the electron density

$$n_e = \frac{N_e}{k_BT_e}(e\phi - m_e\psi). \tag{4.8}$$

If we now go back to the derivation of the general dispersion law, we have for the linearized equation of continuity without streaming

$$n_e = \frac{N_e k u_{ez}}{\omega}, \tag{4.9}$$

while the linearized equation of motion for longitudinal disturbances ($E_z = -ik\phi$) yields

$$u_{ez} = \frac{k\omega(-e\phi + m_e\psi)}{m_e(\omega^2 - k^2c_{se}^2)}. \tag{4.10}$$

Combining equations (4.9) and (4.10), we obtain

$$n_e = \frac{N_e k^2(-e\phi + m_e\psi)}{m_e(\omega^2 - k^2c_{se}^2)} = \frac{N_e}{k_BT_e}(e\phi - m_e\psi) \tag{4.11}$$

when inserting $\omega \ll kc_{se}$ and $m_ec_{se}^2 = k_BT_e$. We can now see that the general dispersion law renders the proper result although, strictly speaking, for the dust-ion-acoustic waves it is applied outside the validity of the fluid description. This is due to the linearization procedure and is in fact a more general remark. For future reference we can now incorporate quasi-inertialess species (denoted with index α) by letting $m_\alpha \to 0$, and carefully retain the nonzero pressure term $m_\alpha c_{s\alpha}^2 = [dP(n_\alpha)/dn_\alpha]_{N_\alpha} = k_BT_\alpha$.

4.5 Dust-acoustic mode

Going to even lower phase velocities so that the phase velocity obeys $c_{sd} \ll \omega/k \ll c_{si}, c_{se}$, the wave dynamics are completely governed by the dust inertia. Now both the electrons and ions supply the necessary pressure and this is the regime of the dust-acoustic wave as first described by Rao et al. [1990]. As the dust-acoustic wave embodies the dynamic behaviour of the dust particles, its frequency is inherently extremely low and typically of the order of a few hertz. Over the years, the existence of the dust acoustic wave has been strikingly confirmed in several laboratory experiments [Barkan et al. 1995, Pieper and Goree 1996] and stimulated many researchers, proven by the avalanche of papers dealing with dust-acoustic waves since their discovery.

Under the aforementioned restrictions the dispersion law (4.2) simplifies in this low frequency regime to

$$\frac{\omega^2}{k^2} = c_{sd}^2 + \frac{\lambda_D^2 \omega_{pd}^2}{1 + k^2 \lambda_D^2} = c_{sd}^2 + \frac{c_{da}^2}{1 + k^2 \lambda_D^2}, \tag{4.12}$$

where $c_{da} = \lambda_D \omega_{pd}$ is the dust-acoustic speed. The Debye length is implicated in the dust-acoustic velocity and the latter can as such be heavily influenced by ion screening effects.

Dust-acoustic waves occur typically for long wavelengths $\lambda \gg \lambda_D$, indeed in this regime the electrons and ions screen the fluctuations of the dust grain charge so that ultimately their pressure gradients drive the oscillation. Since the plasma pressures are much larger than the dust pressures, the dust-acoustic speed c_{da} will be much larger than the dust sound speed c_{sd}, so that in the long wavelength limit ($k\lambda_D \ll 1$) equation (4.12) simply reduces to $\omega = k c_{da}$.

4.6 Dust-Coulomb wave

The previously described modes were derived in a framework wherein the dust charges can be esteemed as constant, because the charging times scales are considered to differ significantly from the wave period. However, another low frequency mode arises solely on condition that both dust charge and density perturbations are taken into account. Indeed, the dust-Coulomb [Rao 1999] wave describes the dust dynamics that are tied up with the dust charge fluctuations and consequently requires the presence of dust grains with variable charges.

Because the dust dynamics are investigated, the characteristic time scales are tuned accordingly and therefore allow the electrons and ions to be treated as being in thermal equilibrium. The electron and ion density are thus Boltzmann distributed

$$n_e = N_e \exp\left(\frac{e\phi}{k_B T_e}\right), \tag{4.13}$$

$$n_i = N_i \exp\left(-\frac{e\phi}{k_B T_i}\right), \tag{4.14}$$

while the continuity and momentum equations for the dust remain

$$\frac{\partial n_d}{\partial t} + \frac{\partial}{\partial z}(n_d u_d) = 0, \tag{4.15}$$

$$\frac{\partial u_d}{\partial t} + u_d \frac{\partial u_d}{\partial z} + \frac{q_d}{m_d}\frac{\partial \phi}{\partial z} + \frac{k_B T_d}{n_d m_d}\frac{\partial n_d}{\partial z} = 0. \tag{4.16}$$

The electrostatic potential ϕ can then be found from Poisson's equation

$$\frac{\partial^2 \phi}{\partial z^2} = \frac{1}{\varepsilon_0}(e n_e - e n_i - q_d n_d) \tag{4.17}$$

and the current balance equation completes the description,

$$\frac{\partial q_d}{\partial t} + u_d \frac{\partial q_d}{\partial x} = I_e + I_i. \tag{4.18}$$

The current balance equation expresses the dust charge fluctuations in terms of the electron and ion currents

$$\begin{aligned} I_e &= -\pi e a^2 n_e(\phi)\sqrt{\frac{8k_B T_e}{\pi m_e}}\exp\left(\frac{eV_d}{k_B T_e}\right), \\ I_i &= \pi e a^2 n_i(\phi)\sqrt{\frac{8k_B T_i}{\pi m_i}}\left(1 - \frac{eV_d}{k_B T_i}\right), \end{aligned} \tag{4.19}$$

that enter or leave the grain. Here $V_d = q_d/4\pi\varepsilon_0 a$ is the instantaneous grain surface potential and a is the grain radius.

Linearizing and Fourier transforming equations (4.13)-(4.18) yields the dispersion relation

$$\frac{\omega^2}{k^2} = \frac{c_{da}^2}{1 + k^2\lambda_D^2 + f\Delta} + c_{sd}^2, \tag{4.20}$$

where the fugacity parameter $f = 4\pi a N_d \lambda_D^2$ has been met in Chapter 2 and Δ is defined as

$$\Delta = \frac{\omega_2}{\omega_1 - i\omega}. \tag{4.21}$$

This involves the characteristic grain charging frequencies

$$\begin{aligned} \omega_1 &= \frac{a}{\sqrt{2\pi}}\left[\frac{\omega_{pi}}{\lambda_{Di}} + \frac{\omega_{pe}}{\lambda_{De}}\exp\frac{eV_{d0}}{\kappa T_e}\right], \\ \omega_2 &= \frac{a}{\sqrt{2\pi}}\left[\frac{\omega_{pi}}{\lambda_{Di}}\left(1 - \frac{eV_{d0}}{\kappa T_i}\right) + \frac{\omega_{pe}}{\lambda_{De}}\exp\frac{eV_0}{\kappa T_e}\right], \end{aligned} \tag{4.22}$$

with $V_{d0} = Q_d/4\pi\varepsilon_0 a$ the equilibrium grain surface potential.

Let us now look at the interesting limits in the relation between the wave period and the charging time scales of the dust grains. When the charging time scale is much larger than the wave period, the dust-Coulomb wave will be absent [Rao 2000]. This result is not much of a surprise, after all the grains in this regime have a nearly constant charge over

a wave period and the existence of grain charge fluctuations is a *conditio sine qua non* for the existence of the dust-Coulomb wave.

On the other hand, when the wave period is much smaller than the characteristic charging times, the grains have ample time to attain an average equilibrium charge over one wave period and consequently charge fluctuations will hardly contribute to wave damping. In this limit, $\omega \ll \omega_1$ so that $\Delta \simeq \omega_2/\omega_1 = \delta$, where the parameter δ can be safely assumed to be constant over a wide range of dust fugacity. Now it becomes clear that the dust-Coulomb wave is a wave that resides in dense dusty plasmas, *i.e.* dusty plasmas with $f\delta \gg 1$. Indeed for $f\delta \gg 1$, the dispersion relation (4.20) reduces to

$$\frac{\omega^2}{k^2} = \frac{c_{dc}^2}{\delta(1 + k^2\lambda_R^2)} + c_{sd}^2, \tag{4.23}$$

with the dust-Coulomb speed $c_{dc} = Q_d/\sqrt{4\pi\varepsilon_0 a m_d}$ and $\lambda_R = 1/\sqrt{4\pi N_d a \delta}$ being a length scale closely related to the intergrain separation. Contrarily, for tenuous dusty plasmas *i.e.* plasmas for which $f\delta \ll 1$, the dust-acoustic wave is recovered and so we can conclude that the value of the plasma fugacity parameter dictates whether the dust-acoustic or dust-Coulomb wave will exist.

4.7 Pure Jeans modes

In the extremely low frequency limit, when plasma effects are unimportant, only the self-gravitational branch of the dispersion law (4.1) remains, namely

$$1 + \sum_\alpha \frac{\omega_{J\alpha}^2}{\omega^2 - k^2 c_{s\alpha}^2} = 0, \tag{4.24}$$

because gravitational forces are negligible among electrons and ions, the summation index in equation (4.24) only runs over the dust species. For one dust species the dispersion law reduces to the archetypal dispersion law for a single neutral self-gravitating species

$$\omega^2 = k^2 c_{s\alpha}^2 - \omega_{J\alpha}^2. \tag{4.25}$$

For an n-component system, the dispersion relation (4.24) has n roots in ω^2, of which at most one can be negative [Fridman and Polyachenko 1984]. The negative root occurs when

$$\sum_{d=1}^{n} \frac{\omega_{Jd}^2}{k^2 c_{sd}^2} > 1 \tag{4.26}$$

and corresponds with an aperiodic instability. All the other modes, corresponding with positive roots, represent coupled acoustic oscillations.

4.8 Other modes

This overview was not intended to be exhaustive and only the most relevant electrostatic modes for the this thesis were recalled and situated concisely. Other electrostatic modes have been described in recent papers, among which the dust-lattice mode and the dust hybrid modes are among the most investigated.

The dust-lattice mode, obtained by Melandsø [1996], Farokhi et al. [1999] and later extended by Farokhi et al. [1999], is also a low frequency mode that only can occur in strongly coupled dusty plasma systems. Dust-lattice waves differ considerably from the acoustic modes that were previously described and exist in an entirely different frequency and phase velocity regime. As the name suggests, it presumes an ordered structure of dust particles and is dealt with using lattice models similar to those applied in solid state physics. Nowadays, dust lattice modes are closely observed and investigated in microgravity experiments, performed in the International Space Station.

The dust hybrid modes are not further discussed, an overview of the dust hybrid modes is given by Verheest [2000].

Chapter 5

Self-gravitation

In astrophysical plasmas which contain a considerable amount of dust, the intergravitational forces between the bulky dust grains can vie successfully with the electric forces acting upon the grains. A large dust cloud in equilibrium may in fact be destabilized through the growth of density perturbations, induced by the self-gravitational attraction forces among the dust particles.

As against in traditional plasmas, the self-gravitational forces are no longer negligible in dusty plasmas and necessitate a reiteration of the age-old problem of gravitational stability in astrophysical systems. For instance, this issue already emerged in the 18th century when Immanuel Kant (1775) and Pierre-Simon de Laplace (1796) posed the first serious theory of the origin of the solar system *i.e.* the nebular hypothesis. But most of the present achievements are greatly indebted to sir James Jeans, who in 1902 formulated the first instability criterion for self-gravitating systems [Jeans 1929]. Later on, several authors refined and extended the study of Jeans instabilities e.g. Chandrasekhar [1954], Nakano [1988], Gehman et al. [1996]. Jeans' analysis was performed for neutral particles only, but the foundations remain the same in the context of dusty plasmas [Avinash and Shukla 1994, Bliokh et al. 1995, Verheest et al. 1997].

Jeans streamlined the analysis radically by presuming the existence of a uniform equilibrium state. As a consequence, the problem is reduced to a small perturbations analysis so that conveniently harmonic waves can be used. The spectral decomposition of the wave equations produces a simple dispersion law containing a critical wavelength, which stipulates that large systems with dimensions exceeding this critical lengthscale will become gravitationally unstable. The aforementioned crucial lengthscale was coined the Jeans length, bearing appropriately the name of the pioneer in the physics of self-gravitating problems.

It is however necessary to advance circumspectly, when drawing conclusions from the small perturbation derivations. The premise of a uniform equilibrium state is not necessarily legitimate in that over larger distances self-gravitation inevitably causes the medium to become nonuniform. Therefore a self-gravitational system may be considered uniform only locally. One often assumes that the critical wavelengths are small compared to the scale lengths over which the system changes so that the perturbation analysis indeed can

be implemented as if the unperturbed configuration satisfies the equilibrium equations, an assumption often referred to rather curtly as the "Jeans swindle" [Spitzer 1978, Boss 1987, Čadež 1990, Vranješ and Čadež 1990]. If this simplifying hypothesis is not valid, the obtained instability criterion possibly allows unphysical solutions as the assumed equilibrium conditions do not satisfy the basic equations. By necessity, it must always be checked whether applying the Jeans swindle is justifiable, a requisite which is often being put on the back burner or even conveniently forgotten!

5.1 Comparison between electrostatic and gravitational forces

It is instructive to compare the magnitudes of the electrostatic and gravitational forces acting upon the dust grains. If we restrict the present forces on the dust grain to electrostatic (F_e) and gravitational forces (F_g), we can calculate the relative importance of these forces between two identical grains,

$$\frac{F_e}{F_g} = \frac{q_d^2}{4\pi\varepsilon_0 r^2}\left(\frac{Gm_d^2}{r^2}\right)^{-1} = \frac{1}{4\pi\varepsilon_0 G}\frac{q_d^2}{m_d^2} = \frac{\omega_{pd}^2}{\omega_{Jd}^2}, \tag{5.1}$$

here $\omega_{Jd}^2 = 4\pi G N_d m_d$ is the Jeans frequency for the dust species. If the capacitance model for the grain charge is used [Houpis and Whipple Jr. 1987] and the dust grain is assumed to be spherical and homogeneous, then the charge and mass of a grain can be expressed as a function of its size a, namely

$$q(a) = 4\pi\varepsilon_0 V_{d0} a \sim a, \tag{5.2}$$

$$m(a) = \frac{4}{3}\pi\rho_0 a^3 \sim a^3, \tag{5.3}$$

where ρ_0 is the mass density of the dust grain. This leads to

$$\frac{F_e}{F_g} = \frac{9\varepsilon_0}{4\pi G}\left(\frac{V_{d0}}{\rho_0 a^2}\right)^2, \tag{5.4}$$

meaning that the electrostatic and gravitational forces are balanced for grains with size

$$a^2 = \sqrt{\frac{9\varepsilon_0}{4\pi G}}\frac{V_{d0}}{\rho_0}. \tag{5.5}$$

For ice particles, the previous equation renders a size $a_{\text{balance}} = 0.018\sqrt{V_{d0}}$.

The equilibrium size can also be expressed in terms of the mass and density of the dust grain

$$\begin{aligned} &\omega_{pd}^2 = \omega_{Jd}^2 \\ &\Rightarrow m_d = \frac{eZ_d}{\sqrt{4\pi\varepsilon_0 G}} \\ &\Rightarrow a = \sqrt[3]{\frac{3m_d}{4\pi\rho_0}}\,. \end{aligned} \tag{5.6}$$

Applied again to ice particles, this gives $a_{\rm balance} \simeq 80 \cdot Z_d^{1/3}$ μm. We can conclude that for singly charged icy grains, the size for which self-gravitation and electric forces counterbalance each other is about 80 μm, for grains which have higher charges this size increases only with the cubic root of the charge.

5.2 Jeans instability and the infamous Jeans swindle

The traditional derivation of the Jeans instability starts from an infinite, homogeneous self-gravitating system which is in a static equilibrium. Yet this outset is flawed, indeed when implementing a constant pressure p_0, a constant density ρ_0 and a mean velocity $\mathbf{v}_0$ which is naught, the equation of motion (3.19) predicts that $\boldsymbol{\nabla}\phi_0 = 0$ but regrettably, this outcome is only reconcilable with Poisson's equation $\nabla^2\phi_0 = 4\pi G\rho_0$ if the mass density ρ_0 is zero. The Jeans swindle now consists of treating Poisson's equation to be valid for the perturbed quantities, while the unperturbed potential is *ad hoc* discarded. One can think of configurations where the Jeans swindle is justifiable [Binney and Tremaine 1987], but in general it may be sensible to look at the use of the Jeans swindle with Argus' eyes.

Having noted the intrinsic weaknesses of Jeans' approach, we can now sketch the physical mechanisms of the Jeans instability when assuming the Jeans swindle to be justifiable. In a neutral gas cloud, there are two antagonists, namely the gas pressure which tries to expand the cloud and the gravitational force which aims at a contraction of the cloud. The gravitational force in a region of radius R and per unit mass is

$$\mathbf{F}_{g1} \simeq -\frac{GM}{R^2}\mathbf{1}_r = -\frac{4}{3}\pi G\rho_0 R\,\mathbf{1}_r, \tag{5.7}$$

with $M = 4\pi\rho_0 R^3/3$ and the counteracting pressure force can be approximated as

$$\mathbf{F}_{p1} \simeq \frac{p_1}{\rho_0 R}\,\mathbf{1}_r = \frac{c_{sn}^2}{R}\,\mathbf{1}_r, \tag{5.8}$$

with the speed of sound defined as $c_{sn}^2 = k_B T_n/m_n$. The oppositely directed pressure forces and gravitational forces will balance each other for regions of radius

$$R_{\rm balance} \simeq \frac{\sqrt{3}c_{sn}}{\sqrt{4\pi G\rho_0}} = \frac{\sqrt{\langle v^2\rangle}}{\sqrt{4\pi G\rho_0}} = \frac{\sqrt{\langle v^2\rangle}}{\omega_J}, \tag{5.9}$$

when a Maxwellian velocity distribution is assumed and with $\langle v^2\rangle = \sqrt{3}c_{sn}$ the average of the squared velocities and ω_J the Jeans frequency. However for regions with dimensions larger than $R_{\rm balance}$, the gravitational forces will be on the upper hand and procure a collapse, the so called Jeans instability.

5.3 Basic state

In order to draw a comparison between the relevant scale lengths and the critical length-scale, we first study the basic, unperturbed state of a self-gravitational plasma in a rather

simple configuration [Verheest et al. 2000a]. We consider a massive plasma cloud of uniform composition, which can be treated as a perfect gas and which is large enough to supply significant self-gravitational forces. The plasma cloud is assumed isothermal, a nonuniform magnetic field $\mathbf{B}_0$ is present and the description further includes the possibility of a nonuniform plasma flow $\mathbf{U}_0$ along the field lines.

The basic state for the plasma can be taken stationary because we assume a sufficiently large electrical conductivity so that Ohmic dissipation and magnetic diffusivity have a negligible effect on the magnetic field, when considering time scales related to the dynamics of the perturbations.

We perform a 1-dimensional analysis in a Cartesian geometry where the z-axis is chosen along the direction of wave propagation and consequently the nabla operator becomes $\boldsymbol{\nabla} = \mathbf{e}_z \partial/\partial z$. On the other hand, the x-axis is chosen along the direction of the magnetic field and particle flow, which are both oriented perpendicularly to the gradients of physical quantities *i.e.* $\mathbf{B}_0 = B_0(z)\mathbf{e}_x$ and $\mathbf{U}_0 = U_0(z)\mathbf{e}_x$. By applying a Cartesian geometry, the correct nonlocal treatment can be restricted to one dimension only, because even in a 3-dimensional description it is impossible to devise a direction along which the medium may be assumed strictly uniform.

The plasma beta $\beta = p_{g0}/p_{m0}$, defined as the ratio of the thermal pressure and the magnetic pressure, is assumed to remain constant in each point of the plasma, which is a realistic assumption in highly conductive plasmas with frozen-in magnetic fields. Because the gas pressure $p_{g0} = R_g T_0 \rho_0$ evolves proportional to the magnetic pressure $p_{m0} = B_0^2/(2\mu_0)$ both the Alfvén speed V_A and the speed of sound c_s are constant,

$$V_A^2 = \frac{B_0^2}{\mu_0 \rho_0} = \text{const}, \tag{5.10}$$

$$c_s^2 = \gamma R_g T_0 = \text{const}. \tag{5.11}$$

Here ρ_0 represents the plasma mass density in the cloud and $R_g = R/M$ is the gas constant of the cloud, with R the universal gas constant and where M denotes the mean molar mass for the cloud. Further, the speed of sound c_s involves the ratio of the specific heats γ and T_0 represents the constant temperature. We have seen that the assumption of a constant β is reflected in a constant Alfvén speed, which implies that the magnetic field is assumed to be stronger in regions with higher densities and weaker in regions with lower densities.

The equations for the basic state now comprise the perfect gas law

$$p_{g0} = R_g \rho_0 T_0, \tag{5.12}$$

the equation of magnetohydrostatic balance

$$-\boldsymbol{\nabla} p_{g0} - \rho_0 \boldsymbol{\nabla} \psi_0 + \frac{1}{\mu_0} (\boldsymbol{\nabla} \times \mathbf{B}_0) \times \mathbf{B}_0 = 0, \tag{5.13}$$

which reduces to

$$\left(1 + \frac{1}{\beta}\right) \frac{dp_{g0}}{dz} = -\rho_0 \frac{d\psi_0}{dz}, \tag{5.14}$$

and the gravitational Poisson equation

$$\frac{d^2\psi_0}{dz^2} = 4\pi G\rho_0, \tag{5.15}$$

which includes the gravitational constant G and from which the gravitational potential ψ_0 can be calculated.

The equations (5.12)-(5.15) yield the following equation for ρ_0

$$\frac{d^2}{dz^2}\ln\rho_0 = -\frac{4\pi G\beta\gamma}{(1+\beta)c_s^2}\rho_0, \tag{5.16}$$

which has the general solution

$$\rho(z) = \frac{(1+\beta)c_s^2}{2\pi\gamma G\beta H^2}\,\mathrm{sech}^2\left(\frac{z+A}{H}\right), \tag{5.17}$$

with A and H constants of integration. If we associate $z = 0$ to the center of the cloud, the constant A accordingly becomes zero and the required solution can be written as

$$\rho_0 = \rho_{00}\mathrm{sech}^2\left(\frac{z}{H}\right), \tag{5.18}$$

wherein ρ_{00}, the equilibrium density measured in the center of the cloud, corresponds to the value of the other integration constant H unambiguously through

$$H^2 = \frac{1+\beta}{2\pi\gamma}\frac{c_s^2}{G\beta\rho_{00}}. \tag{5.19}$$

It follows that H is a lengthscale which quantifies the typical scale of non-uniformity of the basic state.

Using (5.18), the Poisson equation becomes

$$\begin{aligned}\frac{d^2\psi_0}{dz^2} &= 4\pi G\rho_{00}\mathrm{sech}^2\left(\frac{z}{H}\right)\\ &= \omega_{Jd0}^2\mathrm{sech}^2\left(\frac{z}{H}\right),\end{aligned} \tag{5.20}$$

where we have introduced the definition $\omega_{Jd0}^2 = 4\pi G\rho_{00}m_d$, which serves as a local equivalent of the Jeans frequency, measured at $z = 0$. Equation (5.20) can be integrated in order to obtain

$$\frac{d\psi_0}{dz} = \omega_{Jd0}^2 H\tanh\left(\frac{z}{H}\right), \tag{5.21}$$

where the integration constant is zero due to equations (5.14), (5.18) and (5.19).

Since our model started from $\beta \sim \rho_0/B_0^2$ constant, it is evident that

$$B_0 = B_{00}\mathrm{sech}\left(\frac{z}{H}\right), \tag{5.22}$$

where the constant

$$B_{00} = \sqrt{\frac{2\mu_0}{\beta\gamma}c_s^2\rho_{00}} \tag{5.23}$$

stands for the magnitude of the magnetic field at the center of the cloud.

5.4 Linear perturbations

Having obtained the equilibrium values, we move on and perturb the above described basic state in a 1-dimensional configuration. All the amplitudes of the linearly perturbed quantities are z-dependent only and are governed by the standard set of MHD equations together with the gravitational Poisson equation. This linearization procedure leads to the following set of equations for the perturbed quantities,

$$\frac{\partial \rho}{\partial t} + \boldsymbol{\nabla} \cdot (\rho_0 \mathbf{v}) + \boldsymbol{\nabla} \cdot (\rho \mathbf{U}_0) = 0, \tag{5.24}$$

$$\rho_0 \frac{\partial \mathbf{v}}{\partial t} + \rho_0 \mathbf{v} \cdot \boldsymbol{\nabla} \mathbf{U}_0 + \rho_0 \mathbf{U}_0 \cdot \boldsymbol{\nabla} \mathbf{v} = -\boldsymbol{\nabla} p - \rho \boldsymbol{\nabla} \psi_0 - \rho_0 \boldsymbol{\nabla} \psi + \frac{1}{\mu_0} (\boldsymbol{\nabla} \times \mathbf{B}_0) \times \mathbf{B} + \frac{1}{\mu_0} (\boldsymbol{\nabla} \times \mathbf{B}) \times \mathbf{B}_0, \tag{5.25}$$

$$\frac{\partial \mathbf{B}}{\partial t} = \boldsymbol{\nabla} \times (\mathbf{v} \times \mathbf{B}_0) + \boldsymbol{\nabla} \times (\mathbf{U}_0 \times \mathbf{B}), \tag{5.26}$$

$$\nabla^2 \psi = 4\pi G \rho, \tag{5.27}$$

$$\frac{\partial p}{dt} + \mathbf{U}_0 \cdot \boldsymbol{\nabla} p + \mathbf{v} \cdot \boldsymbol{\nabla} p_0 = c_s^2 \left(\frac{\partial \rho}{\partial t} + \mathbf{U}_0 \cdot \boldsymbol{\nabla} \rho + \mathbf{v} \cdot \boldsymbol{\nabla} \rho_0 \right), \tag{5.28}$$

where the last equation expresses the adiabaticity of the perturbations *i.e.* the entropy is conserved because energy dissipation is absent and because a magnetohydrodynamical description implies that the involved macroscopic processes are sufficiently slow.

Fourier transforming the previous set of equations and introducing the total pressure perturbation function $P = p + v_A^2 \rho_0 b_x$ and the new variable $\eta = \rho_0 \xi$, with ξ the Lagrangian displacement in the z-direction ($v_z = -i\omega\xi$) leads to

$$\rho_0 v_x + \eta \frac{dU_0}{dz} = 0, \tag{5.29}$$

$$\frac{d\psi_0}{dz} \frac{d\eta}{dz} + \omega^2 \eta = \frac{dP}{dz} + \rho_0 \frac{d\psi}{dz}, \tag{5.30}$$

$$V_{ms}^2 \frac{d\eta}{dz} = \eta \left[\frac{d \ln \rho_0}{dz} \left(\frac{V_A^2}{2} + \frac{\gamma - 1}{\gamma} c_s^2 \right) \right] - P, \tag{5.31}$$

$$\frac{d^2 \psi}{dz^2} = -4\pi G \frac{d\eta}{dz}, \tag{5.32}$$

where the magnetosonic velocity $V_{ms}^2 = V_A^2 + c_s^2$ is introduced. The last equation can be integrated and with the boundary condition

$$\left. \frac{d\psi}{dz} \right|_{\eta=0} = 0, \tag{5.33}$$

the integration yields

$$\frac{d\psi}{dz} = -4\pi G \eta. \tag{5.34}$$

From the Poisson equation (5.15), we can also obtain

$$\frac{d\psi_0}{dz} = \omega_{Jd0}^2 H \tanh(\frac{z}{H}), \tag{5.35}$$

and thus, up to an arbitrary constant

$$\psi_0 = \omega_{Jd0}^2 H^2 \ln \operatorname{sech}(\frac{z}{H}). \tag{5.36}$$

Finally from equations (5.30) and (5.31), we obtain by eliminating the total pressure perturbation function P the equation

$$\frac{d^2}{dZ^2}(\eta \cosh Z) - \left(\mathcal{N} - \frac{2}{\cosh^2 Z}\right) \eta \cosh Z = 0, \tag{5.37}$$

where $Z = z/H$ and

$$\mathcal{N} = 1 - \frac{\omega^2 H^2}{V_{ms}^2}. \tag{5.38}$$

When using (5.18), the previous equation can be written in the variable $\xi = \eta/\rho_0$ and becomes

$$\frac{d^2}{dZ^2}[\xi \operatorname{sech}(Z)] - \left(\mathcal{N} - 2\operatorname{sech}^2 Z\right) \xi \operatorname{sech}(Z) = 0, \tag{5.39}$$

5.5 Stability analysis

The analysis will only be performed for positive Z, as the solutions of (5.39) will be either symmetric or antisymmetric and it follows that a distinct stability analysis for the positive and negative real parts of the axis is not necessary. Further on in the analysis, it will prove to be convenient to change the dependent variable so that the first derivative vanishes and this can be done (Appendix A) by making a substitution $\xi(Z) = \zeta(Z)\cosh(Z)$. Upon this substitution equation (5.39) becomes

$$\frac{d^2\zeta(Z)}{dZ^2} + \left[1 + \frac{\omega^2 H^2}{V_{ms}^2} - 2\tanh^2(Z)\right] \zeta(Z) = 0, \tag{5.40}$$

where $\zeta(Z)$ evidently has the same roots as $\xi(Z)$, since the cosh-function is nowhere zero. For frequencies $\omega > V_{ms}/H$, we can now use Sturms theorems (Appendix A) to compare the solutions of equation (5.40) and the solutions of

$$\frac{d^2\zeta(Z)}{dZ^2} + \left(\frac{\omega^2 H^2}{V_{ms}^2} - 1\right) \zeta(Z) = 0. \tag{5.41}$$

Equation (5.41) has constant coefficients hence its solutions are quickly calculated as

$$\zeta\left(\frac{z}{H}\right) = \xi\left(\frac{z}{H}\right) \operatorname{sech}\left(\frac{z}{H}\right) = C_1 \cos(kz) + C_2 \sin(kz), \tag{5.42}$$

with C_1, C_2 arbitrary constants and

$$k^2 = \frac{\omega^2}{V_{ms}^2} - \frac{1}{H^2}. \tag{5.43}$$

We can easily deduct from (5.42) that the roots of solutions $\zeta(Z)$ are located at a distance

$$\frac{\pi V_{ms}}{\sqrt{\omega^2 H^2 - V_{ms}^2}} \tag{5.44}$$

from each other. Furthermore, it is obvious that

$$1 + \frac{\omega^2 H^2}{V_{ms}^2} - 2\tanh^2(Z) > \frac{\omega^2 H^2}{V_{ms}^2} - 1. \tag{5.45}$$

Hence for frequencies $\omega > V_{ms}/H$, Sturm's comparison theorem predicts that in each interval of length

$$\frac{\pi V_{ms}}{\sqrt{\omega^2 H^2 - V_{ms}^2}} \tag{5.46}$$

there is at least one root of every non-trivial solution of (5.40). In other words, the distance between two roots of solutions $\zeta(Z)$ cannot be larger than the length of the aforementioned interval. We can conclude that for frequencies above the cut-off frequency *viz.* $\omega > V_{ms}/H$, the solutions for $\zeta(Z)$ and thus also the solutions of $\xi(Z)$ display an oscillating behaviour. For large Z, the solutions of (5.39) will practically coincide with the solutions (5.42) and thus correspond to a dispersion law

$$\omega^2 = k^2 V_{ms}^2 + \frac{V_{ms}^2}{H^2}. \tag{5.47}$$

Equation (5.39) can also be transformed into its self-adjoint form (see Appendix A)

$$\frac{d}{dZ}\left[\operatorname{sech}^2(Z)\frac{d\xi}{dZ}\right] + \frac{\omega^2 H^2}{V_{ms}^2}\xi \operatorname{sech}^2(Z) = 0. \tag{5.48}$$

Applying the theorem of Sonin-Polya, it follows that the absolute values of the relative extrema of each non-trivial solution $\xi(Z)$ of the differential equation form a non-decreasing row. Because we have just seen that a non-trivial solution $\xi(Z)$ has an oscillatory behaviour, non-trivial solutions either diverge or oscillate between constant envelopes, as illustrated in figure 5.1 and figure 5.2, respectively.

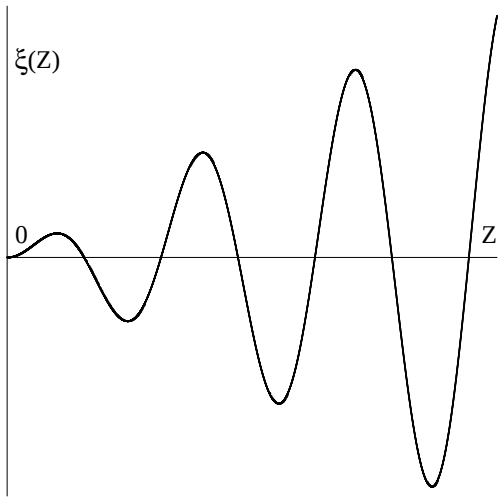

Fig 5.1: Divergent solution

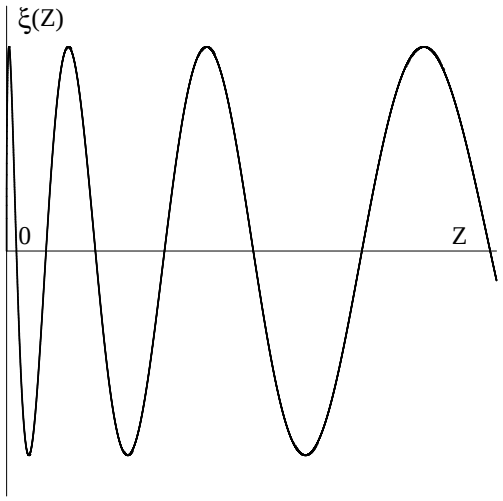

Fig. 5.2: Constant envelopes

Looking at the asymptotic solutions for $\xi(Z)$ at large Z, namely

$$\xi(Z) = \xi\left(\frac{z}{H}\right) = \cosh\left(\frac{z}{H}\right)[C_1 \sin(kz) + C_2 \cos(kz)], \tag{5.49}$$

where k is given by (5.43), we deduce that all non-trivial solutions $\xi(Z)$ are divergent. On the other hand, for frequencies $0 \leqslant \omega \leqslant V_{ms}/H$, the coefficient of the lowest order term in equation (5.40), *viz.*

$$1 + \frac{\omega^2 H^2}{V_{ms}^2} - 2\tanh^2(Z), \tag{5.50}$$

will be negative for sufficiently large arguments $Z > Z_{\max}$. Now Sturm's Comparison theorem implies that there is at most one root for $\xi(Z)$ in the interval $[Z_{\max}, \infty]$, meaning that the behaviour for large Z is non-oscillatory and allows for stable solutions. Indeed, for $0 < \omega < V_{ms}/H$ the asymptotic behaviour of the solutions on the positive axis now displays an evanescent character

$$\xi\left(\frac{z}{H}\right) \sim \exp\left(-\sqrt{\frac{1}{H^2} - \frac{\omega^2}{V_{ms}^2}}\, z\right) \cosh\left(\frac{z}{H}\right). \tag{5.51}$$

Finally, for a zero frequency and also for the cutoff frequency, the solutions of equation (5.39) can be calculated explicitly. For these values of the frequency, the solutions $\eta(Z)$ can be given in terms of the associated Legendre functions. Accordingly for a zero frequency, which relates to $\mathcal{N} = 1$, the solution for $\xi(Z)$ becomes

$$\xi(Z) = \left.\frac{d\xi(Z)}{dZ}\right|_{Z=0} \cdot \frac{\sinh(2Z) + 2Z}{4}, \tag{5.52}$$

because the displacement at the center of the cloud is zero ($\xi(0) = 0$). The cutoff frequency V_{ms}/H corresponds to $\mathcal{N} = 0$ and the solution for $\xi(Z)$ becomes accordingly

$$\xi(Z) = \left.\frac{d\xi(Z)}{dZ}\right|_{Z=0} \cdot \sinh(Z). \tag{5.53}$$

As we had learned from the theorems of Sturm already, these solutions are non-oscillatory, but for these specific cases the solutions are diverging.

We emphasize that we did not work in a (ω, k) phase space but in a (ω, Z)-space, so that instabilities occur when real frequencies lead to infinite displacement amplitudes.

5.6 Uniform basic state

In order to pinpoint the susceptibility for errors ensuing from the Jeans swindle, the standard derivation for the Jeans instability criterium is repeated. The standard approach makes use of the assumption of a uniform, static fluid so that

$$\frac{d\phi_0}{dz} = \frac{d\rho_0}{dz} = \frac{dB_0}{dz} = \frac{dU_0}{dz} = 0. \tag{5.54}$$

Since the aforementioned gradients vanish, the equations (5.30)-(5.32) simplify to the set

$$\begin{aligned} \frac{dP}{dz} &= \omega^2\eta - \rho_0\frac{d\psi}{dz}, \\ V_{ms}^2\frac{d\eta}{dz} &= -P, \\ \frac{d^2\psi}{dz^2} &= -4\pi G\frac{d\eta}{dz}, \end{aligned} \tag{5.55}$$

which yields the acquainted dispersion law

$$\omega^2 = k^2V_{ms}^2 - 4\pi G\rho_0. \tag{5.56}$$

In situations where one can vindicate the Jeans swindle, this dispersion law reveals that an instability occurs for wavenumbers smaller than a critical wavenumber k_{cr}. Indeed for $k < k_{cr} = \omega_{Jd}/V_{ms}$, there are two solutions for ω, one of them having a positive imaginary part. Accordingly, a dust cloud can believed to be subject to a gravitational collapse if its diameter exceeds $2\pi V_{ms}/\omega_{Jd}$ or if the total mass exceeds the Jeans mass M_J, usually defined as

$$M_J = \left(\frac{2\pi}{k_{cr}}\right)^3\rho_0 = \left(\frac{\pi V_{ms}^2}{G}\right)^{3/2}\frac{1}{\sqrt{\rho_0}}\,.$$

Applying the Jeans swindle boils down to considering a local, homogeneous region of the system which is considered to be inhomogeneous only on much larger scales. To check whether this is true, the obtained Jeans length, here denoted as L_J with

$$L_J^2 = \frac{\pi V_{ms}^2}{G\rho_0}, \tag{5.57}$$

must be compared with the lengthscale H,

$$\frac{L_J^2}{H^2} = 2\pi^2 \frac{2+\beta\gamma}{1+\beta} > 1, \tag{5.58}$$

from which we infer that the medium cannot be considered uniform over a Jeans length, a conclusion contravening regrettably the presupposition of a local, uniform state! However, we note that the parameters L_J and H are of the same order, which accounts for the usefulness of an approach that calls upon the Jeans swindle, because the obtained Jeans length determines to what extent a self-gravitating medium with certain dimensions can be considered uniform.

5.7 Summary

In this chapter, we have treated a self-gravitating cloud in a one-dimensional model without invoking the Jeans swindle in order to test the reliability of the classical analysis. On larger lengthscales, a self-gravitating cloud in magnetohydrostatic equilibrium is inevitably inhomogeneous and one obtains a typical lengthscale H that characterizes the typical inhomogeneity lengthscale of the cloud. For perturbations with wavelengths comparable to this inhomogeneity lengthscale H, the stationary density variations necessarily have to be included. If the density inhomogeneities are effectively included, linear waves which would induce a gravitational collapse according to the classical instability criterion, are actually stable.

For the remaining chapters, this causes us to be in two minds about the treatment of the Jeans instability treatment. The treatments in our work and generally those in literature that deal with the Jeans instability mostly presume a uniform basic state and whereas this simplifying assumption proves to be a powerful mathematical instrument, it possesses an Achilles heel, being the Jeans swindle. However, a more exact treatment like the one given in this chapter is not available for multispecies plasmas nor in a more-dimensional model. Nevertheless, while the fruition of a soundly underpinned theory for the study of self-gravitating systems is delayed, applying the Jeans swindle for the examination of self-gravitating systems is often valuable. In case when the acquired instability criterion must be discarded, the instability analysis is not at all futile but the chief virtue of such an approach will then rather shift to the determination of the inhomogeneity length scales of a system. After all, the Jeans length as obtained from the classic Jeans instability criterion is a reliable measure for the scales of non-uniformity of the considered self-gravitating medium.

Chapter 6

Self-gravitation and size distributions

In astrophysical dusty plasmas the dust grains exhibit an abundance of possible sizes and masses. Consequently, the inclusion of a size distribution in any dusty plasma model will deliver more realistic results than a mono-sized dust description and certainly merits a closer look. The size of a dust grain determines the importance of self-gravitational forces on the grain. Whereas grains with radii of the order of microns are still mainly influenced by electric forces, the contribution of self-gravitational forces increases with size and is even dominant for the heavy grains in the size spectrum. Evidently the self-gravitational effects are closely interwoven with the distribution spectrum of the dust sizes, therefore the stability study of self-gravitating plasmas is immediately associated with an investigation of the influences of size distributions.

In this chapter we investigate the influence of self-gravitation and size distributions on waves propagating parallel to the external magnetic field. As mentioned before, the modifications due to the inclusion of self-gravitational forces for parallel waves is strictly limited to the longitudinal modes and consequently only these electrostatic modes are described. We opted for the clear and simple framework of a fluid theory in order to scout the physical mechanisms of self-gravitation orderly. Later on, in chapter 8, the fine tuning lost due to the fluid description is recovered using a kinetic description.

Here, and in all following chapters, issues regarding the validity of the Jeans swindle are given the go-by, the small perturbation analysis is valuable no matter how, if only for the information it provides with respect to the inhomogeneity lengths.

The inclusion of multiple dust species into the description is introduced progressively. We will start with a discrete distribution, dealing only with two dust species. Next, multiple species are included but with some simplifications, namely on the one hand we describe a distribution of cold but charged dust species and on the other hand we recall the distribution of warm but neutral dust species. Afterwards, the more general configuration consisting of multiple warm and charged dust species is tackled. Finally, as an additional application we make a full analysis of a model that depicts two counterstreaming dust

beams. The inclusion of streaming effects engenders the possibility of Jeans-Buneman instabilities [Meuris et al. 1997, Pillay et al. 2000] and we carefully examine the different parameter ranges.

6.1 Distribution functions

The size distribution of dust grains is governed by the formation, growth and destruction processes. These mechanisms are continuously active but are often assumed to be in a dynamic equilibrium. That is, in the life cycle of an individual grain many events can continuously be responsible for breaking up or enlarging the grain, but as the size distribution includes all the present dust grains, the size distribution is some sort of an average and can be considered as being time-independent. However, the treatment of such a variety of dust grains, charged or not, is still very incomplete because of the complexities involved. In the absence of fully self-consistent kinetic theories, we will here adopt a poor man's approach and represent charged dust by a limited number of species in a continuous range.

For some applications however, a continuous model is more realistic than a discrete model. In that case, it is recommended to use a kinetic framework, because a continuous distribution inevitably contains singularities. Such a continuous distribution is treated in chapter 8, where a kinetic model is used in order to retrieve the information lost due to the use of a fluid description.

When dust particles are present in an almost continuous size range, the characterization of the size spectrum can be dealt with through distribution functions. For many astrophysical applications, observations justify the use of a power law distribution [Rosenberg 1993] for charged dust grains in a given range of possible particle sizes. The differential density distribution is then

$$n(a)da = Ka^{-\beta}da \qquad \text{with } a \in [a_{min}, a_{max}], \tag{6.1}$$

where a is the dust grain radius and a_{max} and a_{min} set the maximum respectively minimum grain size. Values of β are documented for several environments and I recall primarily those listed by Meuris [1998]: for the F-ring of Saturn $\beta = 4.6$ [Showalter and Cuzzi 1993] and for the G-ring values of $\beta = 7$, $\beta = 6$ and smaller were obtained [Gurnett et al. 1983, Showalter et al. 1992, Meyer-Vernet et al. 1996]. A value of $\beta = 3.5$ is often found to agree with observations [Mathis et al. 1977, Whittet 1992, Weingartner and Draine 2001]. On the other hand, in cometary environments, a value of $\beta = 3.4$ is observed [McDonnell et al. 1987, McDonnell et al. 1992].

But for dusty plasma experiments the dust sizes often follow a normal distribution [Meuris 1998]

$$n(a)da = \frac{N_{tot}}{\sqrt{\pi}\,\sigma\,\mathrm{erf}(\varepsilon/\sigma)} \exp\left[\frac{(a-\overline{a})^2}{\sigma^2}\right] da, \tag{6.2}$$

where $\overline{a}$ is the average radius, $\varepsilon = (a_{max} - a_{min})/2$ is the center of the size interval and σ stands for the width of the distribution. It is assumed that $\varepsilon/\sigma > 2$ so that $\mathrm{erf}(\varepsilon/\sigma) \simeq 1$.

Of course, more complicated models are also possible, one can think of several intervals of size ranges where some have discrete distributions and others a continuous one.

6.2 Dispersion law

For the study of wave mode modifications due to gravitational effects and the study of gravitational stability, the significant frequencies are those low enough to allow the heavy dust grains to respond to the perturbations and for these low frequencies the electrons and ions can be considered as being effectively Boltzmann distributed. Without self-gravitation, this approach is emblematic of working in the regime of the celebrated dust-acoustic mode, higher frequencies *e.g.* the dust-ion acoustic mode are hardly affected by self-gravitation. Additionally, I suppose that the wavelengths are large enough so that $k^2\lambda_D^2 \ll 1$, this assumption can be justified a posteriori as the wavelengths will prove to be of the order of the Jeans lengths. Using the above approximations, the dispersion law (4.1) simplifies to

$$\left(\frac{1}{k^2\lambda_D^2} - \sum_d \frac{\omega_{pd}^2}{\mathcal{L}_d}\right)\left(1 + \sum_d \frac{\omega_{Jd}^2}{\mathcal{L}_d}\right) + \left(\sum_d \frac{\omega_{pd}\omega_{Jd}}{\mathcal{L}_d}\right)^2 = 0, \tag{6.3}$$

with $\mathcal{L}_d = \omega^2 - k^2 c_{sd}^2$ and where the summations now are restricted to the dust components. When streaming effects are included, the dispersion law (6.3) has the same form, but with $\mathcal{L}_d = (\omega - kU_d)^2 - k^2 c_{sd}^2$ [Bliokh et al. 1995, Bliokh and Yaroshenko 1996, Meuris et al. 1997], all different dust species experience a different, Doppler shifted, frequency. As mentioned before, the electron and ion contributions are retained only via a global plasma Debye length λ_D, defined through

$$\frac{1}{\lambda_D^2} = \frac{1}{\lambda_{De}^2} + \frac{1}{\lambda_{Di}^2} = \frac{\omega_{pe}^2}{c_{se}^2} + \frac{\omega_{pi}^2}{c_{si}^2}. \tag{6.4}$$

For later convenience, I note that equation (6.3) can be rewritten as

$$1 + \sum_d \frac{\omega_{Jd}^2 - k^2\lambda_D^2\omega_{pd}^2}{\mathcal{L}_d} - \frac{k^2\lambda_D^2}{2}\sum_d\sum_{d'} \frac{(\omega_{pd}\omega_{Jd'} - \omega_{pd'}\omega_{Jd})^2}{\mathcal{L}_d\mathcal{L}_{d'}} = 0, \tag{6.5}$$

where in the summations d and d' have been used as dummy indices. This is a polynomial with leading terms

$$\omega^{2N} + \sum_d \left[\omega_{Jd}^2 - k^2(\lambda_D^2\omega_{pd}^2 + c_{sd}^2)\right]\omega^{2N-2} + \ldots = 0, \tag{6.6}$$

where N is the number of dust species. The last term in equation (6.5) clearly represents the modifications due to the presence of different dust species with distinct characteristics and can only vanish when all dust particles have the same charge-to-mass ratio or, equivalently, have the same proportionality between plasma and Jeans frequencies $\omega_{pd}/\omega_{Jd} = \omega_{pd'}/\omega_{Jd'}$.

The dispersion law, written as (6.5), now allows for a systematical approach to study the influence of size distributions on the gravitational stability of sizeable dusty plasmas. First, the dispersion law for a monodisperse dusty plasma is recalled.

6.3 Monodisperse dust description

For a single, neutral dust species and without considering streaming, we recover naturally the classic Jeans instability criterion

$$\omega^2 = k^2 c_{snd}^2 - \omega_{Jnd}^2, \tag{6.7}$$

where the index n has been added to emphasize the neutrality of the dust species under consideration. On the other hand, if we consider a single but charged dust species then equation (6.5) produces a slight adaption of the dispersion law, which becomes

$$\omega^2 = k^2(c_{da}^2 + c_{sd}^2) - \omega_{Jd}^2, \tag{6.8}$$

setting the critical Jeans length to

$$k_{cr}^2 = \frac{\omega_{Jd}^2}{c_{da}^2 + c_{sd}^2}. \tag{6.9}$$

The dust-acoustic mode is recovered if, in addition to ignoring the dust thermal speed, self-gravitational effects are excluded.

We can label equation (6.8) as the archetypal dispersion law for "Jeans" modes in dusty plasmas with a single charged dust component and will encounter this or similar equations frequently. Having outlined the description for a monodisperse dusty plasma, we can now work progressively towards the analysis of a polydisperse dusty plasma and do this by first considering a dusty plasma consisting of two different, charged dust species.

6.4 Two charged dust species

Note that the complexity of the dispersion law (6.5) rapidly increases with the number of dust species, as it is a polynomial of degree N in ω^2, where N is the number of dust species considered. Dealing with only two charged dust species, the modifications due to this most simple configuration of dust mass distributions can be tackled straightforward and in their full generality. For a plasma with only two charged dust components, the dispersion law becomes a biquadratic in ω *viz.*

$$\begin{aligned}&\left[\omega^2 - k^2(c_{sd1}^2 + c_{da1}^2) + \omega_{Jd1}^2\right]\left[\omega^2 - k^2(c_{sd2}^2 + c_{da2}^2) + \omega_{Jd2}^2\right]\\ &= (\omega_{Jd1}\omega_{Jd2} - k^2 c_{da1} c_{da2})^2,\end{aligned} \tag{6.10}$$

revealing the manifest coupling between the two Jeans dust modes, each of which would obey the typical Jeans law (6.8) on its own. In the latter equation a separate dust-acoustic velocity $c_{da\alpha} = \lambda_D \omega_{pd\alpha}$ per dust species α is introduced for notational convenience.

Both roots (in ω^2) of equation (6.10) are real because the discriminant Δ of the bi-quadratic equation is always positive,

$$\begin{aligned}\Delta &= \left(\omega_{Jd1}^2 - \omega_{Jd2}^2 - k^2 c_{da1}^2 - k^2 c_{sd1}^2 + k^2 c_{da2}^2 + k^2 c_{sd2}^2\right)^2 \\ &\quad + 4(\omega_{Jd1}\omega_{Jd2} - k^2 c_{da1}c_{da2})^2 > 0. \end{aligned} \tag{6.11}$$

There is at least one positive root, corresponding to a stable mode. The other root has the same sign as the constant term in (6.10), which represents the product of both real roots. For an instability to occur, this product has to be negative, which can always come about in the event of small enough wavenumbers $k < k_{cr}$, with the critical wavenumber k_{cr} being defined as

$$\begin{aligned} k_{cr}^2 &= \frac{\omega_{Jd1}^2 c_{sd2}^2 + \omega_{Jd2}^2 c_{sd1}^2 + (\omega_{Jd1}c_{da2} - \omega_{Jd2}c_{da1})^2}{c_{sd1}^2 c_{da2}^2 + c_{sd2}^2 c_{da1}^2 + c_{sd1}^2 c_{sd2}^2} \\ &\simeq \frac{(\omega_{Jd1}c_{da2} - \omega_{Jd2}c_{da1})^2}{c_{sd1}^2 c_{da2}^2 + c_{sd2}^2 c_{da1}^2}. \end{aligned} \tag{6.12}$$

The approximate form of k_{cr} stems from the safe assumption of the pure plasma pressures being much larger than the dust pressures, so that for the dust species $c_{sd\alpha} \ll c_{da\alpha}$. Incidentally, the approximate form is not valid in the special case of the two dust species having the same charge-to-mass ratio. As mentioned before, the latter possibility would drastically simplify the dispersion law (6.5) to

$$1 + \sum_d \frac{\omega_{Jd}^2 - k^2\lambda_D^2\omega_{pd}^2}{\omega^2 - k^2 c_{sd}^2} = 0, \tag{6.13}$$

the discussion of which mimics that of a neutral dust cloud [Bliokh et al. 1995], a configuration that will be discussed further on.

If one of the species, *e.g.* the second, is almost cold ($c_{sd2} \to 0$), then (6.12) reduces to

$$k_{cr}^2 = \frac{\omega_{Jd1}^2}{c_{sd1}^2}\left(1 - \frac{q_1 m_2}{q_2 m_1}\right)^2. \tag{6.14}$$

When this cooler species is also the more massive one, then $|q_1 m_2/q_2 m_1| \gg 1$ if we follow the standard, primary charging model [Mendis and Rosenberg 1994, Meuris et al. 1997]. The primary charging model assumes for the charges of the dust grains $q_\alpha \propto a_\alpha$ and for their masses $m_\alpha \propto a_\alpha^3$ with a_α the size of the corresponding dust grain species, all being immersed in the same plasma. A further simplification is now possible and leads to

$$k_{cr}^2 = \frac{\omega_{Jd1}^2 q_1^2 m_2^2}{c_{sd1}^2 q_2^2 m_1^2} \gg \frac{\omega_{Jd1}^2}{c_{sd1}^2}, \tag{6.15}$$

showing that dusty plasmas containing solely charged dust grains are stable on much larger lengthscales than comparable dust clouds with only neutral particles. Summarizing, a rigorous treatment of a dusty plasma with two charged dust species leads to a dispersion law that exemplarily displays the mode coupling between the two Jeans dust modes. Moreover, just as for the monodisperse case, the criterion for gravitational instability is easily recovered, it suffices to set ω^2 equal to zero in order to obtain the critical Jeans wavenumber, a wavenumber that signifies a lower limit for stable wavenumbers.

6.5 Polydisperse, but cold dust species

Dealing with more than two dust species is not much of an obstacle when dealing with only cold dust species, the dispersion law (4.1) remains a biquadratic, independently of the number of dust species [Meuris et al. 1997],

$$\omega^4 + \left(\sum_d \omega_{Jd}^2 - k^2 \lambda_D^2 \sum_d \omega_{pd}^2 \right) \omega^2 - \frac{k^2 \lambda_D^2}{2} \sum_d \sum_{d'} (\omega_{pd} \omega_{Jd'} - \omega_{pd'} \omega_{Jd})^2 = 0. \quad (6.16)$$

or equivalently

$$\left(\omega^2 - k^2 \lambda_D^2 \sum_d \omega_{pd}^2 \right) \left(\omega^2 + \sum_d \omega_{Jd}^2 \right) + \left(\sum_d k \lambda_D \omega_{pd} \omega_{Jd} \right)^2 = 0, \quad (6.17)$$

and the discriminant Δ now becomes

$$\begin{aligned} \Delta &= \left(\sum_d \omega_{Jd}^2 + k^2 \lambda_D^2 \sum_d \omega_{pd}^2 \right)^2 - 4 k^2 \lambda_D^2 \left(\sum_d \omega_{pd} \omega_{Jd} \right)^2 \\ &= \left[\sum_d \left(k \lambda_D \omega_{pd} - \omega_{Jd} \right)^2 \right] \cdot \left[\sum_d \left(k \lambda_D \omega_{pd} + \omega_{Jd} \right)^2 \right] > 0. \end{aligned} \quad (6.18)$$

Again, the discriminant is positive but now the product of both (real) roots will be always negative, independent of the wave number. This results in one positive and one negative real root, so that the presence of the negative root implies an inevitable gravitational instability. We can conclude that without dust pressure a gravitational collapse in a polydisperse dusty plasma is certain, as there is an unstable mode at all possible wavenumbers.

6.6 Multiple neutral dust species

Before dealing with multiple warm, charged dust species, it is useful to consider a polydisperse description of neutral dust species. Naturally, electrostatic effects are absent and the dispersion law reduces to

$$\sum_n \frac{\omega_{Jn}^2}{\omega^2 - k^2 c_{sn}^2} = -1. \quad (6.19)$$

The stability analysis of this multicomponent system shows that there is at most one aperiodic instability that can develop and this instability occurs if [Fridman and Polyachenko 1984]

$$\sum_n \frac{\omega_{Jn}^2}{k^2 c_{sn}^2} > 1, \quad (6.20)$$

obtained by setting $\omega^2 = 0$ in (6.19). Besides the instability, all the other collective modes are combined sound oscillations. This can be well illustrated graphically [Fridman and

Polyachenko 1984]. If we denote the left hand side of equation (6.19) as $f(\omega^2)$, the roots of the dispersion relation (6.19) correspond to the intersecting points of $f(\omega^2)$ and the constant function with value -1. The dispersion law can have only one negative real root and this occurs for configurations where the branch of the dispersion law situated utmost to the left runs as the red curve (fig 6.1). This situation will occur for parameters which obey (6.20), as it is the value of $f(0)$ relative to -1 that predicts whether the cloud is stable or not. The asymptotes of figure 6.1 correspond with the frequency values $\omega^2 = k^2 c_{si}^2$.

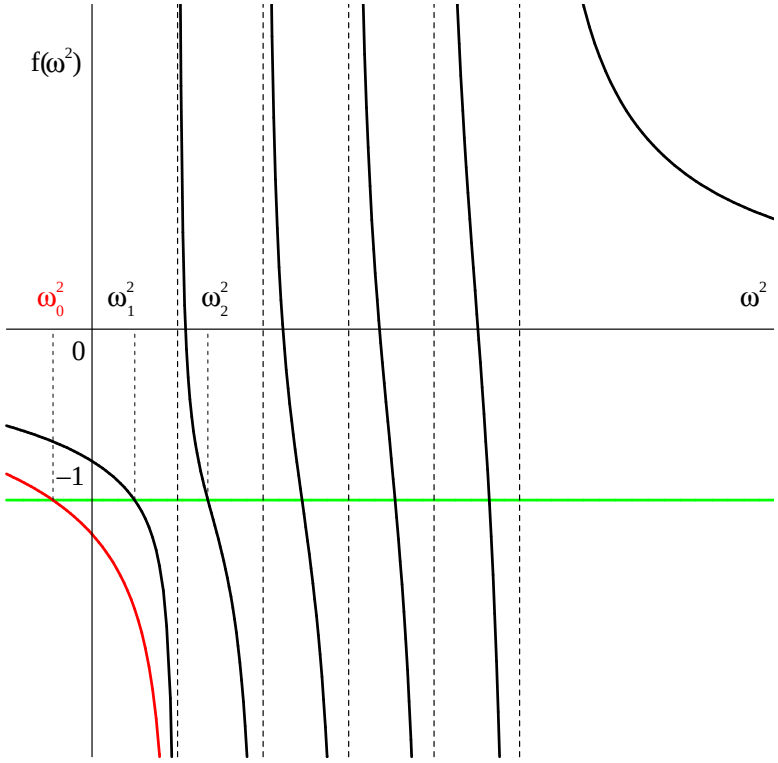

Fig 6.1: multiple neutral species

We can conclude that for a completely neutral description too, the criterion for a Jeans instability to occur can be obtained by simply setting ω equal to zero in the dispersion law.

6.7 Multiple warm, charged dust species

Reverting now to warm but charged dust species, I am primarily interested in finding possible Jeans lengths which give the transition from stable to unstable modes. A thorough analytical investigation of all wave modes tied up with the full dispersion law would not be very informative because of the dramatically long expressions, tangling up the underlying physics of the coupled wave modes. Because of this inherent complexity, it is much more

clarifying to aim immediately for the critical lengths, keeping clear of a detailed wave mode analysis. The simpler cases point out that the onset of the gravitational instability occurs for the value of the wavenumber that renders the constant term zero, in other words the critical wavenumber $k = k_{cr}$ is reached when ω^2 goes through zero. It is then easy to set a lower limit for the unstable wavenumbers in this polydisperse description, as (6.3) is a polynomial in ω^2 with real coefficients.

In effect, this lower limit can be calculated by putting $\omega = 0$ in the dispersion relation, the accompanying wavenumber k_{cr} is then the lower limit for the critical Jeans length we are looking for. Indeed, there will be at least one imaginary root for wavenumbers $k < k_{cr}$ because the (real) constant term changes sign at k_{cr}. We so obtain the expression for k_{cr}

$$\left(1+\sum_{\alpha}\frac{\omega_{p\alpha}^2}{k_{cr}^2c_{s\alpha}^2}\right)\left(1-\sum_{\alpha}\frac{\omega_{J\alpha}^2}{k_{cr}^2c_{s\alpha}^2}\right)+\left(\sum_{\alpha}\frac{\omega_{p\alpha}\omega_{J\alpha}}{k_{cr}^2c_{s\alpha}^2}\right)^2=0, \tag{6.21}$$

and this can be rewritten as

$$1+\sum_{\alpha}\frac{\omega_{p\alpha}^2-\omega_{J\alpha}^2}{k_{cr}^2c_{s\alpha}^2}-\frac{1}{2}\sum_{\alpha}\sum_{\beta}\frac{(\omega_{p\alpha}\omega_{J\beta}-\omega_{p\beta}\omega_{J\alpha})^2}{k_{cr}^4c_{s\alpha}^2c_{s\beta}^2}=0. \tag{6.22}$$

Since

$$(\omega_{p\alpha}\omega_{J\beta}-\omega_{p\beta}\omega_{J\alpha})^2=\frac{4\pi GN_\alpha N_\beta}{\varepsilon_0 m_\alpha m_\beta}(q_\alpha m_\beta-q_\beta m_\alpha)^2, \tag{6.23}$$

we can simplify (6.22) for all combinations involving electrons or plasma ions on the one hand and dust grains on the other. We will use the following, as good as evident, assumptions, $Z_dm_e \ll Z_dm_i \ll m_d$, $c_{sd} \ll c_{si}, c_{se}$ and $\omega_{Je} \ll \omega_{Ji} \ll \omega_{Jd}$. Taking the long wavelength assumption $k_{cr}\lambda_D \ll 1$ then gives for the critical Jeans length

$$k_{cr}^2\left(1+\lambda_D^2\sum_{d}\frac{\omega_{pd}^2}{c_{sd}^2}\right)=\sum_{d}\frac{\omega_{Jd}^2}{c_{sd}^2}+\frac{\lambda_D^2}{2}\sum_{d}\sum_{d'}\frac{(\omega_{pd}\omega_{Jd'}-\omega_{pd'}\omega_{Jd})^2}{c_{sd}^2c_{sd'}^2}, \tag{6.24}$$

or when considering $c_{sd\alpha} \ll \lambda_D\omega_{pd\alpha}$

$$k_{cr}^2 \simeq \frac{\sum_d\sum_{d'}\frac{(\omega_{pd}\omega_{Jd'}-\omega_{pd'}\omega_{Jd})^2}{c_{sd}^2c_{sd'}^2}}{2\sum_d\frac{\omega_{pd}^2}{c_{sd}^2}}. \tag{6.25}$$

6.8 Influence of neutral dust

Until now, we have treated a description that dealt exclusively with charged or conversely neutral dust particles. Now we combine charged and neutral dust species and we start with the most simple case, namely a configuration of only one charged and only one neutral component. The neutral component represents the non-ionized fraction of the dust particles in dust clouds where the amount of electrons is not sufficient to charge all

the grains. The dispersion law (6.10) can easily be adapted to a plasma with one charged and one neutral dust or gas component, by simply setting the charges to zero on one of the species. In doing so, the dispersion law is modified and becomes

$$\left[\omega^2 - k^2(c_{scd}^2 + c_{da}^2) + \omega_{Jcd}^2\right]\left[\omega^2 - k^2 c_{snd}^2 + \omega_{Jnd}^2\right] = \omega_{Jcd}^2\,\omega_{Jnd}^2, \tag{6.26}$$

indicating the coupling between a Jeans dust mode and a purely acoustic gravitational mode in the neutral component. The discriminant remains positive, and the critical Jeans wavenumber follows from (6.12) as

$$k_{cr}^2 = \frac{\omega_{Jcd}^2}{c_{scd}^2 + c_{da}^2} + \frac{\omega_{Jnd}^2}{c_{snd}^2}, \tag{6.27}$$

in accordance with the results of Verheest et al. [1999]. We know that the dust-acoustic velocity squared is a measure of the plasma pressure (due to the electrons and ions) divided by the charged dust mass density, in the same way that in ordinary plasmas the ion-acoustic velocity squared expresses the electron pressure over the ion mass density. Hence, the dust-acoustic velocity is much larger than the dust thermal velocities.

In dusty plasmas where all the dust is charged we find that the critical (Jeans) wavenumbers are of the order ω_{Jd}/c_{da}, which is much smaller than the critical wavenumbers in neutral gases, being typically of an order ω_{Jd}/c_{sd}. It follows that in dusty plasmas with exclusively charged dust particles larger lengths are stabilized than in neutral dust clouds with otherwise similar parameters. However, assuming that $c_{snd} \sim c_{scd} \ll c_{da}$, the presence of even a small fraction of neutral dust and/or gas in a dusty plasma where the bulk of the dust particles is charged, will immediately reduce the unstable wavelengths to the order of the Jeans lengths for purely neutral gases at similar densities and temperatures The same procedure used in order to obtain (6.24) can be applied for a mixture of charged and neutral dust species

$$k_{cr}^2\left(1 + \lambda_D^2 \sum_d \frac{\omega_{pd}^2}{c_{sd}^2}\right) = \sum_n \frac{\omega_{Jn}^2}{c_{sn}^2} + \sum_d \frac{\omega_{Jd}^2}{c_{sd}^2} + \frac{\lambda_D^2}{2}\sum_d \sum_{d'} \frac{(\omega_{pd}\omega_{Jd'} - \omega_{pd'}\omega_{Jd})^2}{c_{sd}^2 c_{sd'}^2}, \tag{6.28}$$

where now indices d only run over charged dust species and index n solely over neutral dust species. For dust distributions the conclusion remains the same as for a monodisperse dusty plasma, the presence of neutrals immediately inhibits the stabilizing effects of the charged dust grains in the absence of frictional coupling between both species. Indeed, at comparable Jeans frequencies, or mass densities really, the fact that $c_{sg} \sim c_{sn} \ll c_{da}$ implies that the terms concerning the neutral species in (6.28) are prevailing.

6.9 Streaming instabilities

If we include the streaming between species, there arise possibly stream or Buneman instabilities in a plasma [Buneman 1958, 1959, Stix 1962, 1992, Verheest 2000]. For dusty plasmas, the additional species provide several new possibilities for streaming mechanisms.

The streaming can be between the dust particles and the electrons and/or ions [Ishihara 1998], but also between different dust species [Havnes 1980] or, for cometary dust grains, between the solar wind and the dust particles [Havnes 1988]. When we incorporate both streaming effects and different dust species, the general expressions become algebraically very complicated [Meuris et al. 1997] and often necessitate a numerical model [Pillay et al. 2000].

An interesting case is that of two dust beams, both with equal parameters but streaming oppositely to each other [Verheest et al. 2000c]. For algebraic reasons of convenience, we will work in the center-of-mass frame, so that the velocities of the beams are opposite but equal, namely $(\pm U)$. Because we aim at typical dust frequencies and wavenumbers, the electrons and ions can be treated as inertialess. Hence, the electrons and ions follow the perturbations instantaneously and cannot induce a Doppler shift. It follows that within the assumption of massless plasma species, the latter are of no influence to the choice of reference frame.

Accordingly, the dispersion law (6.5) becomes a bi-quadratic in ω^2,

$$\omega^4 - 2A\omega^2 + B = 0, \tag{6.29}$$

with coefficients given by

$$\begin{aligned} A &= k^2(U^2 + c_{sd}^2 + c_{da}^2) - \omega_{Jd}^2, \\ B &= k^2(U^2 - c_{sd}^2)\left[2\omega_{Jd}^2 - k^2(c_{sd}^2 + 2c_{da}^2 - U^2)\right]. \end{aligned} \tag{6.30}$$

The discriminant of the biquadratic is given by

$$\begin{aligned} \Delta &= A^2 - B \\ &= (\omega_{Jd}^2 - k^2c_{da}^2)^2 + 4k^2U^2\left[k^2(c_{sd}^2 + c_{da}^2) - \omega_{Jd}^2\right], \end{aligned} \tag{6.31}$$

and is not for all wavenumbers positive.

The roots of the dispersion law (6.29) can be formally written as

$$\omega^2 = A \pm \sqrt{A^2 - B}. \tag{6.32}$$

The discriminant Δ can only vanish for stream velocities $U \geq c_{sd}$ and in that case $\Delta = 0$ requires wavenumbers

$$k_\pm^2 = \frac{2U^2 + c_{da}^2 \pm 2U\sqrt{U^2 - c_{sd}^2}}{4U^2(c_{sd}^2 + c_{da}^2) + c_{da}^4}\omega_{Jd}^2. \tag{6.33}$$

Conversely, for stream velocities $U < c_{sd}$, the discriminant Δ remains strictly positive.

Let us first see what happens in the event of negligible self-gravitational forces. Thus setting $\omega_{Jd} = 0$ in the previous expressions shows that both A and Δ are positive, independent of the wavenumber, whereas B reduces to

$$B = k^4(U^2 - c_{sd}^2)(U^2 - c_{sd}^2 - 2c_{da}^2). \tag{6.34}$$

Since both roots are real and their sum is positive, unstable roots ($\omega^2 < 0$) can only be obtained for negative values of the parameter B. This means that there is a generalized Buneman instability for dust beams that stream oppositely to each other and with velocities

$$c_{sd}^2 < U^2 < c_{sd}^2 + 2c_{da}^2, \tag{6.35}$$

measured relatively to the center-of-mass frame. For this special case, the magnitude of the instability window depends mainly on the dust-acoustic velocity.

Having dealt with beams which are unaffected by self-gravitation, we revert to the general expressions. First we compute for which wavenumbers k_A the parameter A becomes zero,

$$k_A^2 = \frac{\omega_{Jd}^2}{U^2 + c_{sd}^2 + c_{da}^2}, \tag{6.36}$$

and similarly the wavenumbers for which the parameter B vanishes, namely $k = 0$ and $k = k_B$, with the latter given by

$$k_B^2 = \frac{2\omega_{Jd}^2}{c_{sd}^2 + 2c_{da}^2 - U^2}. \tag{6.37}$$

However, k_B only exists for values of U such that $U^2 < c_{sd}^2 + 2c_{da}^2$, otherwise $B > 0$ at all $k > 0$. Because $c_{sd}^2 + 2c_{da}^2 - U^2 < 2(U^2 + c_{sd}^2 + c_{da}^2)$, it follows that $k_A < k_B$. In addition, one can check that Δ evaluated at $k = k_A$ is

$$\Delta(k_A) = k_A^4(c_{sd}^2 - U^2)(3U^2 + c_{sd}^2), \tag{6.38}$$

which is negative for $c_{sd} < U$, whereas the evaluation of Δ at $k = k_B$ yields

$$\Delta(k_B) = \frac{1}{4}k_B^4(3U^2 + c_{sd}^2)^2 > 0, \tag{6.39}$$

provided k_B exists.

For the wavenumbers $k = k_\pm$, we have $\Delta = 0$ or equivalently $B = A^2 > 0$, corresponding with a double, real root in ω^2.

Having established these crucial wavenumber values, we can start the discussion for different streaming velocities.

Case 1: $U < c_{sd}$

First of all, in the regime where $0 < U < c_{sd}$, Δ cannot change sign and is positive for all k, implying that both roots for ω^2 are real. Instability can then occur provided $B < 0$, corresponding to wavenumbers $k < k_B$. For wavenumbers $k < k_B$ one of the roots (in ω^2) effectively becomes negative, as illustrated by Table 6.1.

Since here $U < c_{sd}$, we see that k_B is slightly larger than ω_{Jd}/c_{da}, being the critical Jeans wavenumber in the absence of streaming effects. We conclude that the streaming decreases the Jeans length and hence renders smaller regions susceptible to a gravitational collapse.

Table 6.1: Signs of A, B and Δ when $U < c_{sd}$

k	0		k_A		k_B	
A	$-$	$-$	0	$+$	$+$	$+$
B	0	$-$	$-$	$-$	0	$+$
Δ	$+$	$+$	$+$	$+$	$+$	$+$

This is clearly a Jeans instability, because of the small wavenumbers we obtained and what is more, for $U < c_{sd}$ we found no equivalent instability in the discussion for dust beams void of self-gravitational effects.

Also, the occurrence of $2\omega_{Jd}^2$ and $2c_{da}^2$ is not really surprising, because at equal beam strength $2\omega_{Jd}^2$ is square of the total Jeans frequency for the combined plasma, and likewise $2c_{da}^2 = 2\lambda_D^2\omega_{pd}^2$ stands for the square of the total dust-acoustic velocity.

Case 2: $c_{sd}^2 < U^2 < c_{sd}^2 + 2c_{da}^2$

The next velocity regime to consider is when $c_{sd}^2 < U^2 < c_{sd}^2 + 2c_{da}^2$, corresponding in the absence of self-gravitation to pure beam instabilities. For convenience, we summarize the information about the signs of A, B and Δ for different k values in Table 6.2, which allows to sift the different wavenumber regimes easily.

For large wavenumbers $k \leqslant k_-$ both roots in ω^2 are real and negative, giving each rise to a growing instability with zero real frequency. One instability will be more of the Buneman type, whereas the other will be rather connected with the Jeans instability. We note that the occurrence of instabilities with zero real frequency is a consequence of working in the center-of-mass frame. Table 6.2 further illustrates that in the range $k_- < k < k_+$ both roots for ω^2 will be complex, again there appear two growing instabilities, the latter of which cannot be attributed separately to a clear-cut Jeans or Buneman type of instability. For the smaller wavelengths $k_B < k$ only the Buneman type instability survives, as the involved lengthscales are too small for being able to host a Jeans instability. Finally, the intermediate wavenumber region $k_+ \leqslant k < k_B$ is the only wavenumber window for which the dusty plasma is stable, otherwise either the gravitational or the streaming instabilities occur, or even both together.

Table 6.2: Signs of A, B and Δ when $c_{sd}^2 < U^2 < c_{sd}^2 + 2c_{da}^2$

k	0		k_-		k_A		k_+		k_B	
A	$-$	$-$	$-$	$-$	0	$+$	$+$	$+$	$+$	$+$
B	0	$+$	$+$	$+$	$+$	$+$	$+$	$+$	0	$-$
Δ	$+$	$+$	0	$-$	$-$	$-$	0	$+$	$+$	$+$

To summarize, for large wavelengths corresponding to $k \leqslant k_+$, the self-gravitational forces cause a Jeans instability. The Jeans instability is correlated with the beam instability and for some velocity regimes even completely intertwined. Going towards smaller wavelengths, a frequency window of stable wavenumbers separates the Jeans-like instabilities from a range $k > k_B$ which depicts a pure Buneman instability.

Case 3: $c_{sd}^2 + 2c_{da}^2 < U^2$

In the last velocity range to be considered, $c_{sd}^2 + 2c_{da}^2 < U^2$, we see that $B > 0$ for all wavenumbers and that k_B does not exist. The discussion is fully analogous to the previous case, with the sole exception that there is no longer a Buneman instability at large wavenumbers, instead the configuration is stable for all wavenumbers $k \geqslant k_+$. The instabilities obtained in this velocity range have no analogon in the case of dust beams with absent self-gravitational forces, therefore the driving force for the instability to occur is coming from the self-gravitation.

The different parameter regimes are grouped together and illustrated in figure 6.2

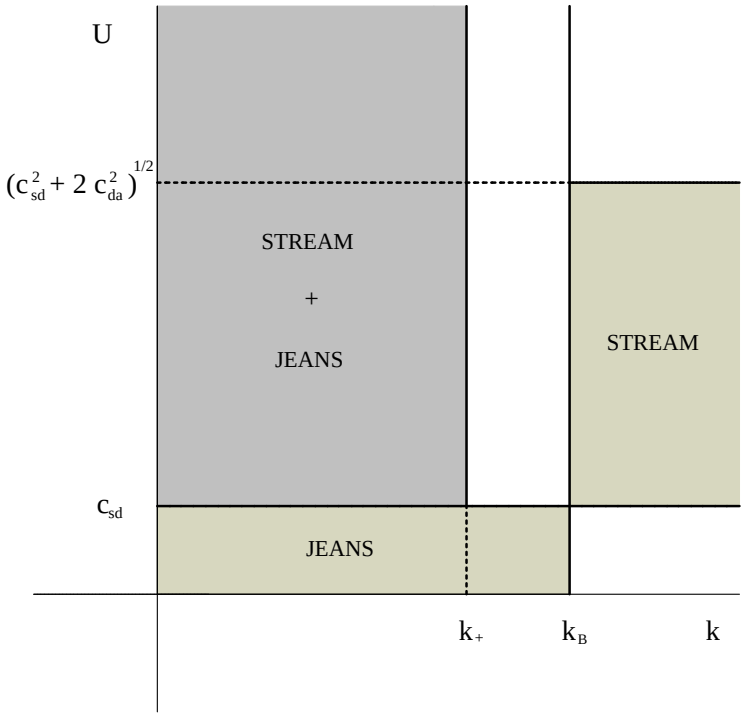

Fig 6.2: Beam instabilities for beams of equal strength

Of course, one can also investigate the special cases where A, B or Δ exactly vanish,

or when $U = c_{sd}$ and $U^2 = c_{sd}^2 + 2c_{da}^2$, but these are too specific and we preferred to concentrate on more generic results. The extension of these results to Buneman-type instabilities where two dust beams have different densities, temperatures and/or streaming velocities leads to a full quartic equation in ω that can only be studied by numerical methods.

Chapter 7

Electromagnetic modes

Having outlined different electrostatic modes, we now revert to the electromagnetic modes. The presence of an external magnetic field not only introduces new phenomena but also causes the coupling mechanisms to become more complicated as a preferred direction is introduced into the system, so perforce the degree of coupling between different wave modes also depends on the direction of the wave propagation.

As we look up the very low frequency end of the wave spectrum, the electromagnetic modes of prime interest are the Alfvénic [Alfvén 1942, 1950] and magnetosonic waves, both originating from the perturbations of the magnetic stress due to the ion and dust inertia.

We will start with the description of the wave modes propagating parallel to the magnetic field. As was noted before, these wave modes are unaffected by self-gravitation thus causing the parallel wave mode description to be easily adaptable for including multiple dust species [Verheest 2000].

On the other hand, for perpendicularly and *a fortiori* for obliquely propagating waves, the wave mode analysis in self-gravitating plasmas becomes tremendously complicated if a size distribution is included [Verheest et al. 2000b]. Therefore, we will advance step by step and so first discuss the simplest size distributions before going over to more generally formulated problems.

The analysis of perpendicularly propagating waves will be mostly restricted to the magnetosonic waves, being a low-frequency transverse wave mode for which the polarization plane is perpendicular to the external magnetic field. The remaining transverse mode for perpendicular propagation then is the ordinary wave mode, which is linearly polarized along the direction of the magnetic field and in the context of this thesis much less interesting because it is unaffected by self-gravitation.

Finally, the low-frequency oblique modes are treated, but mainly for determining the critical wavenumbers, as a full wave analysis is beyond the reach of an analytical study.

7.1 Parallel propagation

For electromagnetic waves propagating parallel to the magnetic field, we recall the dispersion law for the left and righthand circularly polarized modes

$$\omega^2 = c^2k^2 + \omega\left(\sum_p \frac{\omega_{pp}^2}{\omega \pm \Omega_p} + \sum_d \frac{\omega_{pd}^2}{\omega \pm \Omega_d}\right), \tag{7.1}$$

with the index p denoting the plasma species.

Again, the influence of the dust is mainly noticeable for very low frequencies and the modes are supposed having a frequency well below the gyrofrequencies of the plasma species, *viz.* $\omega \ll |\Omega_e|, \Omega_i$. For these low frequencies we enter the regime of the dust-Alfvén waves [Shukla 1992] and upon assuming charge neutrality, the dispersion law becomes

$$\omega^2\left(1 + \frac{c^2}{V_{AR}^2}\right) = c^2k^2 + \omega\sum_d \omega_{pd}^2\left[\frac{1}{\omega \pm \Omega_d} \mp \frac{1}{\Omega_d}\right] + \mathcal{O}\left(\frac{\omega}{\Omega_p}\right)^3, \tag{7.2}$$

where the Alfvén speed V_{AR} is defined over the plasma species only

$$V_{AR}^2 = \frac{B_0^2}{\mu_0 \sum_{p=e,i} N_p m_p}. \tag{7.3}$$

The Alfvén speed V_{AR} can safely be assumed to be much smaller than the speed of light c. Neglecting second order terms and indeed assuming $V_{AR} \ll c$, the dispersion law (7.2) simplifies to

$$\omega^2 - k^2V_{AR}^2 - \frac{V_{AR}^2\omega}{c^2}\sum_d \omega_{pd}^2\left[\frac{1}{\omega \pm \Omega_d} \mp \frac{1}{\Omega_d}\right] = 0. \tag{7.4}$$

The dust grains can be considered immobile in the wave description, corresponding to a frequency limit $|\Omega_d| \ll \omega$. In this frequency regime $|\Omega_d| \ll \omega \ll \Omega_i, |\Omega_e|$, the dispersion law becomes

$$\omega^2 \pm \omega\frac{V_{AR}^2}{c^2}\sum_d \frac{\omega_{pd}^2}{\Omega_d} - k^2V_{AR}^2 = 0 \tag{7.5}$$

For very low frequencies and working in a monodisperse plasma, this dispersion law yields the dust whistler mode [Verheest and Meuris 1995]

$$\omega = c^2k^2\frac{|\Omega_d|}{\omega_{pd}^2} \tag{7.6}$$

On the other hand, when formally taking the frequency limit $\omega \ll |\Omega_d|$, the dispersion law yields

$$\omega = \pm kV_A, \tag{7.7}$$

where now the Alfvén speed

$$V_A^2 = \frac{B_0^2}{\mu_0 \sum_{\alpha=e,i,d} N_\alpha m_\alpha} \tag{7.8}$$

must be computed over all species. In doing so, we recover the Alfvén wave in a description where it is more appropriate to consider the dust grains as heavy ions.

7.2 Magnetosonic modes

As we have seen before, for strictly perpendicularly propagating waves, the dispersion tensor (3.41) decouples into

$$\det[D_{ij}] = D_{xx} \cdot \begin{vmatrix} D_{yy} & D_{yz} & D_{y\psi} \\ D_{yz} & D_{zz} & D_{z\psi} \\ D_{z\psi} & D_{y\psi} & D_{\psi\psi} \end{vmatrix} = 0, \tag{7.9}$$

where $D_{xx} = 0$ represents the ordinary mode

$$\omega^2 = c^2k^2 + \sum_\alpha \omega_{p\alpha}^2. \tag{7.10}$$

The remaining part of the dispersion law is the generalized extraordinary mode and this mode is affected by self-gravitation, as opposed to the ordinary mode. For the low-frequency magnetosonic modes we consider, the lighter species can be treated as being quasi-inertialess. As we have seen before, the assumption of quasi-inertialess electrons and ions can be implemented by taking $m_e, m_i \to 0$ but maintaining the quantities $m_e c_{se}^2, m_i c_{si}^2$ finite. This approximation delineates the frequency regime to the frequencies $\omega \ll \Omega_e, \Omega_i$ and implies that electron and ion Larmor effects can be neglected ($k^2 c_{se}^2/\Omega_e^2, k^2 c_{si}^2/\Omega_i^2 \ll 1$). The inertia needed to sustain the waves is solely provided by the dust grains.

Using these assumptions together with charge neutrality in equilibrium and supposing that $V_{Ad} \ll c$, we find that for low frequencies the elements of the dispersion tensor (3.41) may be simplified to [Verheest et al. 1997, 1999]

$$\begin{aligned}
D_{xx} &= -\sum_d \frac{\omega_{pd}^2}{\omega^2 - k^2 c_{sd}^2 - \Omega_d^2}, \\
D_{xy} &= \sum_d \frac{\omega_{pd}^2(\omega^2 - k^2 c_{sd}^2)}{\Omega_d(\omega^2 - k^2 c_{sd}^2 - \Omega_d^2)} = D_{yx}, \\
D_{x\psi} &= \sum_d \frac{\omega_{pd}\omega_{Jd}}{\omega^2 - k^2 c_{sd}^2 - \Omega_d^2} = D_{\psi x}, \\
D_{yy} &= -\frac{c^2 k^2 V_{ms}^2}{V_{Ad}^2} - \sum_d \frac{\omega_{pd}^2(\omega^2 - k^2 c_{sd}^2)}{\omega^2 - k^2 c_{sd}^2 - \Omega_d^2}, \\
D_{y\psi} &= -\sum_d \frac{\omega_{pd}\omega_{Jd}\Omega_d}{\omega^2 - k^2 c_{sd}^2 - \Omega_d^2} = D_{\psi y}, \\
D_{\psi\psi} &= -1 - \sum_d \frac{\omega_{Jd}^2}{\omega^2 - k^2 c_{sd}^2 - \Omega_d^2} - \sum_g \frac{\omega_{Jg}^2}{\omega^2 - k^2 c_{sg}^2}.
\end{aligned} \tag{7.11}$$

The subscript g refers to the contributions of the neutral dust grains, whereas the dust-

Alfvén V_{Ad} and the magnetosonic velocity V_{ms} are defined respectively as [Rao 1995]

$$V_{Ad}^2 = \frac{B_0^2}{\mu_0 \sum_d N_d m_d}, \tag{7.12}$$

$$V_{ms}^2 = \frac{B_0^2/\mu_0 + P_e + P_i}{\sum_d N_d m_d}, \tag{7.13}$$

where the pressures are specified as $P_\alpha = N_\alpha m_\alpha c_{s\alpha}^2$. The low frequencies we consider are such that $|\omega^2 - k^2 c_{sd}^2 - \Omega_d^2| \ll \omega_{pd}^2$ is satisfied for all dust species.

7.2.1 Average dust dispersion

At first, we consider a simplification of the dispersion law for low-frequency magnetosonic modes. We represent the charged dust by a single species with some average properties and suppose the absence of neutral gas. In this monodisperse description, the dispersion law

$$\det [D_{ij}] = 0, \tag{7.14}$$

where the elements D_{ij} are given by (7.11), simply yields [Verheest et al. 1997, 1999]

$$\omega^2 = k^2 (V_{ms}^2 + c_{sd}^2) - \omega_{Jd}^2. \tag{7.15}$$

The dispersion law (7.15) describes the fast magnetosonic wave, whereas the slow magnetosonic wave has a zero velocity for perpendicular propagation. It is reasonable to suppose that the effective dust pressure P_d is negligible compared to the magnetic pressure B_0^2/μ_0 and to the electron and ion pressures. Naturally this means that the dust pressure P_d can be assumed to be much smaller than the combined magnetic and plasma pressures $B_0^2/\mu_0 + P_e + P_i$ or equivalently that $c_{sd} \ll V_{ms}$, implying that the contribution of the dust thermal effects in dispersion law (7.15) is negligible. Typical parameters for interstellar dust clouds [Whittet 1992, Evans 1994] support the simplifying assumption that dust thermal effects can be omitted. Indeed, within the observational uncertainties, it would seem that $V_{ms} \simeq V_{Ad} \gg c_{sd}$, so that the magnetic pressure is dominant by orders of magnitude [Verheest et al. 1999].

However, when neutral dust or gas is also included, these constituents do not feel any electromagnetic forces, and moreover, they are not directly coupled to the plasma electrons and ions, except through the gravitational Poisson equation. For the neutral gas components of the mixture we are thus forced to explicitly retain the thermal velocities, denoted as c_{sg}.

7.2.2 Two charged dust species

Introducing the possibility of multiple dust species into the description, increases the algebraic complexity of the dispersion laws tremendously. Before addressing a more general dust mass distribution we therefore treat the special case of two charged dust species in the absence of any neutral gas ($\omega_{Jg} = 0$). Although we have seen that in the monodisperse

case the dust thermal effects can be omitted and we would expect similar conclusions to hold when multiple dust species are present, we proceed cautiously and initially retain the dust thermal speeds in the description.

Thus including two charged, dust species the dispersion law (7.14) turns into a biquadratic in ω, namely [Jacobs et al. 2000]

$$A\omega^4 + B\omega^2 + C = 0, \tag{7.16}$$

with coefficients

$$\begin{aligned} A &= \left(\Omega_1\omega_{J1}^2 + \Omega_2\omega_{J2}^2\right)^2, \\ B &= A(\omega_{J,\text{total}}^2 - k^2c_{s1}^2 - k^2c_{s2}^2) - \Omega_1^2\Omega_2^2\omega_{J,\text{total}}^4 \\ &\quad - k^2V_{ms}^2\omega_{J,\text{total}}^2(\Omega_1^2\omega_{J1}^2 + \Omega_2^2\omega_{J2}^2), \\ C &= k^2V_{ms}^2\omega_{J,\text{total}}^2\left[\Omega_1^2\Omega_2^2\omega_{J,\text{total}}^2(1-\mathcal{K}) + \Omega_1^2\omega_{J1}^2k^2c_{s2}^2 + \Omega_2^2\omega_{J2}^2k^2c_{s1}^2\right] \\ &\quad + Ak^2(k^2c_{s1}^2c_{s2}^2 - \omega_{J1}^2c_{s2}^2 - \omega_{J2}^2c_{s1}^2) + \Omega_1^2\Omega_2^2\omega_{J,\text{total}}^2k^2(\omega_{J1}^2c_{s1}^2 + \omega_{J2}^2c_{s2}^2) \\ &\quad -\Omega_1^2\Omega_2^2\omega_{J,\text{total}}^6. \end{aligned} \tag{7.17}$$

In the expressions for the coefficients, we have introduced the total Jeans frequency $\omega_{J,\text{total}}$ through $\omega_{J,\text{total}}^2 = \omega_{J1}^2 + \omega_{J2}^2$, which involves the total mass density. Further a dimensionless coefficient

$$\mathcal{K} = \frac{\omega_{J1}^2\omega_{J2}^2}{\omega_{J,\text{total}}^2}\left(\frac{1}{\Omega_1} - \frac{1}{\Omega_2}\right)^2, \tag{7.18}$$

has been introduced.

We already stated that the thermal velocities c_{s1}, c_{s2} are negligible compared to the magnetosonic velocity V_{ms}, additionally we assume that the coefficient A is of the order of $\Omega_1^2\Omega_2^2\omega_{J,\text{total}}^2\mathcal{K}$. The coefficients B and C of the biquadratic (7.17) can be simplified accordingly and reduce to

$$\begin{aligned} B &= \left[A - \Omega_1^2\Omega_2^2\omega_{J,\text{total}}^2 - k^2V_{ms}^2(\Omega_1^2\omega_{J1}^2 + \Omega_2^2\omega_{J2}^2)\right]\omega_{J,\text{total}}^2, \\ C &= \Omega_1^2\Omega_2^2\omega_{J,\text{total}}^4\left[k^2V_{ms}^2(1-\mathcal{K}) - \omega_{J,\text{total}}^2\right. \\ &\quad \left. + k^2V_{ms}^2\left(\frac{k^2c_{s1}^2\omega_{J2}^2}{\Omega_1^2\omega_{J,\text{total}}^2} + \frac{k^2c_{s2}^2\omega_{J1}^2}{\Omega_2^2\omega_{J,\text{total}}^2}\right)\right]. \end{aligned} \tag{7.19}$$

Only in coefficient C there remain dust thermal effects and we see that they hardly make a contribution if

$$\frac{k^2c_{s1}^2\omega_{J2}^2}{\Omega_1^2\omega_{J,\text{total}}^2} + \frac{k^2c_{s2}^2\omega_{J1}^2}{\Omega_2^2\omega_{J,\text{total}}^2} \ll 1 - \mathcal{K}. \tag{7.20}$$

Again implementing $c_{s1} \ll V_{ms}$ and $c_{s2} \ll V_{ms}$ gives

$$\frac{k^2c_{s1}^2\omega_{J2}^2}{\Omega_1^2\omega_{J,\text{total}}^2} + \frac{k^2c_{s2}^2\omega_{J1}^2}{\Omega_2^2\omega_{J,\text{total}}^2} \ll \frac{k^2V_{ms}^2}{\omega_{J,\text{total}}^2}\left(\frac{\omega_{J2}^2}{\Omega_1^2} + \frac{\omega_{J1}^2}{\Omega_2^2}\right), \tag{7.21}$$

and from the expression for $\mathcal{K}$, *viz.* (7.18), we estimate that

$$\frac{\omega_{J2}^2}{\Omega_1^2} + \frac{\omega_{J1}^2}{\Omega_2^2} = \mathcal{O}(\mathcal{K}). \tag{7.22}$$

We now *ad hoc* introduce a critical wavenumber k_J through

$$k_J^2 = \frac{\omega_{J,\mathrm{total}}^2}{(1-\mathcal{K})V_{ms}^2}. \tag{7.23}$$

and will *a posteriori* see that this is actually the critical Jeans wavenumber. The expressions (7.22) and (7.23) enable to rewrite

$$\frac{k^2 c_{s1}^2 \omega_{J2}^2}{\Omega_1^2 \omega_{J,\mathrm{total}}^2} + \frac{k^2 c_{s2}^2 \omega_{J1}^2}{\Omega_2^2 \omega_{J,\mathrm{total}}^2} \ll \mathcal{O}\left(\frac{\mathcal{K}}{1-\mathcal{K}}\right)\frac{k^2}{k_J^2} \leq 1-\mathcal{K}, \tag{7.24}$$

as far as the orders of magnitudes are concerned. For most astrophysical plasmas the dust Jeans frequencies are small compared to the corresponding gyrofrequencies [Verheest et al. 1999], in particular for interstellar dust clouds when average cloud and dust parameters [Whittet 1992, Evans 1994] are used. Hence, (7.22) indicates that $\mathcal{K}$ typically is very small and we can safely assume $\mathcal{K} \leq \mathcal{O}(1/3)$. The wavenumbers we are interested in are $k \sim k_J$ and for these wavenumbers expression (7.24) predicts that the dust thermal effects may be ignored altogether. For wavenumbers $k \sim k_J$, the coefficient C reduces to

$$C = \Omega_1^2 \Omega_2^2 \omega_{J,\mathrm{total}}^4 \left[k^2 V_{ms}^2 (1-\mathcal{K}) - \omega_{J,\mathrm{total}}^2\right]. \tag{7.25}$$

In that case, the zero-frequency solution of the dispersion law (7.14) needs $C = 0$, yielding a wavenumber $k = k_J$, as already defined in (7.23) and establishing that k_J is indeed the critical Jeans wavenumber. Apparently, the presence of a second charged dust species merely introduces a small correcting factor $1-\mathcal{K}$, which causes k_J to increase and hence relates to smaller Jeans lengths.

Although it is unlikely that the limit $\mathcal{K} = 1$ represents a realistic situation, it is instructive to deliberate about the consequences of such a premise. With the hypothesis that $\mathcal{K} = 1$, expression (7.18) yields the condition

$$\left(\frac{1}{\Omega_1} - \frac{1}{\Omega_2}\right)^2 = \frac{1}{\omega_{J1}^2} + \frac{1}{\omega_{J2}^2}. \tag{7.26}$$

At given values of dust parameters like charges and masses, this condition depicts a specific balance between the dust densities and the strength of the external magnetic field. However, as pointed out already, in most astrophysical plasmas the gyrofrequencies of the dust will be much larger than the Jeans frequencies, which reduces the aforementioned limit to a scarcely applicable exercise.

For determining k_J we have established that leaving out the thermal effects of the charged dust would be of little consequence and we will accordingly apply this simplification further in this section as well in the subsequent general treatment for many charged dust components. In this manner, the discriminant of the biquadratic dispersion law (7.16)

$$\Delta = B^2 - 4AC, \tag{7.27}$$

can be proven to be strictly positive. Indeed, omitting the thermal velocities in the coefficients given by (7.19) yields

$$\begin{aligned}\Delta \;=\; & \omega_{J,\mathrm{total}}^4 \left\{ \left[A + \Omega_1^2\Omega_2^2\omega_{J,\mathrm{total}}^2 - k^2 V_{ms}^2(\Omega_1^2\omega_{J1}^2 + \Omega_2^2\omega_{J2}^2) \right]^2 \right. \\ & \left. + 4k^2 V_{ms}^2 \Omega_1^2\Omega_2^2 \mathcal{K} \left[A + \Omega_1^2\Omega_2^2\omega_{J,\mathrm{total}}^2 \right] \right\} > 0. \end{aligned} \tag{7.28}$$

Because of this, the two roots in ω^2 will be real and the signs of the roots can be determined unambiguously from the signs of the coefficients B and C. A positive value for C implies $k > k_J$, which in turn gives

$$B < -\Omega_1^2\Omega_2^2\omega_{J,total}^2 - \omega_{J1}^2\omega_{J2}^2(\Omega_1 - \Omega_2)^2 < 0, \tag{7.29}$$

and we conclude that both roots for ω^2 are then positive. On the other hand when $C < 0$, which corresponds to $k < k_J$, there will be one positive and one negative root for ω^2, independent of the sign of B. The situation $C < 0$ clearly corresponds to the Jeans unstable case and the transition takes place at $k = k_J$ or $C = 0$. At the critical wavenumber k_J, the roots of (7.16) are given by

$$\omega^2 = \; - \left.\frac{B}{A}\right|_{k=k_J}, \qquad \omega^2 = 0. \tag{7.30}$$

The former corresponds to the high frequency root of the dispersion law [Verheest et al. 1999], and in principle it is possible to rewrite (7.16) in the neighbourhood of marginal stability as

$$A(\omega^2 - \omega_{HF}^2)(\omega^2 - \omega_{LF}^2) = 0, \tag{7.31}$$

where ω_{HF} and ω_{LF} denote the high frequency and low frequency root respectively. A good approximation for the former roots is

$$\omega_{HF}^2 \simeq \; - \frac{B}{A}, \qquad \omega_{LF}^2 \simeq \; - \frac{C}{B}, \tag{7.32}$$

with the coefficient A given by (7.17), B by (7.19) and finally C by expression (7.25).

A possible extension to more dust than two species would result in boundless algebra, and we choose instead to aim at a more systematic treatment, developed in the next section.

7.2.3 Several charged dust species

In the previous section we have seen anew that the gravitational instability occurs when one of the roots (in ω^2) of the dispersion law passes through the origin and thus switches over from positive to negative values. Also for the gravitational instability criterion related to the electromagnetic modes, the dispersion law will generally yield the critical Jeans wavenumber k_J when ω^2 is set to zero. Moreover, the case of two different dust species proved that thermal effects can be omitted, emanating from $c_{sd} \ll V_{ms}$, which expresses that the thermal agitation is negligible compared to propagation velocity of the magnetosonic modes. This allows us to generalize the approach and consider a dusty plasma

which comprises multiple, charged dust species. Since there is no neutral gas ($\omega_{Jg} = 0$) and we have that for the charged dust all $c_{sd} \ll V_{ms}$, the dispersion tensor with elements (7.11) will only contain k in the tensor element D_{yy} and this through $k^2 V_{ms}^2$. It follows that (7.14) can be expanded as

$$F(\omega^2) k^2 V_{ms}^2 = G(\omega^2), \tag{7.33}$$

where F and G are rather complicated functions of ω^2. We have deduced that the critical wavenumber k_J is just about inextricably connected with a zero value of ω^2, so that

$$F(0) k_J^2 V_{ms}^2 = G(0). \tag{7.34}$$

Subsequently we Taylor expand the functions F and G up to first order in ω^2, yielding

$$\left[F(0) + \omega^2 F'(0)\right] k^2 V_{ms}^2 = G(0) + \omega^2 G'(0), \tag{7.35}$$

where $F'(0)$ stands for $dF(\omega^2)/d(\omega^2)$ evaluated at $\omega^2 = 0$ and likewise for $G'(0)$. In effect, (7.35) focusses towards the immediate vicinity of marginally stable regions of the frequency band and will allow both the determination of the critical wavenumber as the determination of the local dispersion law around marginal stability

Following Jacobs et al. [2000], we introduce for the sake of convenience the notations S_n as

$$S_n = \sum_d \frac{\omega_{Jd}^2}{\Omega_d^n} \qquad (n = 0, 1, 2, 3, 4)\,, \tag{7.36}$$

with the summation indices running over all the different dust components and cancelling common factors, we obtain for the Taylor coefficients

$$\begin{aligned} F(0) &= S_0 - S_0 S_2 + S_1^2, \\ F'(0) &= S_2 - S_2^2 + 2 S_1 S_3 - S_0 S_4, \\ G(0) &= S_0^2, \\ G'(0) &= S_0 - S_1^2 + 2 S_0 S_2. \end{aligned} \tag{7.37}$$

In deriving (7.37) we have used the fact that for each dust species

$$\omega_{pd} = \frac{c\,\omega_{Jd}\Omega_d}{V_{Ad}\,\omega_{J,\mathrm{total}}}, \tag{7.38}$$

where we have defined the global Jeans frequency over all charged species through

$$\omega_{J,\mathrm{total}}^2 = \sum_d \omega_{Jd}^2 = S_0. \tag{7.39}$$

The previous definitions allow to rewrite $F(0)$ concisely as

$$F(0) = S_0(1 - \mathcal{K}), \tag{7.40}$$

where the parameter $\mathcal{K}$ is generalized from (7.18) to the (nonnegative) quantity

$$\mathcal{K} = \frac{1}{2\omega_{J,\mathrm{total}}^2} \sum_d \sum_{d'} \omega_{Jd}^2 \omega_{Jd'}^2 \left(\frac{1}{\Omega_d} - \frac{1}{\Omega_{d'}} \right)^2 . \tag{7.41}$$

In this expression for $\mathcal{K}$ and in subsequent expressions, we use d, d' and later also d'' as dummy indices over the different charged dust species. Additionally, in the derivation of the full expression for $\mathcal{K}$ we have made use of the property

$$\left(\sum_p a_p^2 \right) \left(\sum_q b_q^2 \right) - \left(\sum_p a_p b_p \right)^2 = \frac{1}{2} \sum_p \sum_q (a_p b_q - a_q b_p)^2, \tag{7.42}$$

which gave us the opportunity to rewrite combinations like $S_0 S_2 - S_1^2$ in a more convenient form. For rewriting $S_0 S_2 - S_1^2$, we merely have to identify $a_p = \omega_{Jp}$ and $b_q = \omega_{Jq}/\Omega_q$ in (7.42). Implementing all the above, the critical Jeans wavenumber is found from (7.34) afresh as

$$k_J^2 = \frac{\omega_{J,\mathrm{total}}^2}{(1-\mathcal{K}) V_{ms}^2}. \tag{7.43}$$

This critical wavenumber is formally identical to (7.23), but now the generalized expressions for $\omega_{J,\mathrm{total}}$ and $\mathcal{K}$ have to be inserted. We continue by using (7.34) in order to cast (7.35) in the form

$$F(0)^2 V_{ms}^2 (k^2 - k_J^2) = \mathcal{A} \omega^2, \tag{7.44}$$

with the new quantity $\mathcal{A}$ defined as

$$\begin{aligned} \mathcal{A} &= F(0)G'(0) - G(0)F'(0) \\ &= S_0^2 + S_0^3 S_4 - S_0^2 S_2^2 + 3 S_0 S_1^2 S_2 - S_1^4 - 2 S_0^2 S_1 S_3 \\ &= \omega_{J,\mathrm{total}}^4 (1 + \mathcal{L}). \end{aligned} \tag{7.45}$$

Because $\mathcal{L}$ is given by

$$\begin{aligned} \mathcal{L} &= \frac{1}{2\omega_{J,\mathrm{total}}^4} \sum_d \sum_{d'} \omega_{Jd}^2 \omega_{Jd'}^2 \left(\frac{1}{\Omega_d} - \frac{1}{\Omega_{d'}} \right)^2 \times \\ &\quad \times \left[\sum_{d''} \omega_{Jd''}^2 \left(\frac{1}{\Omega_d} + \frac{1}{\Omega_{d'}} - \frac{1}{\Omega_{d''}} \right) \right]^2 \geqslant 0, \end{aligned} \tag{7.46}$$

the parameter $\mathcal{A}$ will be a strictly positive quantity. The parameter $\mathcal{L}$ will only vanish if all charged dust species have the same charge-to-mass ratios, or naturally when we restrict ourselves to one charged dust species. Since $\mathcal{A} > 0$, equation (7.44) shows that $\omega^2 > 0$ for wavenumbers $k > k_J$, and vice versa, wavenumbers $k < k_J$ correspond to the unstable Jeans modes.

In the neighbourhood of marginal stability, k is close to k_J and with the help of the intermediate results, the local dispersion law (7.35) can be written as

$$\omega^2 = \frac{1-\mathcal{K}}{1+\mathcal{L}} \left[(1-\mathcal{K}) k^2 V_{ms}^2 - \omega_{J,\mathrm{total}}^2 \right]. \tag{7.47}$$

Closer inspection of $\mathcal{K}$ and $\mathcal{L}$ shows that $\mathcal{K}$ is of second order in the ratio of typical Jeans over gyrofrequencies, whereas $\mathcal{L}$ is of fourth order in the same quantities. By and large, data for astrophysical plasmas indicates that the Jeans frequencies are relatively small in comparison with the gyrofrequencies [Verheest et al. 1999], so that we can as a rule assume $\mathcal{L} \ll \mathcal{K} \ll 1$. As a result, the local dispersion law (7.47) can be approximated as

$$\omega^2 \simeq (1-\mathcal{K}) \left[(1-\mathcal{K}) k^2 V_{ms}^2 - \omega_{J,\mathrm{total}}^2 \right] . \tag{7.48}$$

Ergo, provided neutral dust is absent, the inclusion of a size distribution for the dust eventuates to lower frequencies and a larger critical wavenumber by comparison with a model that comprises only a single charged dust species. Hence, a polydisperse model of a dust cloud will exhibit a gravitational instability for smaller dimensions.

However, seeing that $\mathcal{K}$ is usually small compared to 1, incorporating a distribution over different charged dust constituents will not significantly enhance the results obtained by describing simply all the charged dust through one species with average properties. Treating all the charged dust as one effective species with average properties evidently comprehends great mathematical advantages and this approach can be expected to yield the same physical insight, except in those cases where $\mathcal{K}$ and $\mathcal{L}$ are not so small.

On a final note, we point out that it was tacitly assumed that $F(0) > 0$ when writing (7.34). Because (7.37) states that $G(0) > 0$ a negative value for $F(0)$ would imply that k_J does not exist. According to expression (7.40), $F(0) > 0$ is equivalent to assuming $\mathcal{K} < 1$. Suppose conversely we would naively let $\mathcal{K} \to 1$, then (7.34) would produce for the critical wavenumbers $k_J \to \infty$ and apparently the system would be inclined to instability even at arbitrarily small lengthscales. However, presuming $\mathcal{K} \to 1$ is at variance with our simplifying assumption that the dust thermal effects are negligible compared to those pressures that determine the magnetosonic velocity. As was already evident from the discussion of a dust cloud with two charged dust components it is therefore not allowed to let $\mathcal{K} \to 1$ unless we would abandon the reduction $c_{sd} \ll V_{ms}$.

7.2.4 Presence of a neutral component

Whereas the previous sections dealt with purely charged dust species, we now investigate the influence of the presence of one or more neutral dust or gas species. We could follow the outline marked by the description of the previous sections, but the obtained dispersion law would be cumbersome and too disorderly for a proper analysis. Instead of calculating long dispersion laws that are not physically transparent at all, we reduce our analysis to determining the critical Jeans wavenumbers, in the same manner as we did for the electrostatic modes. Accordingly, the critical Jeans numbers can be acquired by putting $\omega = 0$ in the appropriate dispersion law. In the general case, we evaluate the elements (7.11) of the dispersion tensor at $\omega = 0$ and find that k_J obeys

$$k_J^2 = \frac{1}{1-\mathcal{K}} \left[\frac{\omega_{J,\mathrm{total}}^2}{V_{ms}^2} + \sum_g \frac{\omega_{Jg}^2}{c_{sg}^2} \right] , \tag{7.49}$$

where the index g denotes the neutral component and $\omega^2_{J,\mathrm{total}}$ is summed over the charged dust species only. This results generalizes the unstable Jeans lengths obtained by Verheest et al. [1999] and (7.49) show that the effects of the dust mass distribution appear through the introduction of a relatively small correcting factor $(1-\mathcal{K})$. Because of the wide disparity between the values of the characteristic magnetosonic speed (V_{ms}) and the thermal speed of the neutral gas c_{sg}, we observe once again that if a neutral component is present, it almost exclusively determines the effective Jeans number and completely nullifies the possibly stabilizing role of the charged dust.

7.3 Oblique modes

For obliquely propagating waves, we must use the full dispersion law (7.14) as a starting point. Because all the present wave modes are coupled, the calculation of the polynomial dispersion law becomes extremely complicated, especially when multiple dust species are taken into account.

We can simplify the dispersion law by assuming the electrons and ions to be inertialess, furthermore we assume $\omega^2 \ll c^2k^2$ and suppose sufficiently long wavelengths $k^2\lambda_D^2 \ll 1$. With these assumptions, the elements of the dispersion law become

$$
\begin{aligned}
D_{xx} &= \frac{\omega^2\tan^2\theta}{k^2\lambda_D^2} - c^2k^2 - \omega^2\sum_d \frac{\omega_{pd}^2(\omega^2 - k^2c_{sd}^2 - \Omega_d^2\sin^2\vartheta)}{\omega^2(\omega^2-\Omega_d^2) - k^2c_{sd}^2(\omega^2-\Omega_d^2\cos^2\vartheta)}\\
D_{xy} &= D_{yx} = \omega\sum_d \frac{\omega_{pd}^2\Omega_d(\omega^2 - k^2c_{sd}^2)\cos\vartheta}{\omega^2(\omega^2-\Omega_d^2) - k^2c_{sd}^2(\omega^2-\Omega_d^2\cos^2\vartheta)},\\
D_{xz} &= D_{zx} = \frac{\omega\tan\theta}{k^2\lambda_D^2} + \omega\sum_d \frac{\omega_{pd}^2\Omega_d^2\sin\vartheta\cos\vartheta}{\omega^2(\omega^2-\Omega_d^2) - k^2c_{sd}^2(\omega^2-\Omega_d^2\cos^2\vartheta)},\\
D_{x\psi} &= D_{\psi x} = -\omega\sum_d \frac{\omega_{pd}\omega_{Jd}\Omega_d^2\sin\vartheta\cos\vartheta}{\omega^2(\omega^2-\Omega_d^2) - k^2c_{sd}^2(\omega^2-\Omega_d^2\cos^2\vartheta)},\\
D_{yy} &= -c^2k^2 - \omega^2\sum_d \frac{\omega_{pd}^2(\omega^2 - k^2c_{sd}^2)}{\omega^2(\omega^2-\Omega_d^2) - k^2c_{sd}^2(\omega^2-\Omega_d^2\cos^2\vartheta)},\\
D_{yz} &= D_{zy} = -\omega^2\sum_d \frac{\omega_{pd}^2\Omega_d\sin\vartheta}{\omega^2(\omega^2-\Omega_d^2) - k^2c_{sd}^2(\omega^2-\Omega_d^2\cos^2\vartheta)},\\
D_{y\psi} &= D_{\psi y} = \omega^2\sum_d \frac{\omega_{pd}\omega_{Jd}\Omega_d\sin\vartheta}{\omega^2(\omega^2-\Omega_d^2) - k^2c_{sd}^2(\omega^2-\Omega_d^2\cos^2\vartheta)},\\
D_{zz} &= \frac{1}{k^2\lambda_D^2} - \sum_d \frac{\omega_{pd}^2(\omega^2 - \Omega_d^2\cos^2\vartheta)}{\omega^2(\omega^2-\Omega_d^2) - k^2c_{sd}^2(\omega^2-\Omega_d^2\cos^2\vartheta)},\\
D_{z\psi} &= D_{\psi z} = \sum_d \frac{\omega_{pd}\omega_{Jd}(\omega^2 - \Omega_d^2\cos^2\vartheta)}{\omega^2(\omega^2-\Omega_d^2) - k^2c_{sd}^2(\omega^2-\Omega_d^2\cos^2\vartheta)},
\end{aligned}
\tag{7.50}
$$

$$D_{\psi\psi} = -1 - \sum_d \frac{\omega_{Jd}^2(\omega^2 - \Omega_d^2\cos^2\vartheta)}{\omega^2(\omega^2-\Omega_d^2) - k^2c_{sd}^2(\omega^2-\Omega_d^2\cos^2\vartheta)}.$$

Clearly, the complexity of the dispersion law $\det[D_{ij}] = 0$ will increase tremendously with the number of dust species, therefore we will consider only one effective dust species. The inclusion of only one dust species and the assumption of inertialess electrons and ions brings us to the configuration of the so called "classic" dusty plasma. After some tedious but straightforward algebra, the result is a cubic polynomial in ω^2 with real coefficients,

$$\begin{aligned}\omega^6 &- \left[\Omega_d^2\kappa^2\left((1+\kappa^2)\cos^2\vartheta+1\right)+\Delta\right]\omega^4 \\ &+ \left[(\Omega_d^2+\Delta)\kappa^2+2\Delta\right](\Omega_d^2\kappa^2\cos^2\vartheta)\omega^2 - (\Omega_d^4\kappa^4\cos^4\vartheta)\Delta = 0. \end{aligned} \tag{7.51}$$

Here $\kappa = ck/\omega_{pd}$, and we note that all thermal and self-gravitational effects are consistently grouped together in Δ, which is defined as

$$\Delta = k^2(c_{da}^2 + c_{sd}^2) - \omega_{Jd}^2. \tag{7.52}$$

Solving $\Delta = 0$ corresponds to setting $\omega^2 = 0$ and gives the familiar result for the critical wavelength

$$k_{cr}^2 = \frac{\omega_{Jd}^2}{c_{da}^2 + c_{sd}^2}. \tag{7.53}$$

The other two roots which are also associated with $\Delta = 0$ are the solutions of the bi-quadratic

$$\omega^4 - \Omega_d^2\kappa_{cr}^2[(1+\kappa_{cr}^2)\cos^2\theta + 1]\omega^2 + \Omega_d^4\kappa_{cr}^4\cos^2\theta = 0, \tag{7.54}$$

with a positive discriminant

$$\Omega_d^4\kappa^4\{[(\kappa_{cr}^2-1)\cos^2\theta+1]^2 + 4\kappa_{cr}^2\cos^4\theta\} > 0, \tag{7.55}$$

and where

$$\kappa_{cr} = \frac{c\,\omega_{Jd}}{c_{da}\omega_{pd}}. \tag{7.56}$$

It follows that the two remaining roots, which also correspond to $\Delta = 0$ are real and positive.

For the analysis of the cubic dispersion law (7.51), we make use of Descartes' rule of signs. This rule indicates that the number of positive real roots of a polynomial with real coefficients, is either equal to the number of sign variations in the coefficients of the polynomial or else is less than this number by an even integer. We note that in the determination of the number of sign variations, the terms with a zero coefficient can be ignored. Furthermore, if one denotes the polynomial with real coefficients as $p(x)$, Descartes' rule of signs implies also that the number of negative roots of $p(x) = 0$ is either equal to the number of sign variations in the coefficients of $p(-x)$ or else is less than this number by an even integer.

Hence, for negative Δ, but small in absolute value, Descartes' rule of signs predicts that there is one negative, real root, therefore a gravitational instability is certain. For the

corresponding wavenumbers $k < k_{cr}$, the negative root for ω^2 corresponds to the purely growing Jeans instability.

On the other hand, for small, positive Δ, we deduce analogously that the polynomial (7.51) has three positive roots in ω^2 and represents a stable configuration. Since both the self-gravitational effects and the thermal effects of all species (electrons, ions and dust) only appear in Δ, the analysis for a self-gravitating plasma with positive Δ is congruent to a dusty plasma for which $\omega_{Jd} \simeq 0$ applies. Naturally a plasma with negligible self-gravitational forces will be stable, as in this model there are no physical mechanisms included which are possibly destabilizing.

We conclude that for positive Δ there is gravitational stability and the transition towards instability occurs when Δ and one of the roots ω^2 go simultaneously through zero. These results are in concordance with those obtained by Mamun et al. [1999] and we note already that the gyromagnetic effects do not sway the value of the critical wavenumber.

Since the dust thermal speed is usually much smaller than the dust-acoustic speed, we obtain

$$k_{cr}\lambda_D \simeq \frac{\omega_{Jd}}{\omega_{pd}}, \tag{7.57}$$

and as we have used the long wavelength assumption it is necessary that $\omega_{Jd} \ll \omega_{pd}$ in order to assure that $k_{cr}\lambda_D \ll 1$. On the other hand, when the magnitudes of the Jeans and plasma frequencies are comparable, the critical wavelengths are of the order of the Debye length ($k_{cr}\lambda_D \simeq 1$). This means that wavenumbers which are allowed in a fluid description ($k\lambda_D \ll 1$) are invariably smaller than the critical wavenumber and thus are automatically located in the unstable band. This could have been expected as $\omega_{pd} \sim \omega_{Jd}$ indicates rather heavy dust grains, which naturally go hand in hand with substantial self-gravitational forces.

When adding more dust species to the dusty plasma model, treating the unabridged dispersion law would become extremely laborious and the obtained, lengthy polynomial would be well nigh impossible to unravel. Instead, we choose to cut this Gordian algebraic knot and to go directly to the desired critical lengths. The simpler cases of parallel and perpendicular propagation and the discussion of the "classic" dusty plasma given above, indicate that the onset of the instability comes about at $\omega^2 = 0$. Furthermore, the critical lengths are typically of the form $k_{cr} \simeq \omega_J/V$, where ω_J stands for a global Jeans frequency and V for some average thermal or magnetosonic velocity.

A shortcut to procure the Jeans lengths at oblique propagation is to immediately put $\omega = 0$ in the elements (7.50) of the dispersion tensor. This purposive approach is justifiable, except for nearly perpendicularly propagating perturbations ($\vartheta \neq 90^{\circ}$), which would necessitate a separate treatment. The nonzero elements of the dispersion tensor are now very simple expressions and with k_{cr} the desired critical Jeans length they become

$$\begin{aligned} D_{xx} &= D_{yy} = -c^2 k_{cr}^2, \\ D_{zz} &= 1 + \sum_{\alpha} \frac{\omega_{p\alpha}^2}{k_{cr}^2 c_{s\alpha}^2}, \end{aligned}$$

$$D_{z\psi} \;=\; D_{\psi z} \;=\; -\sum_{\alpha} \frac{\omega_{p\alpha}\omega_{J\alpha}}{k_{cr}^2 c_{s\alpha}^2}, \tag{7.58}$$

$$D_{\psi\psi} \;=\; -1 + \sum_{\alpha} \frac{\omega_{J\alpha}^2}{k_{cr}^2 c_{s\alpha}^2}.$$

Conveniently, the result of the dispersion law

$$\left(1 + \sum_{\alpha} \frac{\omega_{p\alpha}^2}{k_{cr}^2 c_{s\alpha}^2}\right)\left(1 - \sum_{\alpha} \frac{\omega_{J\alpha}^2}{k_{cr}^2 c_{s\alpha}^2}\right) + \left(\sum_{\alpha} \frac{\omega_{p\alpha}\omega_{J\alpha}}{k_{cr}^2 c_{s\alpha}^2}\right)^2 = 0, \tag{7.59}$$

is independent of the angle of wave propagation ϑ and could have been obtained just as well from (3.48) by putting $\omega = 0$, except that the validity is now extended to all angles of propagation aside from strictly perpendicular propagation. This result brings us to the conclusion that in the presence of an external magnetic field, tracing the conditions for gravitational instability in a dust cloud with isotropic pressures can be narrowed to two main directions, namely the parallel direction and one perpendicular to the magnetic field. In this description, all perpendicular directions are alike and a representative can be chosen arbitrarily. For the directions in between, the terms for a gravitational collapse will be almost identical to those for the direction aligned with the magnetic field. This means that for $\vartheta \to 90^{\rm o}$ an abrupt transition will occur to the critical lengths, the latter of which must be determined from the appropriate treatment of the extraordinary mode at strictly perpendicular propagation. This discontinuous change in the structure of the Jeans lengths is a consequence of the fact that the limits $\omega \to 0$ and $\vartheta \to 90^{\rm o}$ are not freely interchangeable.

Therefore, in the absence of neutral species, a dust cloud with isotropic pressure disturbances can in terms of gravitational stability be characterized by only two crucial lengthscales, namely

$$\begin{aligned} L_{cr,\,\not\perp} \;&\simeq\; \frac{2\pi\omega_{Jd}}{c_{da}}, \\ L_{cr,\,\perp} \;&\simeq\; \frac{2\pi\omega_{Jd}}{V_{ms}}, \end{aligned} \tag{7.60}$$

with ω_{Jd}, c_{da} and V_{ms} some sort of average over the different dust species. Oppositely, when neutrals are present, the role of the charged dust particles is completely swamped. Hence, since the neutrals are not influenced by any magnetic field, there will be no distinction between directions and only a single crucial lengthscale $L \simeq 2\pi\omega_{Jd}/c_{sg}$ is called for.

It follows that (7.59) reduces to the expression (6.9) for one dust species, whereas in case of a combination of charged and neutral dust the expression (6.27) is recovered.

7.4 Summary

Whereas in the previous chapter we studied the influence of a dust size distribution on the electrostatic modes, we explored here the modifications due to a size distribution as regards the electromagnetic modes. In the light of the incapacity of the gravitational forces

to exert influence on the parallel, electromagnetic modes, these are of no importance for the gravitational stability analysis. Since we primarily aim at self-gravitational phenomena, the impact of dust dispersion on these transverse, electromagnetic wave modes was therefore only briefly recalled.

On the other hand, at perpendicular propagation, the generalized extraordinary mode embodies the coupling between the Jeans modes and the magnetosonic modes and will as such be influenced by dust dispersion. In order to establish a pattern, we started with the case of two dust species and from this we learned that the dust thermal speeds play a minor part compared to the magnetosonic velocity. This assessment provided a stepping stone for more general discrete dust distributions and in leaving out the secondary thermal effects in a general polydisperse description, a factor $(1-\mathcal{K})$ is introduced into the expression for the critical Jeans lengths. The parameter $\mathcal{K}$ is quite small for astrophysical dusty plasmas, so that the influence of a dust distribution is rather insignificant as far as the gravitational stability criterion is concerned. The moral being that in future associated research, efforts can be drastically saved by modelling only one dust species with some average properties instead of including the whole spectrum of different dust species.

Finally, we turned to the obliquely propagating waves in order to explore the transition between the parallel, electrostatic modes and the magnetosonic modes. Whereas the former pictured the coupling between the Langmuir oscillations and the Jeans modes, the latter combine the magnetosonic and Jeans modes. However, at intermediate angles the general dispersion law enshrouds all the involved modes much more thoroughly and calls for a more purposive approach. A blow-by-blow treatment would indeed stand little chance for providing meaningful conclusions and instead we choose to head directly for the critical Jeanslengths.

For the involved ultra low frequencies, the electrons and ions can be safely assumed to be inertialess. This assumption of inertialess plasma species together with a restriction to only one dust species corresponds to the "classic" dusty plasma model, which provided a reliable testcase for a dusty plasma model that includes several charged dust components.

Curiously enough, the outcome is that critical Jeans lengths for oblique modes are exactly the same as derived from electrostatic parallel modes, except at or close to perpendicular propagation. For quasi-perpendicular directions, the evolution of the Jeans lengths associated with the parallel wavemodes towards the critical lengths determined from the extraordinary mode will occur intermittently, because the limits $\omega \to 0$ and $\vartheta \to 90^{\mathrm{o}}$ are not freely interchangeable.

Chapter 8

Kinetic analysis

In the previous chapters we have primarily studied the modifications of the dust-acoustic wave due to self-gravitation. For the sake of convenience, all derivations were based on a hydrodynamic approach instead of a kinetic one. We now evoke the kinetic model in order to excavate the information that has been lost due to the inability of the hydrodynamic model to incorporate the behaviour of the particles which travel at speeds of the order of the phase velocity. Since it is particularly the particles travelling at or near the phase velocity of the wave that interact most strongly with the wave, the kinetic treatment ferrets out the phenomenon of wave damping as a result of energy exchange between the wave and resonant particles. This collisionless damping mechanism is known as Landau damping and is well studied in Maxwellian electron-ion plasmas [Krall and Trivelpiece 1973, Akhiezer et al. 1975]. We note that collisionless wave damping can also occur as a consequence of the interaction between the waves and the fluctuating charges of the dust [Havnes et al. 1992, Melandsø et al. 1993a,b]. The analysis of charge fluctuation-damping has been explored also in self-gravitational dusty plasmas with high fugacity by Rao and Verheest [2000].

Recently, Melandsø et al. [1993a] and Brattli et al. [1997] have already studied the propagation of dust-acoustic modes in dusty plasmas within a kinetic model, but without including self-gravitational effects. On the other hand, Binney and Tremaine [1987] and Fridman and Polyachenko [1984] have used both descriptions in application to a neutral self-gravitating medium and concluded that each model yields the same instability criterion. However, the spectrum of wave oscillations differs in that short-wavelength sound waves do not continue to exist when going over from a fluid to a kinetic treatment.

Here, we join the facets of both self-gravitation and electrostatic interactions for low frequency modes in dusty plasmas within the formalism of a kinetic theory. We investigate if the Jeans instability criterion, obtained in a hydrodynamical approach, is modified and furthermore examine the damping rates of the eigenmodes of dust-acoustic and dust Langmuir modes. The aspects of linear Landau damping are firstly explored for a monodisperse dusty plasma, which will serve as a preamble for the case of polydisperse plasmas, which will get a chance in the next chapter. The wave frequencies of the dust-acoustic and dust-Langmuir waves are assumed to differ considerably from the charging frequencies so that

the dust charges are effectively constant.

8.1 Kinetic model of a dusty self-gravitating plasma

When we neglect collisions and possible sink or source terms, we can make use of the previously discussed kinetic dispersion law (3.17) for electrostatic waves in self-gravitating dusty plasmas [Yaroshenko et al. 2001b]

$$\varepsilon(\omega, k) = \varepsilon_p + \frac{K^2}{\varepsilon_G} = 0, \tag{8.1}$$

with ε_p a plasma function, which stems only from the electrostatic interactions and is given by

$$\varepsilon_p = 1 + \frac{1}{\varepsilon_0 k^2} \sum_\alpha \frac{q_\alpha^2}{m_\alpha} I_\alpha, \tag{8.2}$$

and where ε_G is a dispersion function correlated exclusively with the gravitational interactions [Bliokh et al. 1995]

$$\varepsilon_G = 1 - \frac{4\pi G}{k^2} \sum_\alpha m_\alpha I_\alpha. \tag{8.3}$$

Just as in a fluid description for self-gravitating plasmas, these functions are combined in the dispersion law through a coupling factor [Bliokh and Yaroshenko 1996]

$$K = \sqrt{\frac{4\pi G}{\varepsilon_0}} \frac{1}{k^2} \sum_\alpha q_\alpha I_\alpha. \tag{8.4}$$

In these definitions, I_α is given as

$$I_\alpha = \int \frac{\mathbf{k} \cdot \boldsymbol{\nabla}_v f_{\alpha 0}}{\omega - \mathbf{k} \cdot \mathbf{v}} d^3\mathbf{v}. \tag{8.5}$$

8.2 Monodisperse description

First, we will treat a monodisperse dusty, self-gravitating plasma with the velocity distribution of the plasma particles assumed to be Maxwellian, so that for the unperturbed part of the distribution functions

$$f_{\alpha 0} = \frac{n_{\alpha 0}}{\left(\pi c_{s\alpha}^2\right)^{3/2}} \exp\left(-\frac{v^2}{c_{s\alpha}^2}\right). \tag{8.6}$$

In order to be in accordance with the majority of kinetic treatments in the literature, we redefine the thermal velocities as $c_{s\alpha} = \left(2k_B T_\alpha / m_\alpha\right)^{1/2}$. If one describes the three dimensional velocity phase space within a rectangular coordinate system (v_x, v_y, v_z), where

the v_x-axis is chosen to be aligned with the wave vector $\mathbf{k}$, the integral over all velocities in (3.16) can be calculated as

$$I_\alpha = \frac{2n_{\alpha 0}k}{\sqrt{\pi}c_{s\alpha}^3}\int_{-\infty}^{\infty}\frac{v_x}{kv_x-\omega}\exp\left(-\frac{v_x^2}{c_{s\alpha}^2}\right)dv_x, \tag{8.7}$$

if one makes use of

$$\int_{-\infty}^{\infty}\exp\left(-\frac{v^2}{c_{s\alpha}^2}\right)dv = \sqrt{\pi}c_{s\alpha}, \tag{8.8}$$

for the calculation of the integrals over v_y and v_z. If we use again (8.8) and subsequently substitute $v_x = c_{s\alpha}\xi$, expression (8.7) can be rewritten as

$$\begin{aligned} I_\alpha &= \frac{2n_{\alpha 0}}{c_{s\alpha}^2}\left[1+\frac{\omega}{\sqrt{\pi}c_{s\alpha}}\int_{-\infty}^{\infty}\frac{1}{kv_x-\omega}\exp\left(-\frac{v_x^2}{c_{s\alpha}^2}\right)dv_x\right] \\ &= \frac{2n_{\alpha 0}}{c_{s\alpha}^2}\left[1+\frac{\omega}{\sqrt{\pi}kc_{s\alpha}}\int_{-\infty}^{\infty}\frac{1}{\xi-\frac{\omega}{kc_{s\alpha}}}\exp\left(-\xi^2\right)d\xi\right] \end{aligned} \tag{8.9}$$

where the involved integral is frequently encountered in descriptions treating Landau damping [Landau 1946, Fried and Conte 1961, Melandsø et al. 1993a].

8.3 Determination of the critical wavenumbers

The discussions within the framework of a fluid description provided ample indications that the boundary between stable and unstable solutions occurs at $\omega = 0$ and we reasonably not expect a deviation from this maxim here. Following this prescript $\omega = 0$ reduces the integral (8.9) to

$$I_{\alpha,cr} = \frac{2n_{\alpha 0}}{c_{s\alpha}^2}. \tag{8.10}$$

Next, we substitute (8.10) into (8.2)–(8.4) and use (8.1), which yields the following equation for the critical wavenumber k_{cr}

$$\left(1+\frac{1}{k_{cr}^2\lambda_D^2}\right)\left(1-\frac{1}{k_{cr}^2\lambda_{Jd}^2}\right)+\frac{1}{k_{cr}^2\lambda_{Dd}^2} = 0, \tag{8.11}$$

where we have defined a characteristic Jeans lengths per species, given through $\lambda_{J\alpha}^2 = k_B T_\alpha/4\pi G n_{\alpha 0} m_\alpha^2 = 2\omega_{Jd}^2/c_{sd}^2$. With the redefinition of the thermal speeds in this chapter, the Debye length now reads as $\lambda_D^2 = 2\omega_{pd}^2/c_{sd}^2$. The gravitational influences due to ions or electrons is so insignificant in self-gravitational plasmas that they are never included in a wave description. Terms proportional to λ_{Je}^{-1} and λ_{Ji}^{-1} can thus be neglected, which is equivalent to the assumptions $|q_d|/m_d \ll |q_i|/m_i, e/m_e$. As a consequence, the electron and ion contributions are retained only through the global plasma Debye length λ_D.

The bi-quadratic equation (8.11) has two real solutions of opposite sign in k^2, of which the positive solution corresponds to the critical wavenumber. The equation is now solved for two different wavenumber regimes, both of which stand for a characteristic type of low-frequency waves in dusty self-gravitating plasmas.

Dust-acoustic regime ($k_{cr}^2\lambda_D^2 \ll 1$)

As mentioned in the discussion of the dust-acoustic mode, the physical phenomena that bring about the dust-acoustic wave are long wavelength phenomena ($\lambda \gg \lambda_D$) and this long wavelength approximation yields a critical wavenumber

$$k_{cr}^2 = \frac{\omega_{Jd}^2}{c_{da}^2}\,\frac{1}{1+\lambda_{Dd}^2/\lambda_D^2}. \tag{8.12}$$

If the dust is specified to be cold, the result (8.12) formally reduces to the critical wavenumber k_{cr} for dust-acoustic waves obtained within a fluid description.

Dust Langmuir wave regime ($k_{cr}^2\lambda_D^2 \gg 1$)

On the other hand, when $k_{cr}^2\lambda_D^2 \gg 1$, the critical wavenumber k_{cr} is given by

$$k_{cr}^2 = \frac{2(\omega_{Jd}^2-\omega_{pd}^2)}{c_{sd}^2}, \tag{8.13}$$

an expression which naturally is effective only for warm dust species and requires the domination of the self-gravitational forces over the electrostatic forces ($\omega_{Jd} > \omega_{pd}$).

8.4 Growth rates in case of gravitational instability

Now we check if perturbations associated with wavenumbers $k < k_{cr}$ indeed correspond to a gravitational instability, as was the case for the wave treatment in self-gravitating plasmas within the framework of a fluid description. For that we substitute $\omega = i\gamma$ into (8.7), with γ real and positive, since Jeans instabilities are of a purely growing nature. Using the relation

$$\int_0^\infty \frac{x^2}{x^2+b^2}\exp(-x^2)dx = \frac{\sqrt{\pi}}{2}\left[1-\sqrt{\pi}b\exp(b^2)\,\mathrm{erfc}(b)\right], \tag{8.14}$$

where

$$\begin{aligned}\mathrm{erfc}(b) &= 1-\mathrm{erf}(b)\\ &= 1-\frac{2}{\sqrt{\pi}}\int_0^b \exp\left(-\xi^2\right)d\xi,\end{aligned} \tag{8.15}$$

denotes the complementary error function, we find that

$$\begin{aligned}I_\alpha &= \frac{2n_{\alpha 0}}{c_{s\alpha}^2}\left[1-\sqrt{\pi}b_\alpha\exp(b_\alpha^2)\,(1-\mathrm{erf}(b_\alpha))\right] \\ &\equiv \frac{2n_{\alpha 0}}{c_{s\alpha}^2}F_\alpha.\end{aligned} \tag{8.16}$$

Here $b_\alpha = \gamma/kc_{s\alpha}$ and F_α is short-hand for the expression between square brackets. The equations (8.1)–(8.4) thus result in the following expression for the general dispersion law

$$\left(1 + \frac{F_e}{k^2\lambda_{De}^2} + \frac{F_i}{k^2\lambda_{Di}^2}\right)\left(1 - \frac{F_d}{k^2\lambda_{Jd}^2}\right) + \frac{F_d}{k^2\lambda_{Dd}^2} = 0, \tag{8.17}$$

which will be analyzed in the regimes for dust Langmuir and dust-acoustic waves, respectively.

Dust Langmuir waves

The relation (8.17) is plotted in Fig. 8.1 for the dimensionless variables $\omega^2/(\omega_{Jd}^2 - \omega_{pd}^2)$ and k^2/k_{cr}^2. In order to discern the modifications due to the kinetic description, the dispersion relation for the fluid model is also plotted. The latter corresponds to

$$\frac{\omega^2}{\omega_{Jd}^2 - \omega_{pd}^2} = \frac{k^2}{k_{cr}^2} - 1. \tag{8.18}$$

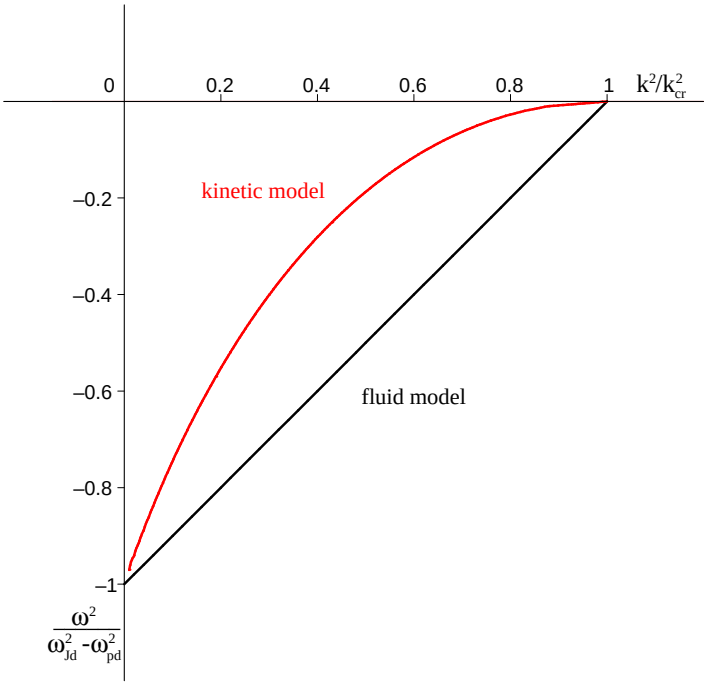

Fig 8.1: Unstable branch of the dispersion relation (8.17) for dust Langmuir waves ($k^2\lambda_D^2 \gg 1$) in a fluid and kinetic description.

As could be anticipated, the perturbations indeed grow for wavenumbers smaller than k_{cr}, but the growth rates generally are quite different in both plasma models. This result

conforms to the kinetic analysis of a self-gravitating neutral system [Binney and Tremaine 1987], which becomes clear if one replaces the Jeans frequency of the neutral species by an effective Jeans frequency, defined as $\omega^2_{J,\mathrm{eff}} = \omega^2_{Jd} - \omega^2_{pd}$.

Dust-acoustic waves

We continue the analysis of the approximate solutions of (8.17), now in the regime of the dust-acoustic waves ($k^2_{cr}\lambda^2_D \ll 1$), when $k \to k_{cr} - 0$. Introducing dimensionless variables $y = \omega^2/\omega^2_{Jd}$ and $x = k^2/k^2_{cr}$, we can expand the functions $F_\alpha\left(\sqrt{-y/2x}\right)$ for small arguments, i.e. $y/x \ll 1$. Then one can obtain the simplified dispersion relation as

$$y = -x(1-x)^2/\pi \tag{8.19}$$

or

$$\omega^2 = -\frac{k^2 c^2_{da}}{\pi}\left(1 + \frac{\lambda^2_{Dd}}{\lambda^2_D}\right)\left[1 - \frac{k^2}{k^2_{cr}}\right]^2. \tag{8.20}$$

The difference in growth rate of the dust-acoustic perturbations between the kinetic and fluid approach is illustrated in Fig. 8.2, for wavenumbers located as $k \to k_{cr} - 0$.

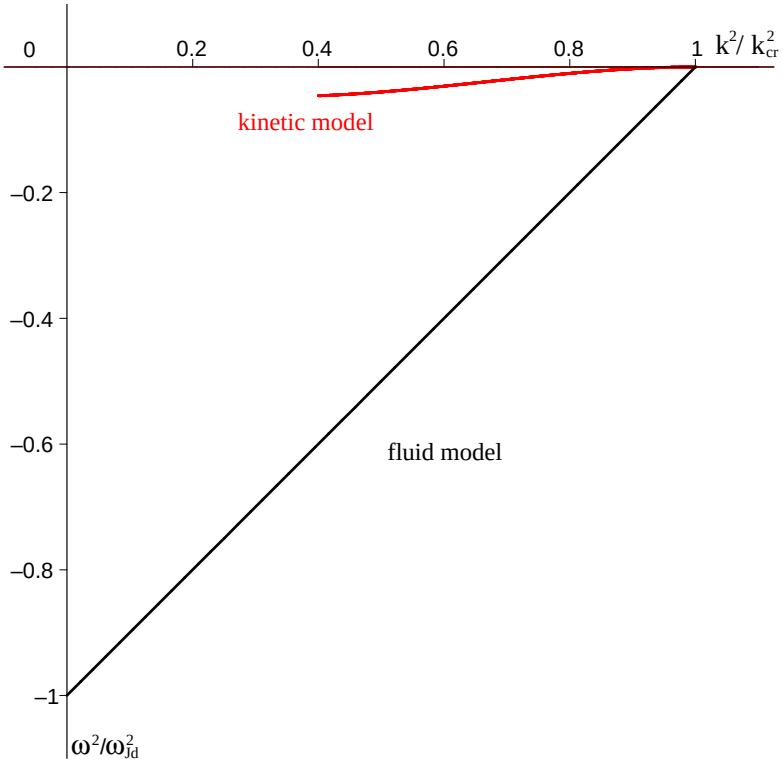

Fig 8.2: Dispersion relations analogous to Fig.8.1 but now in the dust-acoustic regime ($k^2\lambda^2_D \ll 1$)

Note that the validity of the curve associated to the kinetic model is limited to the vicinity of $k \to k_{cr} - 0$ and therefore not plotted for the entire range wavenumber range $k < k_{cr}$. We conclude that for the dust Langmuir waves and the dust-acoustic waves there is a gravitational instability for $k < k_{cr}$ both in a fluid as in a kinetic model. The growth rates however differ significantly, the perturbations in the fluid description grow much faster than in the kinetic one.

8.5 Electrostatic waves in self-gravitating plasmas

After having dealt with the unstable wavenumber regions, we now turn to $k > k_{cr}$ and analyze the concomitant stable modes in a self-gravitating dusty plasma. The denominator of the integrand in (8.9) represents a complex pole and for rather weak instabilities ($0 \ll |\Im(\omega)| \ll \Re(\omega)$), we must apply Landau's prescription for specifying the integration contour [Landau 1946]. Accordingly, the contour of integration in the complex v plane bypasses the pole singularity at $\omega = kv$ from below and we obtain from (8.9) [Fridman and Polyachenko 1984, p. 32-33]

$$I_\alpha = \frac{2n_{\alpha 0}}{c_{s\alpha}^2} \left(1 + i\sqrt{\pi} z_\alpha W(z_\alpha)\right), \tag{8.21}$$

where $z_\alpha = \omega / k c_{s\alpha}$ is a dimensionless frequency and W is the Kramp function [Faddeeva and Terentjev 1954, Fridman and Polyachenko 1984]

$$W(z) = \exp(-z^2) \left[1 + \frac{2i}{\sqrt{\pi}} \int_0^z \exp x^2 dx\right]. \tag{8.22}$$

The last term between the square brackets in (8.22) is visibly related to the Error function for complex arguments and as such this result is a extension of expression (8.16).

In other textbooks, one rather deals with the Plasma Dispersion function ($\equiv i\sqrt{\pi} W[z]$) [Fried and Conte 1961] or a function $Z(z) \equiv i\sqrt{\pi} z W(z)$ [Faddeeva and Terentjev 1954]. The book written by Ishimaru [1973] uses yet another closely related function ($\equiv W[z/\sqrt{2}]$).

Implementing the previous expressions, we are able to write the dispersion equation (8.1) in the form

$$\varepsilon(\omega, k) = 1 + \sum_{\alpha=e,i,d} \frac{1 + i\sqrt{\pi} z_\alpha W(z_\alpha)}{k^2 \lambda_{D\alpha}^2} + \frac{\left[\sum\limits_{\alpha=e,i,d} \dfrac{1 + i\sqrt{\pi} z_\alpha W(z_\alpha)}{k^2 \lambda_{D\alpha} \lambda_{J\alpha}}\right]^2}{1 - \sum\limits_{\alpha=e,i,d} \dfrac{1 + i\sqrt{\pi} z_\alpha W(z_\alpha)}{k^2 \lambda_{J\alpha}^2}} = 0. \tag{8.23}$$

Further on in the analytic analysis the asymptotic expansions of the dispersion function $W(z)$ are called for, both for small and large arguments and here we list these asymptotic approximations, according to Faddeeva and Terentjev [1954],

a) $|z| \gg 1$, $\mathrm{Re}\{z\} \gg \mathrm{Im}\{z\}$, $\mathrm{Im}\{z\} < 0$

$$\begin{aligned} W(z) &= \frac{i}{\sqrt{\pi}z}\left(1+\sum_{n=1}^{\infty}\frac{(2n)!}{n!\,(2z)^{2n}}\right)+\exp(-z^2) \\ &= \frac{i}{\sqrt{\pi}z}\left(1+\sum_{n=1}^{\infty}\frac{1\cdot 3\ldots(2n-1)}{(2z^2)^n}\right)+\exp(-z^2) \\ &= \frac{i}{\sqrt{\pi}z}\left(1+\frac{1}{2z^2}+\frac{3}{4z^4}+\ldots\right)+\exp(-z^2). \end{aligned} \tag{8.24}$$

b) $|z| \ll 1$

$$W(z) = 1+\frac{2iz}{\sqrt{\pi}}+\ldots \tag{8.25}$$

The wave frequency ω as well as the dispersion relation $\varepsilon(\omega,k)$ are split in their respective real and imaginary parts and for this we use the standard notations $\omega = \omega_0 + i\gamma$ and $\varepsilon(\omega,k) = \varepsilon_r + i\varepsilon_i$. Furthermore, as already mentioned for the calculation of the Landau contour, we assume that the instabilities are sufficiently weak so that $|\gamma| \ll |\omega_0|$ and analogously $|\varepsilon_i| \ll |\varepsilon_r|$.

We prefer to study the very low wave frequencies for which the dust dynamics are involved in the wave processes, more specifically we restrict the analysis to those wave frequencies that obey the inequality $kc_{sd} \ll \omega \ll kc_{si}, kc_{se}$. For a orderly discussion of these low-frequency waves in self-gravitating plasmas, we define a parameter

$$\Delta = \frac{\omega_{Jd}^2}{\omega_{pd}^2}\left(1+\frac{1}{k^2\lambda_D^2}\right), \tag{8.26}$$

which is essentially a measure for the influence of self-gravitation. For the aforementioned phase velocities $\omega \gg kc_{sd}$, the dispersion relation (8.23) can be transformed into the form

$$\begin{aligned} 1 &+ \frac{1}{k^2\lambda_D^2}\left[1+\frac{i\omega\sqrt{\pi}}{k(1+\delta)}\left(\frac{1}{c_{si}}+\frac{\delta}{c_{se}}\right)\left(1+\frac{\omega_{Jd}^2}{\omega^2}\right)\right] \\ &- (1-\Delta)\left[\frac{\omega_{pd}^2}{\omega^2}\left(1+\frac{3k^2c_{sd}^2}{2\omega^2}\right)-i\sqrt{\pi}\frac{\omega}{kc_{sd}}\frac{1}{k^2\lambda_{Dd}^2}\exp\left(-\frac{\omega^2}{k^2c_{sd}^2}\right)\right]=0, \end{aligned} \tag{8.27}$$

with the newly introduced parameter

$$\delta = \frac{\lambda_{Di}^2}{\lambda_{De}^2} = \frac{T_i}{T_e}\frac{n_e}{n_i} \tag{8.28}$$

measuring the influence of the electron component on the dust modes. For dusty plasmas where the dust particles are negatively charged due to the adsorption of electrons, the resulting electron density depletion sees to it that typically $\delta < 1$ or even $\delta \ll 1$. In

astrophysical dusty plasmas that are characterized by such extremely small values of δ, the plasma electrons have been almost completely devoured by the dust grains and allows for a model consisting only of ions and charged dust grains [Goertz 1989]. On the other hand, values for δ larger than unity can occur in isothermal plasmas ($T_e \simeq T_i$) with positively charged grains.

Because of the inequalities $|\gamma|, kc_{sd} \ll \omega \ll kc_{si}$, the imaginary part of (8.27) is small compared to the real part and we can easily Taylor expand the dispersion relation around $\gamma = 0$, which yields a real frequency

$$\omega_0^2 = \frac{\omega_{pd}^2(1-\Delta)}{1+\frac{1}{k^2\lambda_D^2}} \left[1 + \frac{3k^2\lambda_{Dd}^2\left(1+\frac{1}{k^2\lambda_D^2}\right)}{1-\Delta} \right], \tag{8.29}$$

and a growth rate

$$\begin{aligned} \gamma &= -\varepsilon_i(\omega_0) \left[\left. \frac{\partial \varepsilon_r}{\partial \omega} \right|_{\omega=\omega_0} \right]^{-1} \\ &= -\frac{\sqrt{\pi}\omega_0^4}{2k^3\lambda_D^2\omega_{pd}^2(1-\Delta)} \left[\frac{\frac{1}{c_{si}}+\frac{\delta}{c_{se}}}{(1-\Delta)(1+\delta)} + \frac{(1-\Delta)\beta}{c_{sd}} \exp\left(-\frac{\omega_0^2}{k^2c_{sd}^2}\right) \right]. \end{aligned} \tag{8.30}$$

In the latter expression, the parameter

$$\beta = \frac{\lambda_D^2}{\lambda_{Dd}^2} = \frac{2c_{da}^2}{c_{sd}^2} \tag{8.31}$$

has been introduced, so that β typically is quite large. From this, we deduce that the condition $\omega \gg kc_{sd}$ necessitates

$$k^2\lambda_{Dd}^2 + \frac{1}{\beta} \ll |1-\Delta|. \tag{8.32}$$

As a consequence, weakly damped low-frequency modes with frequencies (8.29) can only exist in the long-wavelength range $k^2\lambda_{Dd}^2 \ll |1-\Delta|$ and in self-gravitating dusty plasmas for which $1 \ll \beta|1-\Delta|$. As the self-gravitational influences increase, these requirements for the low-frequency modes will become harder to fulfill and certainly more stringent than in the usual dusty plasmas.

Again, we will subdivide the further study of the eigenmodes two-ways, and treat the limits which either involve much shorter or much larger wavelengths than the plasma Debye length.

8.6 Analogue of dust-acoustic modes

In the long-wavelength limit $k^2\lambda_D^2 \ll 1$ we encounter the analogue of the classic dust-acoustic mode in dusty self-gravitating plasmas and will discuss its modifications due to

self-gravitation. The real frequency (8.29) and damping decrement (8.30) reduce to

$$\omega_0^2 \simeq k^2 c_{da}^2 \left[(1-\Delta)(1-k^2\lambda_D^2) + \frac{3}{\beta} \right], \tag{8.33}$$

and

$$\begin{aligned} \gamma \;=\; & -\sqrt{\frac{\pi}{8}} k c_{da} \left\{ \left(\frac{\omega_{pd}}{\omega_{pi}} + \frac{\omega_{pd}}{\omega_{pe}} \delta^{3/2} \right) (1+\delta)^{-3/2} \right. \\ & \left. + (1-\Delta)^2 \beta^{3/2} \exp\left[-\frac{3+(1-\Delta)\beta}{2} \right] \right\}, \end{aligned} \tag{8.34}$$

and for these small wavenumbers we can safely redefine the parameter Δ as $\Delta \simeq \omega_{Jd}^2/k^2 c_{da}^2$. If self-gravitation is negligible, we simply set $\Delta = 0$ and the expressions (8.33) and (8.34) lead to the recovery of the dispersion relations obtained earlier in a kinetic approach for dust-acoustic waves [Melandsø et al. 1993b].

We have seen that in the dust-acoustic regime, the stable modes correspond to $k > k_{cr} = \omega_{Jd}/c_{da}$, so that for these stable modes always $\Delta < 1$. Having established the precise form of the real frequency and damping decrement in the dust-acoustic regime, these expressions are now explored in order to establish the influence of self-gravitation. First of all, we should note that dust-acoustic waves usually are almost nondispersive in the long-wavelength regime. Since $k^2\lambda_D^2 \ll 1$, the phase velocity of long-wavelength disturbances reads as $v_{ph} = \omega_{pd}\lambda_D$, which indeed reflects the independency of the phase velocity with respect to the wavelength. In a self-gravitating plasma however, dust-acoustic mode is slightly modified and no longer nondispersive, as shown by the expression for the phase velocity

$$v_{ph} \simeq \omega_{pd}\lambda_D \sqrt{1 - \frac{\omega_{Jd}^2}{k^2 c_{da}^2}}. \tag{8.35}$$

Clearly, the dispersive part of the phase velocity is solely due to the self-gravitational effects. Furthermore, a peculiarity of the dust-acoustic wave in a self-gravitating plasma is its damping (8.34). By and large, the electron depletion in astrophysical plasmas is quite important, and for convenience we compare the different terms in (8.34) for a case $\delta \simeq 0$. Then the global Debye length λ_D reduces to λ_{Di} and (8.34) becomes

$$\gamma \simeq -\sqrt{\frac{\pi}{8}} \frac{k c_{da}^2}{c_{si}} \left\{ 1 + (1-\Delta)^2 \beta \frac{c_{si}}{c_{sd}} \exp\left[-\frac{(1-\Delta)\beta}{2} \right] \right\}. \tag{8.36}$$

Because usually $\beta c_{si} \gg c_{sd}$, we see that the second term between curly brackets makes the main contribution to the damping rate and this term is largely controlled by self-gravitation. Also for other values of δ, the heavy nature of the dust particles will see to it that the second term in (8.34) dominates. But when dealing with large values of the parameter β, one has to be more cautious, the exponential term will diminish quickly for larger β and so will the influence of self-gravitation on the damping rate. Hence, when studying self-gravitational effects we have to restrict our analysis to those values of β for which the second term of (8.34) prevails. This is equivalent to stating that inside the

curly brackets the term $\beta^{3/2}\exp(-\beta/2)$ has a much larger part than $\omega_{pd}/\omega_{pi}+\omega_{pd}\delta^{3/2}/\omega_{pe}$. Moreover, for the dust the Jeans frequency ω_{Jd} must be larger than the plasma frequency ω_{pd} but not all too much as otherwise the self-gravitational effects again become insignificant. Deliberating carefully these considerations indicates that the modifications due to gravitational influences are significant for parameter values that keep β smaller than 50 [Yaroshenko et al. 2001b].

The typical evolution of the wave decrement of the dust-acoustic wave in such self-gravitational plasmas is illustrated in Fig. 8.3, where the ratio $|\gamma|/kc_{da}$ is shown as a function of Δ and where the parameter β is fixed to a value $\beta = 20$.

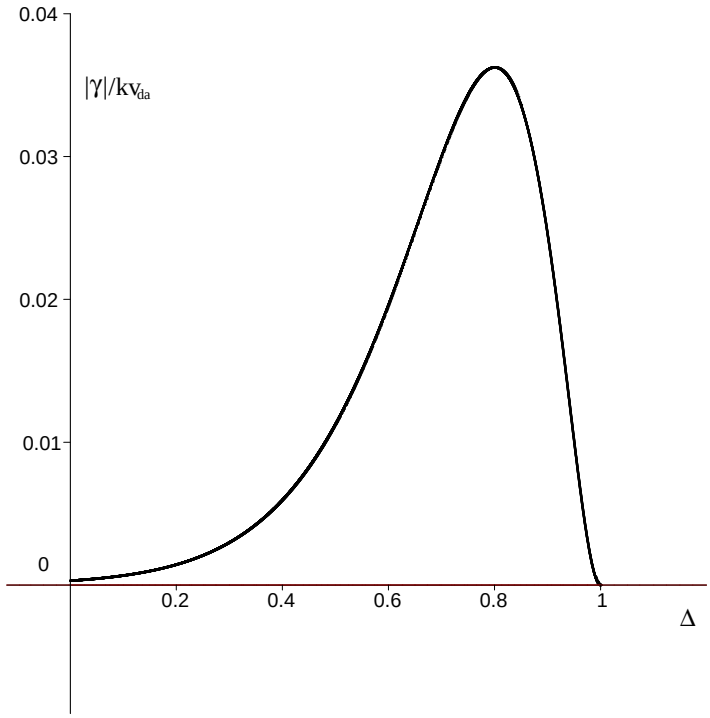

Fig 8.3: Effect of self-gravitation on Landau damping of the dust-acoustic wave for $\beta = 20$

The curve in Fig. 8.3 demonstrates that the damping effect can grow considerably when the gravitational interactions intensify, especially when $\Delta \to 1$ is realized. We see that the decrement rate corresponding with the peak practically dwarfs the decrement rate for a usual dust-acoustic wave in dusty plasmas without self-gravitation, in case of which $\Delta = 0$. In the near vicinity of $\Delta = 1$ the damping drops to zero, an observation that is not at all surprising because this situation is associated with a relation $\omega_{Jd}^2 = k^2 c_{da}^2$ or $k = k_{cr}$. In other words, $\Delta = 1$ implies a marginally stable configuration and thus denotes a turning point for the sign of the damping rate.

From a physical point of view, the explanation of the rather high damping rate for $\Delta \to 1$ is quite simple. The damping rate of a wave is proportional to the difference in numbers of slow and fast captured particles, *i.e.* the particles that are slower respectively faster than the phase velocity of the wave. Because primarily the particles near the phase velocity determine the damping rate, this difference in numbers is proportional to the following expression

$$N_{\text{slow}} - N_{\text{fast}} \sim - \left. \frac{df_{0d}}{dv} \right|_{v=\frac{\omega_0}{k}}, \tag{8.37}$$

which is a positive quantity since a Maxwellian distribution makes sure that there are more particles with velocities smaller than the phase velocity than there are with larger velocities. It follows that for a Maxwellian distribution (8.6), the number N of dust particles which can effectively interact with the dust-acoustic wave can be expressed as

$$N \sim (1-\Delta)^{1/2} \exp\left[-\frac{(1-\Delta)\beta}{2} \right]. \tag{8.38}$$

When the influence of self-gravitation strengthens and thus $\Delta \to 1$, the number of resonant dust particles N is forced up too and achieves a maximum at $\Delta_m = 1 - 1/\beta$. When the parameter Δ approaches unity, the number of resonant particles thus becomes so large that the damping rate builds up crucially and surpasses the Landau damping rate for usual dust-acoustic waves considerably. We remark that $\Delta \sim \Delta_m$ implies $1/\beta \simeq |1-\Delta|$, so that the condition (8.32) is not satisfied in the immediate vicinity of Δ_m. This means that the picture of absorption of the dust-acoustic waves is not entirely accurate in the neighbourhood of Δ_m, where this approach rather serves as a rough indication for the anomalous damping rate due to self-gravitational effects.

The increase of the damping rate due to the self-gravitational interactions can be demonstrated also from another perspective. This is established by considering the dimensionless damping rate $|\gamma|/\omega_{Jd}$, obtained from (8.34), as a function of the normalized wavenumbers k/k_{cr}. Here, the critical Jeans wavenumber is approximately $k_{cr} \simeq \omega_{Jd}/c_{da}$ and we focus on arguments $k/k_{cr} > 1$ as we are investigating the eigenmodes of the dust-acoustic wave. The functional relation between $|\gamma|/\omega_{Jd}$ and k/k_{cr} is illustrated in Fig. 8.4 for different values of β, all smaller than 50.

Again we see that the perturbations damp strongly when $k \to k_{cr} + 0$ and we notice also that larger values of β enfeeble the influence of self-gravitation. The latter points out that particularly the parameter β is of a major influence on the decrement rate in the wavenumber region where the damping is at its peak. For large values of β, the modifications of the usual damping rate for dust-acoustic waves will be rather minor.

Both approaches make abundantly clear that for self-gravitational dusty plasmas in which the parameter β has a typical value of no more than 50, the existing disturbances, characterized by wavenumbers

$$k \sim \left(1 + \frac{1}{2\beta} \right) \frac{\omega_{Jd}}{c_{da}}, \tag{8.39}$$

are subjected to a strong attenuation because of the self-gravitational effects. In other words, for given values of the dust plasma and Jeans frequencies, the dust-acoustic waves

with $k \sim \omega_{Jd}(1 + 1/2\beta)/c_{da}$ can hardly propagate in surroundings where $10 < \beta < 50$ holds.

This detailed study of the kinetic model for dust sound waves in dusty self-gravitating plasmas pinpoints the deficiencies of the fluid model. Whereas stable wave modes with small wavelengths $\lambda < 2\pi c_{da}/\omega_{Jd}$ survive unhindered in a fluid approach, the kinetic analysis shows that they are in fact strongly damped due to collisionless Landau damping, in particular for wavenumbers $k \to k_{cr} + 0$. However, the fluid dispersion equation succeeds in providing exactly the same critical wavenumber as the much more intricate kinetic dispersion relation.

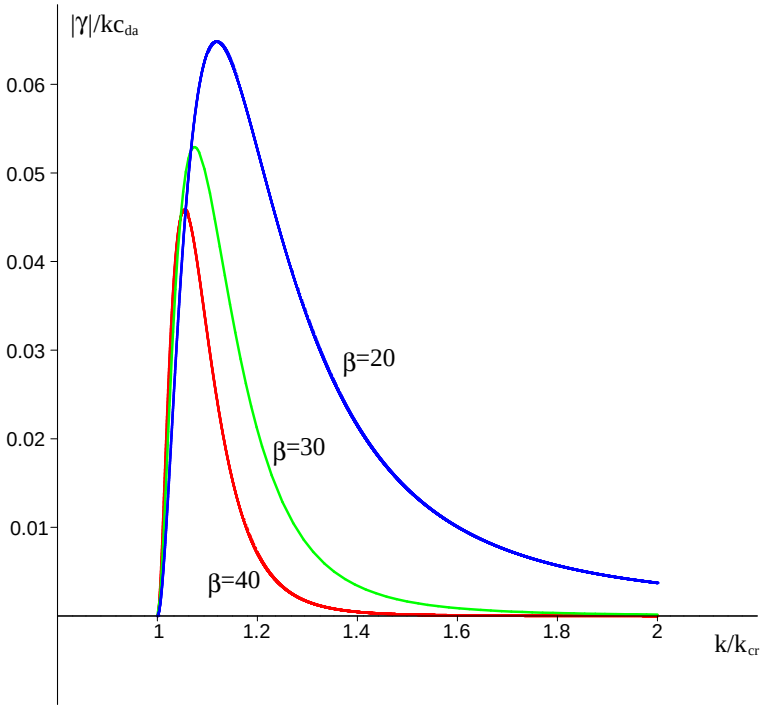

Fig 8.4: Landau damping vs k/k_{cr} for the analogue of the dust-acoustic wave in self-gravitating plasmas

8.7 Dust Langmuir waves

Finally, we turn back to the dust Langmuir regime, for which we determined the critical wavenumber in (8.13). In order to meet the imposed requirement (8.32), the wavenumbers must comply with both $k^2\lambda_D^2 \gg 1$ and $k^2\lambda_{Dd}^2 \ll |1 - \Delta|$. In this regime, the spectrum reads as

$$\begin{aligned} \omega_0^2 &\simeq \omega_{pd}^2 \left(1 - \Delta + 3k^2\lambda_{Dd}^2\right), \\ &= \omega_{pd}^2 - \omega_{Jd}^2 + 3k^2 c_{sd}^2 \end{aligned} \tag{8.40}$$

where the dimensionless parameter Δ is now defined as $\Delta = \omega_{Jd}^2/\omega_{pd}^2$. For stable wave modes, we have $\Delta < 1$ and the corresponding damping decrements are given by

$$\gamma \simeq -\sqrt{\frac{\pi}{8}}\frac{\omega_{pd}}{k^3\lambda_D^3}\left\{\left(\frac{\omega_{pd}}{\omega_{pi}}+\frac{\omega_{pd}}{\omega_{pe}}\delta^{3/2}\right)(1+\delta)^{-3/2} + (1-\Delta)^2\beta^{3/2}\exp\left[-\frac{3}{2}-\frac{(1-\Delta)\omega_{pd}^2}{k^2c_{sd}^2}\right]\right\}. \tag{8.41}$$

In the determination of the critical wavenumbers, it was already noted that the analogon of dust Langmuir waves in self-gravitating plasmas takes after the usual Langmuir waves if one introduces the effective plasma frequency of the dust particles, defined through $\omega_{p,\mathrm{eff}}^2 = \omega_{pd}^2 - \omega_{Jd}^2$. Indeed, the equations (8.40) and (8.41) formally reduce to the dispersion relations for ion Langmuir waves in electron-ion plasmas [Krall and Trivelpiece 1973, Akhiezer et al. 1975], with the effective plasma frequency being the acting representative of the plasma frequency. For the dust Langmuir waves, the parameter Δ is independent of the wave number and for self-gravitating dusty plasmas where the plasma frequency is close to but smaller than the Jeans frequency ($\Delta \to 1$), the dust Langmuir waves also diminish with large damping decrements. The mechanisms responsible for the strong damping are akin to their counterparts in the dust-acoustic wave description and conclusions can be borrowed from the previous section, except that the requirements for β are less stringent because of the different argument in the exponential.

8.8 Conclusions

The use of a kinetic procedure in the stability analysis of low-frequency waves in homogeneous self-gravitating plasmas bears out the Jeans instability criterion as obtained from a hydrodynamical approach. In both models a critical wavenumber is obtained, which separates the stable and the instable modes. But the more general kinetic approach makes clear that the fluid model overlooks the strong attenuation of the dust-acoustic modes for very short wavelengths. The mechanism responsible for complicating the propagation of these stable modes is the collisionless Landau damping. This mechanism is particularly effective for wavenumbers slightly larger than the critical wavenumber and can only be studied in a kinetic framework. It is found that the damping of the dust-acoustic perturbations in self-gravitating plasmas strongly depends on the values of the plasma parameters, especially on β. For parameter values of $10 < \beta < 50$, the impact of Landau damping is considerable and accordingly the damping rate is much higher than for the usual dust-acoustic waves, which is predominantly noticeable for wavenumbers near the critical values. This means that in such self-gravitating plasmas, there exists a range of wavenumbers in which dust-acoustic modes can barely be excited. On the other hand, for larger values, typically $\beta > 50$, the damping rates are just about unchanged. Moreover, the growth rates of the Jeans instability are also quite different, the unstable seeds of instability grow much faster in a fluid approach than in an approach which is outlined by kinetic considerations.

Chapter 9

Continuous dust size distributions

In many astrophysical dusty plasmas, the size of the dust components spans a wide, almost continuous range. For this reason, we will now generalize the kinetic approach for dust-acoustic modes to self-gravitating plasmas which comprise a continuous size distribution. The framework of a kinetic analysis is necessary for an accurate description of a continuous size spectrum, as treating such a spectrum in a hydrodynamical manner inevitably poses some fundamental problems [Bliokh et al. 1995, Verheest 2000]. Indeed, a hydrodynamical treatment of a continuous size spectrum involves integration procedures which are complicated by the fact that the denominator of the integrand will vanish for some arguments. In order to deal with the poles of the integrands, a procedure akin to the procedures encountered in a treatment of Landau damping is required, which is unavoidably outside the reach of a fluid approach.

Observational data indicate that a realistic dust size distribution can be approximated quite accurately by means of a decreasing power law [Meuris 1998] and we therefore focus on such distributions. The precise value of the exponent of the involved power law is decisive for the relative importance of the larger dust grains in the self-gravitational mechanisms and it turns out that the larger dust grains come into force only for power laws that decrease faster than a quartic. Further, the damping effects for analogues of dust-acoustic modes are investigated, to show whether a power-law distribution of dust-particle sizes influences the Landau damping in a self-gravitating dusty plasma [Yaroshenko et al. 2001a].

As we have established in the previous chapter, the inclusion of self-gravitation fortifies the influence of Landau damping in certain parameter ranges. In this way, we generalize the results for continuous size distributions of Brattli et al. [1997] to self-gravitational plasmas. In these investigations, we have preferred an analytical approach, which implies far more flexibility concerning the parameter input than the study of Brattli et al. [1997] does, but their numerical analysis allowed for the inclusion of charge fluctuations, whereas we assumed constant dust charges.

9.1 Dispersion relation for a continuous dust mass spectrum

For the kinetic analysis of the dust-acoustic mode in a self-gravitating plasma containing multiple dust species, we keep the assumption of inertialess electrons and ions and continue using the dispersion relation (8.23),

$$\varepsilon(\omega,k) \equiv 1 \; + \sum_{\alpha=e,i,d} \frac{1+i\sqrt{\pi}z_\alpha W(z_\alpha)}{k^2\lambda_{D\alpha}^2} + \frac{\left[\displaystyle\sum_{\alpha=e,i,d} \frac{1+i\sqrt{\pi}z_\alpha W(z_\alpha)}{k^2\lambda_{D\alpha}\lambda_{J\alpha}}\right]^2}{1-\displaystyle\sum_{\alpha=e,i,d} \frac{1+i\sqrt{\pi}z_\alpha W(z_\alpha)}{k^2\lambda_{J\alpha}^2}} = 0, \quad (9.1)$$

but now the summation index runs over every dust species, which are all assumed to be negatively charged. We recall that the dimensionless arguments are defined per species α through $z_\alpha = \omega/kc_{s\alpha}$ and that $W(z)$ denotes the Kramp function [Faddeeva and Terentjev 1954].

In realistic astrophysical applications of dusty plasmas, the dust grains tend to come in all sizes and the plenitude of possible dust sizes can often be well modelled by a continuous spectrum that goes as a power law in the interspace between a minimal diameter value $a_{\min}$ and a maximum diameter $a_{\max}$. In general, this power law will be decreasing since in astrophysical situations the smaller particles are encountered more frequently. Accordingly, we investigate the influence of dust mass distributions through a differential density, defined as

$$n_d(a)da = N_0 a_0^{\mu-1} a^{-\mu} da \qquad (\mu > 0), \quad (9.2)$$

where the total number density N_0 is given by the expression

$$N_0 = \int_{a_{\min}}^{a_{\max}} n_d(a)da. \quad (9.3)$$

In the definition (9.2), we have introduced a characteristic size a_0, which is completely determined by the peculiarities of the power law distribution because of the normalization procedure (9.3) that defines the equilibrium density N_0. The characteristic size a_0 is connected with the boundaries $a_{\min}$ and $a_{\max}$ of the size interval and also with the exponent μ of the power law through

$$\frac{a_0^{\mu-1}}{\mu-1}\left(a_{\min}^{1-\mu} - a_{\max}^{1-\mu}\right) = 1. \quad (9.4)$$

If the range of sizes is fairly wide, then $a_{\min} \ll a_{\max}$ and for exponents $\mu > 1$, the relation (9.4) can be approximated as

$$\left(\frac{a_0}{a_{min}}\right)^{\mu-1} \simeq \mu - 1. \quad (9.5)$$

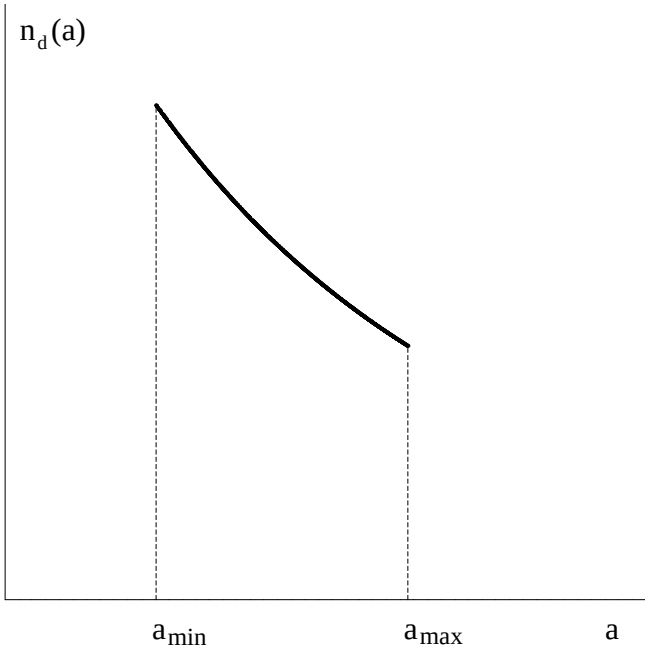

Fig 9.1: Differential density modelled as a decreasing power law

We are led by the standard dusty plasma model and thus assume homogeneous, spherical dust particles with the charges being congregated on the outer layer, so that the mass and charge can be expressed as

$$\begin{aligned} m(a) &= \frac{4}{3}\pi\rho a^3, \\ q(a) &= 4\pi\varepsilon_0 a\varphi_0, \end{aligned} \tag{9.6}$$

where ρ is the mass density of the grain material and φ_0 the electric surface potential at equilibrium. For simplicity, we presume the mass density and surface potential to be equal and time independent for all dust grains, assumptions both of which can be considered as a fair approximation in many astrophysical environments.

For power laws that decrease faster than a quadratic, the equation of quasi-neutrality is given by

$$\begin{aligned} q_i n_{i0} &= e n_{e0} + \int_{a_{\min}}^{a_{\max}} n_d(a) q_d(a) da, \\ &\simeq e n_{e0} + N_0 q_1 \frac{\mu - 1}{\mu - 2} \qquad (\mu > 2), \end{aligned} \tag{9.7}$$

where $q_1 = q(a_{\min}) = 4\pi\varepsilon_0\varphi_0 a_{\min}$ is the charge of the smallest grains, q_i the charge of the ions, and n_{e0} and n_{i0} are the unperturbed electron and ion densities.

For a continuous distribution, such as (9.2), the discrete summation over different grain

species in (9.1) is replaced by an integral, so that the dispersion law is now of the form

$$\left[1+\sum_{\alpha=e,i}\frac{1+i\sqrt{\pi}z_\alpha W(z_\alpha)}{k^2\lambda_{D\alpha}^2}+\int_{a_{\min}}^{a_{\max}}\frac{1+i\sqrt{\pi}z(a)W[z(a)]}{k^2\lambda_{Dd}^2(a)}da\right]\times$$
$$\times\left[1-\int_{a_{\min}}^{a_{\max}}\frac{1+i\sqrt{\pi}z(a)W[z(a)]}{k^2\lambda_{Jd}^2(a)}da\right]+\left[\int_{a_{\min}}^{a_{\max}}\frac{1+i\sqrt{\pi}z(a)W[z(a)]}{k^2\lambda_{Dd}(a)\lambda_{Jd}(a)}da\right]^2=0. \quad (9.8)$$

Here the generalizations

$$\begin{aligned}\lambda_{Dd}^2(a) &= \frac{\varepsilon_0 k_B T}{q^2(a)n_d(a)},\\ \lambda_{Jd}^2(a) &= \frac{k_B T}{4\pi m^2(a)n_d(a)},\end{aligned} \quad (9.9)$$

for the analogues of the Debye and Jeans lengths have been introduced, both of which quantities now display explicitly their size dependence. In these definitions, we have used the assumption of an equal temperature for all the dust particles ($T(a)=T\neq T_e,T_i$) and further we introduce extensions of the definitions used in the previous chapter, namely $z_{e,i}=\omega/kc_{se,si}$, $z(a)=\omega/kc_s(a)$ and $c_s^2(a)=2k_BT/m(a)$. We recall that due to their relative smallness all terms proportional to $\lambda_{Ji}^{-1}\sim m_i$ and *a fortiori* to $\lambda_{Je}^{-1}\sim m_e$ were omitted in the derivation of the dispersion law (9.8), which is now investigated specifically in the dust-acoustic regime.

9.2 Dust-acoustic modes in self-gravitating plasmas

In the dust-acoustic regime, the requirements for the phase velocity $kc_s(a_{\min})\ll\omega\ll kc_{si}$, c_{se}, result in the conditions $z_e,z_i\ll 1$ and $z(a_{min})\gg 1$. Consequently, we can apply anew the asymptotic expansions (8.24) for the Kramp function. Inserting these expansions into the dispersion law (9.8) yields [Yaroshenko et al. 2001a]

$$\left[1+\sum_{\alpha=e,i}\frac{1+\frac{i\sqrt{\pi}\omega}{kc_{s\alpha}}}{k^2\lambda_{D\alpha}^2}-\frac{\Omega_p^2}{\omega^2}\left(1+\frac{\Delta_p}{\omega^2}\right)+i\omega C_p\right]\cdot\left[1+\frac{\Omega_J^2}{\omega^2}\left(1+\frac{\Delta_J}{\omega^2}\right)-i\omega C_J\right]$$
$$+\left[\frac{\Omega_{pJ}^2}{\omega^2}\left(1+\frac{\Delta_{pJ}}{\omega^2}\right)-i\omega C_{pJ}\right]^2=0, \quad (9.10)$$

where the notations Ω_p, Ω_J and Ω_{pJ} stand for the effective dust plasma, Jeans and hybrid frequencies, respectively. Inherently, these effective frequencies are size independent and

are defined as

$$\Omega_p^2 = \int_{a_{\min}}^{a_{\max}} \frac{q^2(a) n_d(a)}{\varepsilon_0 m(a)} da = \int_{a_{\min}}^{a_{\max}} \widetilde{\omega}_p^2(a) da, \tag{9.11}$$

$$\Omega_J^2 = \int_{a_{\min}}^{a_{\max}} 4\pi G m(a) n_d(a) da = \int_{a_{\min}}^{a_{\max}} \widetilde{\omega}_J^2(a) da, \tag{9.12}$$

$$\Omega_{pJ}^2 = \int_{a_{\min}}^{a_{\max}} \widetilde{\omega}_p(a) \widetilde{\omega}_J(a) da. \tag{9.13}$$

The equations (9.11) and (9.12) define the quantities $\tilde{\omega}_p^2(a)$ and $\tilde{\omega}_J^2(a)$, and furthermore the newly introduced notations Δ_p, Δ_J and Δ_{pJ} represent the thermal corrections and are given through

$$\Delta_p = \frac{3k^2}{2\Omega_p^2} \int_{a_{\min}}^{a_{\max}} \widetilde{\omega}_p^2(a) c_s^2(a) da, \tag{9.14}$$

$$\Delta_J = \frac{3k^2}{2\Omega_J^2} \int_{a_{\min}}^{a_{\max}} \widetilde{\omega}_J^2(a) c_s^2(a) da, \tag{9.15}$$

$$\Delta_{pJ} = \frac{3k^2}{2\Omega_{pJ}^2} \int_{a_{\min}}^{a_{\max}} \widetilde{\omega}_p(a) \widetilde{\omega}_J(a) c_s^2(a) da. \tag{9.16}$$

Finally, the structure of (9.10) has been made more compact by representing the imaginary parts through the coefficients C_p, C_J and C_{pJ}, standing for

$$C_p = \frac{\sqrt{\pi}}{k^3} \int_{a_{\min}}^{a_{\max}} \frac{\exp\left[-\omega^2/k^2 c_s^2(a)\right]}{c_s(a) \lambda_{Dd}^2(a)} da, \tag{9.17}$$

$$C_J = \frac{\sqrt{\pi}}{k^3} \int_{a_{\min}}^{a_{\max}} \frac{\exp\left[-\omega^2/k^2 c_s^2(a)\right]}{c_s(a) \lambda_{Jd}^2(a)} da, \tag{9.18}$$

$$C_{pJ} = \frac{\sqrt{\pi}}{k^3} \int_{a_{\min}}^{a_{\max}} \frac{\exp\left[-\omega^2/k^2 c_s^2(a)\right]}{c_s(a) \lambda_{Jd}(a) \lambda_{Dd}(a)} da. \tag{9.19}$$

The complexity of the dispersion law (9.10) is tremendous and for this reason Brattli et al. [1997] have dealt with the kinetic effects of a size distribution on dust-acoustic waves in a numerical fashion. Their paper covers the possibility of fluctuating dusty charges but does not include the self-gravitational effects. We choose to continue analytically in order to determine the damping decrements and wave frequencies of dust acoustic modes for different size spectra.

We start with the imaginary part of the dispersion law (9.10), and denote the integrals (9.17)–(9.19) as

$$C_\nu = Q \int_{a_{\min}}^{a_{\max}} a^\nu \exp\left[-\omega^2/k^2 c_s^2(a)\right] da, \tag{9.20}$$

with Q being constant. This type of integral can be rewritten with the help of the following relation [Abramowitz and Stegun 1972]

$$\begin{aligned} C_\nu &= Q \int_{a_{\min}}^{a_{\max}} a^\nu \exp(-ba^3) da \\ &= -\frac{Q}{3} b^{-\frac{\nu+1}{3}} \Gamma\left(\frac{\nu+1}{3}, ba^3\right)\Big|_{a_{\min}}^{a_{\max}}, \end{aligned} \tag{9.21}$$

where, because of (9.6), the parameter $b = \omega^2/a^3 k^2 c_s^2(a)$ is independent of the dust diameter a and with $\Gamma(p,x)$ denoting the incomplete Gamma function

$$\Gamma(p,x) = \int_x^\infty \exp(-t)\, t^{p-1} dt. \tag{9.22}$$

Since the dust-acoustic regime corresponds to $kc_s(a) \ll \omega$, the second argument of the incomplete Gamma function in (9.21) satisfies $ba^3 = \omega^2/k^2 c_s^2(a) \gg 1$. Using the asymptotic expansion of $\Gamma(p,x)$ for large arguments x [Abramowitz and Stegun 1972], one can obtain

$$\begin{aligned} C_\nu &= -\frac{Q}{3b} a^{\nu-2} \exp\left(-ba^3\right)\Big|_{a_{\min}}^{a_{\max}} \\ &= -\frac{ak^2 c_s^2(a)}{3\omega^2} Q a^\nu \exp\left[-\frac{\omega^2}{k^2 c_s^2(a)}\right]\Big|_{a_{\min}}^{a_{\max}}. \end{aligned} \tag{9.23}$$

In this approximation, the expressions (9.17)–(9.19) can be noted in a simple fashion, namely as

$$C_p = \omega_p^2(a)\mathcal{E}(a)\big|_{a_{\min}}^{a_{\max}}, \tag{9.24}$$

$$C_J = \omega_J^2(a)\mathcal{E}(a)\big|_{a_{\min}}^{a_{\max}}, \tag{9.25}$$

$$C_{pJ} = \omega_p(a)\omega_J(a)\mathcal{E}(a)\big|_{a_{\min}}^{a_{\max}}, \tag{9.26}$$

where we have introduced

$$\begin{aligned} \omega_p^2(a) &= \frac{N_0 q^2(a)}{\varepsilon_0 m(a)}, \\ \omega_J^2(a) &= 4\pi G N_0 m(a), \end{aligned} \tag{9.27}$$

and where $\mathcal{E}(a)$ is shorthand for

$$\mathcal{E}(a) = -\frac{2\sqrt{\pi}}{3\omega^2 k c_s(a)} \left(\frac{a_0}{a}\right)^{\mu-1} \exp\left(-\frac{\omega^2}{k^2 c_s^2(a)}\right). \tag{9.28}$$

Using the notations (9.27) yields for the effective frequencies

$$\Omega_p^2 = -\frac{1}{\mu}\left(\frac{a_0}{a}\right)^{\mu-1}\omega_p^2(a)\Big|_{a_{\min}}^{a_{\max}}, \tag{9.29}$$

$$\Omega_J^2 = -\frac{1}{\mu-4}\left(\frac{a_0}{a}\right)^{\mu-1}\omega_J^2(a)\Big|_{a_{\min}}^{a_{\max}}, \tag{9.30}$$

$$\Omega_{pJ}^2 = -\frac{1}{\mu-2}\left(\frac{a_0}{a}\right)^{\mu-1}\omega_p(a)\omega_J(a)\Big|_{a_{\min}}^{a_{\max}}, \tag{9.31}$$

and for the associated thermal corrections

$$\Delta_p = -\frac{3k^2}{2\Omega_p^2}\left(\frac{a_0}{a}\right)^{\mu-1}\frac{\omega_p^2(a)c_s^2(a)}{\mu+3}\Big|_{a_{\min}}^{a_{\max}}, \tag{9.32}$$

$$\Delta_J = -\frac{3k^2}{2\Omega_p^2}\left(\frac{a_0}{a}\right)^{\mu-1}\frac{\omega_J^2(a)c_s^2(a)}{\mu-1}\Big|_{a_{\min}}^{a_{\max}}, \tag{9.33}$$

$$\Delta_{pJ} = -\frac{3k^2}{2\Omega_p^2}\left(\frac{a_0}{a}\right)^{\mu-1}\frac{\omega_p(a)\omega_J(a)c_s^2(a)}{\mu+1}\Big|_{a_{\min}}^{a_{\max}}. \tag{9.34}$$

For the further study of the dispersion law (9.1) in the dust-acoustic regime, we make the usual assumptions $|\omega_r| \gg |\gamma|$ and $|\varepsilon_r| \gg |\varepsilon_i|$, wherein the notations concerning the real and complex parts of $\varepsilon(\omega, k)$ and ω of the previous chapter remain. Now we describe the influence of the size distribution on the peculiarities of the dust-acoustic modes in dusty and self-gravitating plasmas and determine the sway of the precise form of the power law therein.

In order to provide a benchmark, we firstly consider a dusty plasma without self-gravitation ($\Omega_J = 0 = \Omega_{pJ}$), so that the coefficients Δ_J, Δ_{pJ}, C_J and C_{pJ} are equal to zero. In this case, the dispersion relation of Brattli et al. [1997] for dust-acoustic modes in a plasma with a dust size distribution is recovered, provided constant dust charges are assumed. The numerical analysis of Brattli et al. [1997] seems to indicate that the Landau damping in a dusty plasma with a power-law dust size distribution deviates only slightly from the Landau damping in a monodisperse dusty plasma wherein the dust particles all have a size equal to the average particle size of the distribution.

For a size spectrum (9.2) with values $\mu > 1$ and covering a substantial size range of the dust particles, so that $a_{\max} \gg a_{\min}$, the dispersion relation (9.10) reduces to

$$1 + \frac{1}{k^2\lambda_D^2}\left[1 + \frac{i\sqrt{\pi}\omega}{k(1+\delta)}\left(\frac{1}{c_{si}} + \frac{\delta}{c_{se}}\right)\right] - \frac{\Omega_p^2}{\omega^2}\left(1 + \frac{3\mu k^2 c_s^2(a_{min})}{2(\mu+3)\omega^2}\right) + \frac{2i\sqrt{\pi}\mu\Omega_p^2}{3\omega k c_s(a_{min})}\exp\left(-\frac{\omega^2}{k^2 c_s^2(a_{min})}\right) = 0, \tag{9.35}$$

where the parameter δ has the same meaning as in the previous chapter, namely $\delta = \lambda_{Di}^2/\lambda_{De}^2$. Note that the obtained dispersion law is insensitive to the upper limit of integration as long as $a_{\max} \gg a_{\min}$ holds, being in accordance with the conclusions of Brattli

et al. [1997]. For the study of the dust-acoustic mode, we can insert $k^2\lambda_D^2 \ll 1$, which yields for the frequency and damping rate, respectively

$$\omega_r^2 \;=\; \frac{1}{2}k^2U_{da}^2(1-k^2\lambda_D^2)\left[1+\sqrt{1+\frac{12\mu(1+k^2\lambda_D^2)}{(\mu+3)\beta}}\right], \tag{9.36}$$

and, for parameter values $\beta \gg 12\mu/(\mu+3)$,

$$\begin{aligned}\gamma \;\simeq\; & -\sqrt{\frac{\pi}{8}}kU_{da}\left\{(1+\delta)^{-3/2}\left(\frac{\Omega_p}{\omega_{pi}}+\frac{\Omega_p}{\omega_{pe}}\delta^{3/2}\right)\right. \\ & \left.+\frac{2\mu}{3}\sqrt{\beta}\exp\left[-\frac{\beta}{4}\left(1+\sqrt{1+\frac{12\mu}{(\mu+3)\beta}}\right)\right]\right\}. \end{aligned} \tag{9.37}$$

The dust-acoustic velocity $U_{da} = \Omega_p\lambda_D$ has been introduced and β is now given through

$$\beta = \frac{\lambda_D^2}{\lambda_{D1}^2} = \frac{2U_{da}^2}{c_s^2(a_{\min})}, \tag{9.38}$$

the definition of which incorporates the new quantity $\lambda_{D1}^2 = c_s^2(a_{min})/2\Omega_p^2$. Because of the assumptions $\mu > 1$ and $a_{\min} \ll a_{\max}$, the effective plasma frequency becomes

$$\Omega_p^2 = \frac{(\mu-1)\omega_p^2(a_{\min})}{\mu}. \tag{9.39}$$

We emphasize that a comparison with a monodisperse dusty plasma cannot be made by substituting $\mu = 0$, since all the previous equations require $\mu > 1$. Instead, we compare (9.36) and (9.37) to corresponding values in a monodisperse plasma, where all the dust particle have a size $a = a_{\min}$ and the total dust density equals N_0. Using the equation of charge neutrality (9.7), we can easily compute the ratios of the real frequencies and damping rates for both situations, with and without size distribution respectively. It turns out that both ratios depend only faintly on the parameter μ and this in a similar fashion, namely

$$\frac{\omega_{r,\mathrm{poly}}}{\omega_{r,\mathrm{mono}}} \sim \frac{\mu-2}{\sqrt{\mu(\mu-1)}} \sim \frac{\gamma_{r,\mathrm{poly}}}{\gamma_{r,\mathrm{mono}}}, \qquad \mu > 2. \tag{9.40}$$

However, the relative damping rate γ/ω_r for dust-acoustic modes in dusty plasmas with a power law dust size distribution is almost independent of μ, akin to the results of Brattli et al. [1997].

Including now the self-gravitational aspects of dusty plasmas, the general dispersion law (9.10) will display a stronger dependence on μ, due to the occurrence of the gravitational (Ω_J, Δ_J) and hybrid terms (Ω_{pJ}, Δ_{pJ}). Tacitly, it is assumed that μ differs from the critical values that would cause one of the denominators in (9.29)–(9.34) to vanish. For these critical values, one would simply have to establish the appropriate limiting expressions. For the terms purely associated with the electrostatic plasma interactions, *viz.* the terms (9.29) and (9.32), are almost entirely determined by the particles with the minimal size

$a_{\min}$. On the other hand, the dominant influence on the effective Jeans frequency (9.12) and the hybrid frequency can originate from either the smallest or largest grains, depending on the precise magnitude of μ. Since for distributions with a sufficiently wide size range $a_{\min} \ll a_{\max}$, the effective frequencies (9.29)–(9.31) can be rewritten as

$$\Omega_p^2 = \frac{\mu-1}{\mu}\omega_p^2(a_{\min})\left[1-\left(\frac{a_{min}}{a_{max}}\right)^{\mu}\right], \tag{9.41}$$

$$\Omega_J^2 = \frac{\mu-1}{\mu-4}\omega_J^2(a_{\min})\left[1-\left(\frac{a_{min}}{a_{max}}\right)^{\mu-4}\right], \tag{9.42}$$

$$\Omega_{pJ}^2 = \frac{\mu-1}{\mu-2}\omega_p(a_{min})\omega_J(a_{min})\left[1-\left(\frac{a_{min}}{a_{max}}\right)^{\mu-2}\right]. \tag{9.43}$$

It follows that for $\mu > 4$, primarily the smaller sized particles act upon the expressions for Ω_J and Ω_{pJ}, because of their abundant presence. Vice versa, the upper limit ($a_{\max}$) has the upper hand in the assessment of the effective Jeans frequency when $\mu < 4$, additionally the maximal diameter $a_{\max}$ also dominates the hybrid term when $\mu < 2$. Bearing in mind the observational data concerning dust distributions in real dusty plasma objects, especially the cases $\mu > 4$ and $2 < \mu < 4$ merit a further investigation.

9.2.1 Power law distributions with $\mu > 4$

For the case $\mu > 4$, we can reevaluate the real part of the general dispersion equation in the dust-acoustic regime (9.10), which becomes upon neglecting the small thermal terms,

$$\omega^4 - \omega^2\left(k^2U_{da}^2 - \Omega_J^2\right) - Ck^2U_{da}^2\Omega_J^2 = 0, \tag{9.44}$$

where the constant C is given through

$$C = \frac{4}{(\mu-2)^2}. \tag{9.45}$$

As the product of the roots of (9.44) for ω^2 is negative, there will always be one positive solution for ω^2, corresponding to a stable mode, as well as a purely imaginary mode for which $\omega^2 < 0$.

First, we discuss the case of a self-gravitating plasma wherein the self-gravitational effects are hardly influencing the propagation of the dust-acoustic mode, corresponding to $k^2U_{da}^2 \gg \Omega_J^2$. In this limit, the roots of (9.44) are given by

$$\omega_1^2 \simeq k^2U_{da}^2 - \Omega_J^2(1-C) \tag{9.46}$$

and

$$\omega_2^2 \simeq -C\Omega_J^2. \tag{9.47}$$

The first solution represents a generalized dust-acoustic wave, the size distribution of the dust grains is communicated through a increase of the dust-acoustic phase velocity, because

the distribution effectively reduces the effective Jeans frequency. Here, the definition of Δ, used in the previous chapter, would relate to a term $\Omega_J^2(1-C)/k^2U_{da}^2$, so that the influence of the size distribution is noticeable through both the factor $(1-C)$ and the definitions of Ω_p and Ω_J. Reinstating the earlier omitted thermal effects makes clear that they only act for a slight correction for the dust-acoustic branch (9.46), namely

$$\omega_1^2 \simeq k^2U_{da}^2\left(1+\frac{3\mu}{(3+\mu)\beta}\right)-\Omega_J^2(1-C). \tag{9.48}$$

This particular wave is always damped, and the damping decrement can be easily calculated in the same fashion as (9.37), yielding

$$\begin{aligned}\gamma \;=\; & -\sqrt{\frac{\pi}{8}}kU_{da}\left\{(1+\delta)^{-3/2}\left(\frac{\Omega_p}{\omega_{pi}}+\frac{\Omega_p}{\omega_{pe}}\delta^{3/2}\right)\right.\\ & \left.+\frac{2\mu\sqrt{\beta}}{3}\exp\left[-\frac{1}{2}\left(\frac{3\mu}{\mu+3}+\beta\right)+\frac{\beta\Omega_J^2(1-C)}{2k^2U_{da}^2}\right]\right\}.\end{aligned} \tag{9.49}$$

Both the real frequency and the expression for the damping decrement are strikingly similar to what was obtained for the dust-acoustic wave (9.36)–(9.37), but the damping rate can clearly be considerably influenced by self-gravitation and the size distribution, especially for power law distributions with a large exponent μ. The exception is dusty plasmas that are characterized by very large values of β, in case of which the exponential term in (9.49) hardly contributes to the damping rate and the expression for the damping rate practically mimics the expression (9.37) for the mono-sized dust case.

Since we are interested in the modifications due to the self-gravitational effects, we restrict therefore our analysis again to those values of β for which the second term of (9.49) is estimated to prevail, namely $\beta < 50$. In order to examine the influence of the size distribution on the damping rate of the dust-acoustic mode, we take a closer look at the self-gravitational terms in (9.49), the relative importance of which is proportional to

$$\frac{\Omega_J^2(1-C)}{k^2U_{da}^2}=\frac{\omega_J^2(a_{\min})\mu}{k^2\lambda_{Di}^2\omega_p^2(a_{\min})(\mu-4)}\left[1-\frac{4}{(\mu-2)^2}\right], \tag{9.50}$$

attaining a maximal value of

$$\left.\frac{\Omega_J^2(1-C)}{k^2U_{da}^2}\right|_{\mu=4}=\frac{4\omega_J^2(a_{\min})}{k^2\lambda_D^2\omega_p^2(a_{\min})}, \tag{9.51}$$

for the limit $\mu = 4$.

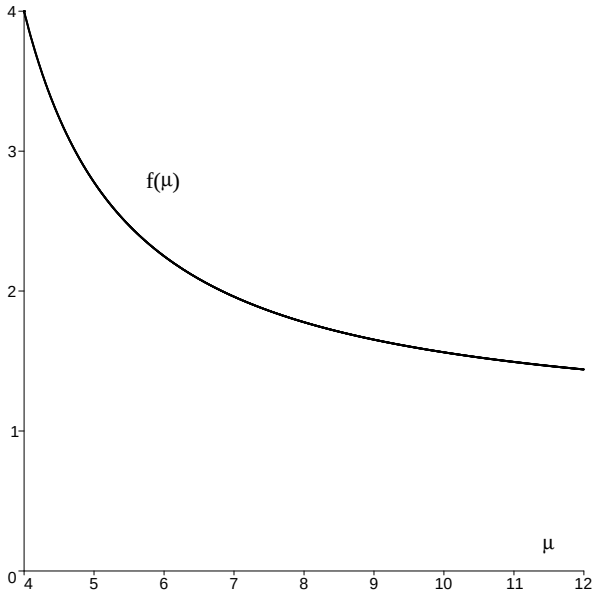

Fig 9.2: Variation of $f(\mu) = \frac{\mu}{\mu-4}\left[1 - \frac{4}{(\mu-2)^2}\right]$ for $\mu > 4$.

The figure 9.2 makes clear that for values of $\mu \sim 5 \div 7$ the contribution of the gravitational term is rather enhanced due to the size distribution. For very large values, typically $\mu > 10$, the influence of self-gravitation on the damping rate will be negligible as the dependence (9.50) will tend to 1. Moreover for large values of the exponent in the size distribution, the influence of the distribution on $U_{da} = \lambda_D \Omega_p$ is also small, as can be seen in the expression (9.41).

The negative root (9.47) gives rise to a weakly unstable mode, the frequency of which is negative and varies with μ as

$$\omega_2^2 = -\frac{\mu - 1}{\mu - 4}\left[1 - \frac{4}{(\mu-2)^2}\right]\omega_J^2(a_{\min}). \tag{9.52}$$

This new mode arises due to the presence of a size distribution and is thus a dust distribution instability. In this way the results of Meuris et al. [1997] are repeated and equation (9.44) matches the equation (32) of Meuris et al. [1997], provided one replaces the double summation in their equation by a double integral. Following the notations of Meuris et al. [1997], the situation $k^2 U_{da}^2 > \Omega_J^2$ corresponds to their condition $A > B$.

Next we consider the opposite case, when $k^2 U_{da}^2 \ll \Omega_J^2$. In this limit, the self-gravitational effects dominate and the roots of (9.44) are of the form

$$\omega_1^2 \simeq -\Omega_J^2 + k^2 U_{da}^2 (1 - C) \tag{9.53}$$

and

$$\omega_2^2 = C k^2 U_{da}^2. \tag{9.54}$$

The mode $\omega_1^2 < 0$ represents a modified Jeans instability, and the presence of a dust size distribution will only slightly affect the corresponding growth rate. The other solution $\omega_2^2 > 0$ has no analogon in a monodisperse plasma and thus represents a new stable mode, originating from the size dispersion. This mode is always attenuated, with a decrement

$$\gamma = -\sqrt{\frac{\pi}{8}} k U_{da} \left\{ (1+\delta)^{-3/2} \left(\frac{\Omega_p}{\omega_{pi}} + \frac{\Omega_p}{\omega_{pe}} \delta^{3/2} \right) + \frac{2\mu\sqrt{\beta}}{3} \exp\left[-\frac{C\beta}{2} \right] \right\}. \quad (9.55)$$

These results corroborate qualitatively with the analysis of dust-acoustic waves in a plasma with a number of discrete charged and neutral dust species, performed by Meuris et al. [1997]. However, the results of Meuris et al. [1997] are obtained within a fluid description and therefore provide no information about the damping effect for the different investigated modes.

9.2.2 Power law distributions with $2 < \mu < 4$

Finally, we turn to the dust-acoustic modes in self-gravitating plasmas with the exponent μ of the size distribution being sufficiently small, namely $2 < \mu < 4$. In that case, the gravitational terms in the general dispersion law (9.10) are practically insensitive to the smaller dust particles, being nearly exclusively determined by the heavier dust particles. In this limit the dispersion relation (9.44) is still valid but since now the gravitational terms are nearly exclusively determined by the heavier dust particles, the values of Ω_J^2 and C change accordingly to

$$\Omega_J^2 = \frac{\mu - 1}{4 - \mu} \omega_J^2(a_{\min}) \left(\frac{a_{\max}}{a_{\min}} \right)^{4-\mu}, \quad (9.56)$$

$$C = 1 - \frac{\mu(4-\mu)}{(\mu-2)^2} \left(\frac{a_{\min}}{a_{\max}} \right)^{4-\mu} \simeq 1. \quad (9.57)$$

It follows that there now is an almost complete factorization of (9.44), *viz.*

$$(\omega^2 - k^2 U_{da}^2)(\omega^2 + \Omega_J^2) \simeq 0. \quad (9.58)$$

We thus conclude that for $2 < \mu < 4$ the plasma and gravitational disturbances decouple and can develop almost independently. This is a consequence of the rather mild decline of the differential density $n_d(a)$ so that the larger particles, although smaller in absolute numbers, can dominate the self-gravitational effects, in contradistinction to the case $\mu > 4$.

9.3 Results

In this chapter we have extended the kinetic analysis of dust-acoustic modes in a self-gravitating dusty plasma by including a continuous dust size distribution, in order to mimic astrophysical situations more realistically. Following observational results, we treated a size distribution that decreases as a power law in a certain range of dust particle sizes.

Our kinetic analysis recovers the dust distribution instability and a stable mode that solely exists due to the size distribution of the dust particles, both of which have been described earlier by Meuris et al. [1997], but within a hydrodynamical approach and in the case of a discrete dust size spectrum. Not only does the present kinetic approach comprise the damping and growth rates of the dust-acoustic modes, but it additionally allows for investigating the precise influence of the shape of the power law distribution.

We found that because of their abundance the effective plasma terms will always be weighted towards the smallest particles, whereas the effective Jeans and hybrid terms can be determined by either the smallest or the largest grains, depending on the precise slope of the power law distribution. For steeply descending power laws, characterized by an exponent $\mu > 4$, the sheer quantity of the lighter dust particles will mainly determines the effective Jeans and hybrid terms. In effect, in this case the dust-acoustic modes are practically insensitive to the upper boundary of the size distribution. For $\mu > 4$, we retrieve a generalization of the dust-acoustic mode and the Jeans acoustic mode, as well as the just mentioned dust distribution instability and a stable mode which is nonexistent in monodisperse plasmas. On the other hand, for $2 < \mu < 4$, the larger dust grains take over the main role in the issue of self-gravitation, causing a decoupling between the plasma and gravitational perturbations.

Moreover, we investigated in both parameter regimes of μ the influence of the dust particles sizes on the Landau damping, which will be only measurable in self-gravitating dusty plasmas and for certain parameter values, as was already stated in the previous chapter.

Chapter 10

Influence of dust-ion collisions

In all the previous chapters, collisional mechanisms were not taken into account. However, in many astrophysical dusty plasmas, the collisions between particles may not be neglected in an accurate wave analysis [D'Angelo 1998, Winske and Rosenberg 1998, Shukla et al. 1999, Ivlev et al. 1999, Ostrikov et al. 2000]. The exchange of momentum between species, caused by the different types of collisions, can be a source of considerable damping for the low-frequency modes under study and thus merit further investigations.

If neutral dust or gas species are present, the most relevant collisions in dusty plasmas are those occurring between the charged dust species and the neutral dust species. Since in the larger part of this thesis we have worked within a model restricted to charged dust species only, we also now study the influence of collisions in dusty self-gravitating plasmas without neutrals. In this case, the dominant collision mechanism occurs between the ions and the (charged) dust species [Shukla and Mamun 2002, p.76], the physics of which were already inspected by D'Angelo [1998], but in the absence of self-gravitation. One of the most relevant papers concerning a combination of self-gravitational effects and collisions in a dusty plasma model is that of Shukla and Verheest [1999], in which self-gravitating collisional dusty plasmas are studied but wherein the possibly important ion inertia is neglected.

In our study, the stability of self-gravitating plasmas is examined using elementary principles of rootlocus theory, a semi-analytical tool often used in control engineering. This method produces straightforward criteria for gravitational collapse, while only requiring a minimal amount of algebra. Moreover, this procedure provides a relatively easy means for visualizing the qualitative evolution of the real frequencies and damping decrements of the dust-acoustic and ion-acoustic modes, for increasing values of the dust-ion collision frequency.

Our treatment shows that collisions between ions and dust grains do not change the criteria for gravitational collapse at any value of their collision frequency, but diminish the growth rate of unstable self-gravitating plasmas [Jacobs et al. 2002].

10.1 General formalism

The model we investigate is a collisional dusty plasma consisting of electrons, ions and charged dust grains where only the dust-ion collisions are retained. We consider electrostatic waves propagating along the z-axis with phase velocities much smaller than the thermal speeds of the electrons. Furthermore, the wave period is assumed to differ considerably from the dust charge fluctuation time, so that we can treat the dust charges as effectively constant. Because the phase speed of the waves under consideration is negligible compared to the thermal speeds of the electrons, the electrons are treated as being Boltzmann distributed, consequently the electron density is given by

$$n_e = n_{e0} \exp\left(\frac{e\phi}{k_B T_e}\right). \tag{10.1}$$

On the other hand, since the ions are involved in collision processes, the inertia of the ions is retained, so that our basic equations further include the continuity equations

$$\frac{\partial n_i}{\partial t} + \frac{\partial}{\partial z}(n_i v_i) = 0, \tag{10.2}$$

$$\frac{\partial n_d}{\partial t} + \frac{\partial}{\partial z}(n_d v_d) = 0, \tag{10.3}$$

and the equations of motion for the ions and dust particles, respectively,

$$\frac{\partial v_i}{\partial t} + v_i \frac{\partial v_i}{\partial z} + \frac{q_i}{m_i}\frac{\partial \phi}{\partial z} + \frac{\partial \psi}{\partial z} + \frac{c_{si}^2}{n_i}\frac{\partial n_i}{\partial z} + \nu_{id}(v_i - v_d) = 0, \tag{10.4}$$

$$\frac{\partial v_d}{\partial t} + v_d \frac{\partial v_d}{\partial z} + \frac{q_d}{m_d}\frac{\partial \phi}{\partial z} + \frac{\partial \psi}{\partial z} + \frac{c_{sd}^2}{n_d}\frac{\partial n_d}{\partial z} + \nu_{di}(v_d - v_i) = 0. \tag{10.5}$$

The different definitions for the collision frequencies, *viz.* ν_{di} and ν_{id}, are related to each other through

$$\nu_{di} = \frac{m_i n_{i0}}{m_d n_{d0}} \nu_{id}. \tag{10.6}$$

As usual, the electric (ϕ) and gravitational (ψ) potentials can be computed from the Poisson equations

$$\frac{\partial^2 \phi}{\partial z^2} = \frac{1}{\varepsilon_0}(n_e e - n_i q_i - n_d q_d), \tag{10.7}$$

$$\frac{\partial^2 \psi}{\partial z^2} = 4\pi G(m_i n_i + m_d n_d). \tag{10.8}$$

For the sake of generality, the gravitational Poisson equation (10.8) also includes the ion mass density, but in general the term $m_i n_i$ will only be of secondary importance.

10.2 Dispersion relation

We investigate linear waves in dusty plasma, which are presumed to be homogeneous in both space and time, so that the equations (10.1)-(10.8) can be linearized and Fourier transformed, yielding the following dispersion relation

$$\left[\omega\left(\omega + i\nu_{id}\frac{\omega_{Ji}^2}{\omega_{Jd}^2}\right) - k^2c_{sd}^2 + \omega_{Jd}^2 - A\omega_{pd}^2\right]\left[\omega\left(\omega + i\nu_{id}\right) - k^2c_{si}^2 + \omega_{Ji}^2 - A\omega_{pi}^2\right]$$
$$= \left[A\omega_{pi}\omega_{pd} - \omega_{Ji}\omega_{Jd} + i\omega\nu_{id}\frac{\omega_{Ji}}{\omega_{Jd}}\right]^2. \tag{10.9}$$

For convenience, the abbreviated notation A is introduced, which stands for

$$A = \left(1 + \frac{1}{k^2\lambda_{De}^2}\right)^{-1}, \tag{10.10}$$

and we note that this parameter depends on the wavelength. Starting from the dispersion relation (10.9), we can easily recover equation (27) of Meuris et al. [1997] but without streaming, if we leave out the dust-ion collisions in (10.9), neglect the terms that include the Jeans frequency of the ions (ω_{Ji}) and only incorporate cold dust species. The results of D'Angelo [1998], valid for dusty plasmas with negligible self-gravitational effects, can also be retrieved through setting $k^2\lambda_{De}^2 \ll 1$, $Z_i = 1$, $q_d = -eZ_d$ and $\omega_{Ji}^2 = 0 = \omega_{Jd}^2$ in (10.9), which then becomes

$$\omega^4 - k^2[\lambda_{De}^2(\omega_{pi}^2 + \omega_{pd}^2) + c_{si}^2]\omega^2 + k^4\lambda_{De}^2\omega_{pd}^2c_{si}^2$$
$$+i\nu_{di}\omega\left\{\omega^2 - k^2\left[c_{si}^2 + \lambda_{De}^2\omega_{pi}^2\left(1 - \frac{n_{d0}}{n_{i0}}Z_d\right)\right]\right\} = 0, \tag{10.11}$$

and equals equation (21) of D'Angelo [1998], provided one sets there $\tau_L = \infty$ and $\alpha = 0$. In the latter paper, figures of growth rates for different plasma and dust parameters can be found.

When substituting $\omega = i\Omega$ in the dispersion relation (10.9), we obtain a quartic equation with real coefficients *viz.*

$$P(\Omega, 0) + \nu_{id}\Omega\left[\Omega^2 - \Lambda\right] = 0, \tag{10.12}$$

where $P(\Omega, 0) = 0$ denotes the collisionless dispersion relation, which is a biquadratic equation in Ω, namely

$$P(\Omega,0) = \left[\Omega^2 + A\omega_{pd}^2 + k^2c_{sd}^2 - \omega_{Jd}^2\right]\left[\Omega^2 + A\omega_{pi}^2 + k^2c_{si}^2 - \omega_{Ji}^2\right]$$
$$-\left[A\omega_{pi}\omega_{pd} - \omega_{Ji}\omega_{Jd}\right]^2. \tag{10.13}$$

The parameter Λ, occurring in (10.12) can be computed as

$$\Lambda = \omega_{Jd}^2 - k^2c_{sd}^2\left(1 + \frac{n_{i0}T_i}{n_{d0}T_d}\right) - A\omega_{pd}^2\left(1 + \frac{n_{i0}Z_i}{n_{d0}Z_d}\right)^2, \tag{10.14}$$

provided we implement the obvious relation $\omega_{Ji} \ll \omega_{Jd}$. Further on, the full dispersion relation (10.12) is noted as $P(\Omega, \nu_{id}) = 0$.

For dusty plasmas with very heavy dust particles, so that

$$\left(1 + \frac{n_{i0}Z_i}{n_{d0}Z_d}\right)\omega_{pd} < \omega_{Jd} \tag{10.15}$$

is satisfied, Λ is always positive. On the other hand, for lighter dust species that satisfy

$$\left(1 + \frac{n_{i0}Z_i}{n_{d0}Z_d}\right)\omega_{pd} > \omega_{Jd}, \tag{10.16}$$

the sign of Λ depends on the wavenumber. For negatively charged dust grains, the following equalities are valid, *viz.* $n_{i0}Z_i = n_{e0} + n_{d0}Z_d > n_{d0}Z_d$ and $n_{i0}T_i \gg n_{d0}T_d$, which leads to

$$\Lambda \simeq \omega_{Jd}^2 - k^2 c_{si}^2 \left(\frac{n_{i0}m_i}{n_{d0}m_d}\right) - A\omega_{pd}^2 \left(\frac{n_{i0}Z_i}{n_{d0}Z_d}\right)^2. \tag{10.17}$$

We now compare the two negative terms of the expression (10.17),

$$\frac{k^2 c_{si}^2 \left(\dfrac{n_{i0}m_i}{n_{d0}m_d}\right)}{A\omega_{pd}^2 \left(\dfrac{n_{i0}Z_i}{n_{d0}Z_d}\right)^2} = \frac{\lambda_{Di}^2}{\lambda_{De}^2}(1 + k^2\lambda_{De}^2) \ll 1, \tag{10.18}$$

and deduce that for the long wavelength perturbations we are investigating, the second term in (10.17) and also in (10.14) can be neglected. For dusty plasmas that obey the inequality (10.16), we introduce the wavenumber k_Λ as

$$k_\Lambda^2 = \frac{\omega_{Jd}^2}{\left[\left(1 + \dfrac{n_{i0}Z_i}{n_{d0}Z_d}\right)^2 \omega_{pd}^2 - \omega_{Jd}^2\right]\lambda_{De}^2}, \tag{10.19}$$

and we see that Λ is negative for $k > k_\Lambda$ and positive for $k < k_\Lambda$. As usual we assume long wavelengths $k^2\lambda_D^2 \simeq k^2\lambda_{Di}^2 \ll 1$, hence it is clear that $k_\Lambda < \omega_{Jd}/c_{da}$. Further on, it will become clear that the dust-ion collisions exert a different influence on wavenumber regions separated by k_Λ.

10.2.1 Collisionless dispersion relation

Before tackling the full dispersion relation, the dispersion relation (10.12) is discussed in the collisionless limit. First, we compute the discriminant D^* of this biquadratic equation,

$$\begin{aligned} D^* \;=\; & \left[A(\omega_{pi}^2 - \omega_{pd}^2) + k^2(c_{si}^2 - c_{sd}^2) - (\omega_{Ji}^2 - \omega_{Jd}^2)\right]^2 \\ & + 4(A\omega_{pi}\omega_{pd} - \omega_{Ji}\omega_{Jd})^2 \geqslant 0, \end{aligned} \tag{10.20}$$

which implies that both roots (in Ω^2) of equation (10.13) are real. These roots are denoted as r_{ia} and r_{da}, since they actually represent the ion-acoustic and dust-acoustic mode, respectively, as will become clear momentarily. Indeed, the expressions

$$r_{ia,da} = -\frac{1}{2}\left[A(\omega_{pi}^2 + \omega_{pd}^2) + k^2(c_{si}^2 + c_{sd}^2) - (\omega_{Ji}^2 + \omega_{Jd}^2) \pm \sqrt{D^*}\right], \tag{10.21}$$

with r_{ia} corresponding to the +sign and r_{da} to the −sign, make clear that $r_{ia} \gg r_{da}$, hence the roots of $P(\omega, 0) = 0$ can be approximated as

$$r_{ia} \simeq -A\omega_{pi}^2 - k^2 c_{si}^2 \tag{10.22}$$

$$r_{da} \simeq \omega_{Jd}^2 - k^2(c_{da}^2 + c_{sd}^2), \tag{10.23}$$

proving that r_{ia} and r_{da} represent the ion-acoustic and the dust-acoustic branch of the dispersion relation, respectively.

Whereas r_{ia} is always negative, the sign of r_{da} switches at the familiar critical wavenumber

$$k_{cr}^2 = \frac{\omega_{Jd}^2}{c_{da}^2 + c_{sd}^2} \simeq \frac{\omega_{Jd}^2}{c_{da}^2}. \tag{10.24}$$

In accordance with the earlier results, we conclude that wavenumbers $k \geqslant k_{cr}$ yield a stable solution

$$\Omega^2 = -\omega^2 = r_{da} \leqslant 0, \tag{10.25}$$

and vice versa the very small wavenumbers $k < k_{cr}$ imply a gravitational instability, because $-\omega^2 = r_{da} > 0$.

We now pay extra attention to a dusty plasma with negligible self-gravitational interactions, and in that special case we obtain

$$r_{ia} \cdot r_{da} = k^2[k^2 c_{si}^2 c_{sd}^2 + A(\omega_{pi}^2 c_{sd}^2 + \omega_{pd}^2 c_{si}^2)] \geqslant 0, \tag{10.26}$$

meaning that in this case $r_{da} \leqslant 0$ holds for all wavelengths. An evident result, because in the absence of both collisions and self-gravitation, there is no mechanism included that can be responsible for instabilities.

All the previous allows for a more compact and practical form for the general dispersion relation (10.12), namely

$$(\Omega^2 - r_{ia})(\Omega^2 - r_{da}) + \nu_{id}\Omega(\Omega^2 - \Lambda) = 0, \tag{10.27}$$

and we note that $r_{da} - \Lambda$ is always positive because of the following relation,

$$r_{da} - \Lambda > \frac{1}{2}[\sqrt{D^*} - \omega_{Jd}^2 - A(\omega_{pi}^2 - \omega_{pd}^2) - k^2(c_{si}^2 - c_{sd}^2)] > 0. \tag{10.28}$$

10.2.2 Small and large collision frequencies

Before tackling the general dispersion relation, it is instructive to determine the solutions of the dispersion law (10.27) in the limits of very small and very large collision frequencies. For small collision frequencies ν_{id}, we can easily compute the corrections for the collisionless solutions $\Omega \simeq r_{ia}$ and $\Omega \simeq r_{da}$. Calculated up to first order in ν_{id}, the solution for $\Omega \simeq r_{ia}$ becomes

$$\begin{aligned} \Omega &= \sqrt{r_{ia}} - \frac{\nu_{id}}{2}\frac{(r_{ia}-\Lambda)}{(r_{ia}-r_{da})} \\ &\simeq \sqrt{r_{ia}} - \frac{\nu_{id}}{2}, \end{aligned} \tag{10.29}$$

because $|r_{da}|, |\Lambda| \ll |r_{ia}|$. Performing a similar first order approximation for $\Omega \simeq \sqrt{r_{da}}$ yields

$$\begin{aligned} \Omega &= \sqrt{r_{da}} - \frac{\nu_{id}}{2}\frac{(r_{da}-\Lambda)}{(r_{da}-r_{ia})} \\ &\simeq \sqrt{r_{da}} + \frac{\nu_{id}}{2}\frac{(r_{da}-\Lambda)}{r_{ia}} \end{aligned} \tag{10.30}$$

and we note that the second term on the right hand side of both expression (10.29) and expression (10.30) is always real, the latter of which because of (10.28).

On the other hand, for very large collision frequencies, we can formally calculate the corrections for $\Omega \simeq 0$ and $\Omega \simeq \sqrt{\Lambda}$. For negative Λ, the roots of the equation $P(\Omega, \pm\infty) = 0$ are $\Omega = 0, \pm i\sqrt{|\Lambda|}$ and we start with the determination of the first terms of the series expansion for $\Omega \simeq i\sqrt{|\Lambda|}$ in the small parameter ν_{id}^{-1}

$$\begin{aligned} \Omega &= i\sqrt{|\Lambda|} + \frac{(r_{ia}+|\Lambda|)(r_{da}+|\Lambda|)}{2\nu_{id}|\Lambda|} \\ &\simeq i\sqrt{|\Lambda|} + \frac{r_{ia}(r_{da}+|\Lambda|)}{2\nu_{id}|\Lambda|}. \end{aligned} \tag{10.31}$$

The expressions for positive Λ are obviously very similar and not given here. Finally, for $\Omega \simeq 0$ we obtain

$$\Omega \simeq \frac{r_{ia}r_{da}}{\nu_{id}\Lambda}. \tag{10.32}$$

The equations (10.31) and (10.32) are mentioned here because the semi-analytical method, that is used in the next section, requires the mathematical solution for infinite collision frequencies. We emphasize that in these equations, the collision frequency is treated as a purely mathematical parameter. After all, the mathematical solutions for very large collision frequencies may not be physically meaningful, as in that situation our basic equations are not valid anymore. However, since the analysis is not compromised by extending the use of the parameter ν_{id} beyond its physical relevance, there is no objection for calculating the solutions for all values of the collision frequency, provided the results for very large ν_{id} are interpreted carefully and possibly discarded afterwards.

10.3 Rootlocus method applied on stability analysis

Equation (10.27) is a full quartic equation in Ω and can be written in the form

$$D(\Omega) + \nu_{id} N(\Omega) = 0, \tag{10.33}$$

where $N(\Omega)$ and $D(\Omega)$ are polynomials with real coefficients in the complex variable Ω and are clearly independent of the parameter ν_{id}. These are the exact requirements for being able to draw a so called rootlocus plot [Willems 1970], which shows how the roots of the dispersion relation (10.27) move in the complex plane as the collision frequency ν_{id} increases.

In rootlocus theory, one mostly uses the form

$$1 + \nu_{id} \frac{N(\Omega)}{D(\Omega)} = 0, \tag{10.34}$$

and accordingly labels the roots of the polynomial $N(\Omega)$ as the zeros of the equation, whereas the roots of the denominator $D(\Omega)$ are called the poles. Because here ν_{id} is a positive parameter, the loci of the solutions of the dispersion relation (10.27) will originate in the poles and terminate in the zeros if one increases ν_{id}, starting from zero towards infinity. In effect, the strengths of this method are primarily revealed in a numerical analysis, but this approach can be highly advantageous in analytical investigations too. For relatively simple equations like (10.27), one can easily predict the general form of the rootlocus plot for fixed values of r_{ia}, r_{da} and Λ, but even without actually plotting the rootlocus, one can already derive some of its properties by just studying the rational function $N(\Omega)/D(\Omega)$.

Before continuing, we first mention some of the trivial solutions of the dispersion relation (10.27), namely $(\Omega, \nu_{id}) = (0, \infty)$, $(\pm i\sqrt{|r_{ia}|}, 0)$, $(\pm\sqrt{r_{da}}, 0)$ and $(\pm\sqrt{\Lambda}, \infty)$. Note that some of these trivial roots in Ω can be purely imaginary but there are no other purely imaginary roots for finite, nonzero values of the collision frequency. Indeed, a purely imaginary solution $\Omega = ix$ with $x \in \mathbb{R}_0$, would require that

$$(x^2 + r_{ia})(x^2 + r_{da}) - ix\nu_{id}(x^2 + \Lambda) = 0. \tag{10.35}$$

Identifying the real and imaginary parts of this equation results in the following system of equations

$$\begin{cases} (x^2 + r_{ia})(x^2 + r_{da}) &= 0, \\ x\nu_{id}(x^2 + \Lambda) &= 0, \end{cases}$$

and considering $r_{ia} \neq 0$ and $r_{da} \neq \Lambda$, we find that (10.35) can never be satisfied for $x \in \mathbb{R}_0$ and a finite $\nu_{id} \neq 0$. Because $|r_{ia}| \gg |r_{da}|$, we can also see that the frequency

$$\Omega = -\sqrt{-r_{ia}}, \tag{10.36}$$

with the following value for the collision frequency

$$\nu_{id} = 2\frac{r_{ia} + r_{da}}{r_{ia} + \Lambda}\sqrt{-r_{ia}} \simeq 2\sqrt{-r_{ia}}, \tag{10.37}$$

is a real and negative solution of the dispersion relation, moreover it is a double root.

10.3.1 Properties of the rootlocus plots

- Since the coefficients of equation (10.27) are real, the conjugate of every root is a solution too. This explains one of the general properties of rootlocus plots, namely that they are symmetrical with respect to the real axis.

- Because $\omega = i\Omega$, stable solutions require Ω to have a negative real part and therefore all roots located in the right half of the complex plane can be recognized as unstable solutions.

- For the dispersion relation (10.27), the rootlocus plot will cross the imaginary axis only in poles or zeros because for $\nu_{id} \neq 0$ and $\nu_{id} \neq \infty$ there are no purely imaginary roots, as proven before. This will be an important remark for the determination of the stability of the system.

- We can easily deduct which parts of the real axis correspond to sets of solutions (Ω, ν_{id}) of equation (10.27) and are thus part of the rootlocus plot. To clarify this, we write the equation (10.33) in the form

$$1 + \nu_{id} \frac{\prod_{i=1}^{q}(\Omega - z_i)}{\prod_{i=1}^{p}(\Omega - p_i)} = 0, \tag{10.38}$$

  where p_i stand for the poles, z_i for the zeros and p and q for the number of poles and zeros, respectively. Suppose a certain Ω is real and we rewrite (10.38) as

$$\frac{\prod_{i=1}^{p}(\Omega - p_i)}{\prod_{i=1}^{q}(\Omega - z_i)} = -\nu_{id} < 0. \tag{10.39}$$

  Because the collision frequency is real and positive, we can calculate the complex phase angles of both sides of the latter equation, which yields

$$\sum_{i=1}^{p} \arg(\Omega - p_i) - \sum_{i=1}^{q} \arg(\Omega - z_i) = (2l+1)\pi. \tag{10.40}$$

  From this expression, we now go over to a geometric interpretation, as illustrated in Fig. 10.1 and we recall that Ω is chosen to be real. As can be seen in figure 10.1, an expression $\arg(\Omega - x)$ corresponds to a phase angle between the real axis and the line segment that connects x and Ω, where the line segment has a direction that points towards Ω. Further on, we will reason on the contributions of the poles only, the interpretation for the zeros is exactly the same. In Fig 10.1 and all the following plots of this chapter, the crosses will correspond to the poles and the circles to the zeros.

  First, we note that complex conjugate roots do not contribute in (10.40). Indeed, for the complex conjugate poles S and $\overline{S}$ in Fig. 10.1, we have $\arg(\Omega - S) + \arg(\Omega - \overline{S}) = \alpha + \beta = 0$ and conclude that the phase angles of complex conjugate poles cancel each other out. Real roots located to the left of Ω (represented by a pole I in the

figure) do not contribute either, because the phase angles $\eta = \arg(\Omega - I)$ will be zero. Finally, we deduce that real roots located to the right of Ω correspond to a phase angle π, as illustrated for the pole R with $\gamma = \arg(\Omega - R) = \pi$ in the figure.

It follows from (10.40) that an interval on the real axis belongs entirely to a rootlocus plot if the sum of the number of poles, located to the right of this interval, and the number of zeros, each also located to the right of this interval, is odd.

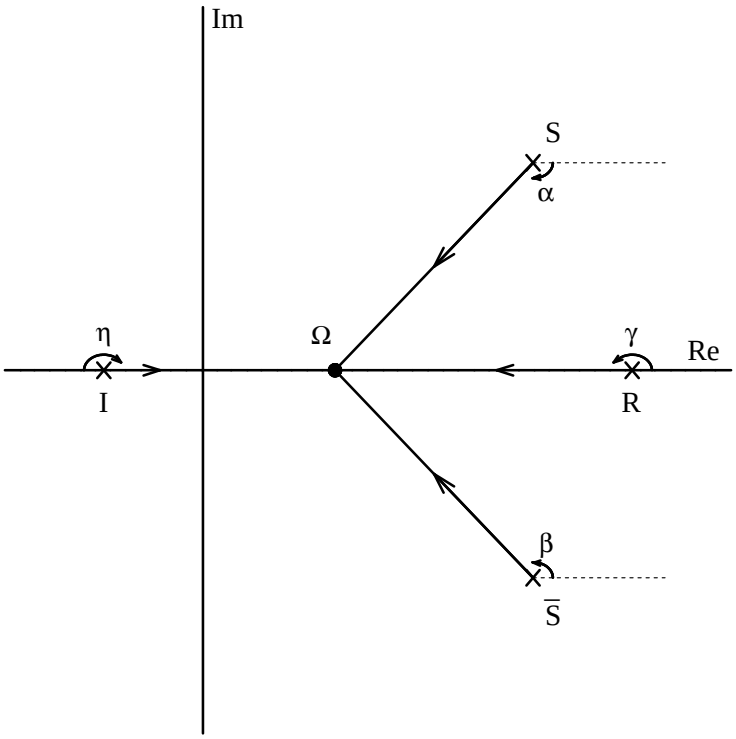

Fig 10.1: Geometric interpretation of phase angles

- The asymptotes for the rootlocus plot, being the straight lines that coincide with the plot for $\nu_{id} \to \infty$ can also be calculated quite easily. It can be proven [Willems 1970] that there are $n - m$ asymptotes. These asymptotes run through the center σ (located on the real axis)

$$\sigma = -\frac{\sum_{i=1}^{p} p_i - \sum_{i=1}^{q} z_i}{p - q}, \tag{10.41}$$

and have directions

$$\theta = \frac{(2l+1)\pi}{p - q}, \tag{10.42}$$

where θ denotes the angle of the asymptotes with the horizontal axis [Willems 1970].

Equation (10.27) has four poles and three zeros, hence there will be only one asymptote, being the negative real axis.

- Furthermore, expressions for the starting angles in the poles (θ_s) and the ending angles in the zeros (θ_e) can be determined [Willems 1970], namely

$$\theta_s(p_k) = \frac{1}{\mu}[(2l+1)\pi + \sum_{j=1}^{q}(z_j - p_k) - \sum_{\substack{i=1 \\ i\neq k}}^{p}(p_i - p_k)], \tag{10.43}$$

$$\theta_e(z_k) = \frac{1}{\mu}[(2l+1)\pi + \sum_{i=1}^{p}(p_i - z_k) - \sum_{\substack{j=1 \\ j\neq k}}^{q}(z_j - z_k)], \tag{10.44}$$

where μ stands for the multiplicity of the respective pole or zero.

- There is another class of important points needed to determine a rootlocus unambiguously, the breakaway points [Willems 1970]. These so called breakaway points are defined as points on the real axis where two or more branches of the rootlocus depart from or arrive at. We wish to note here that the determination of the breakaway points will prove to be redundant for obtaining the instability criterion. However, for determining qualitatively the evolution of the roots for increasing ν_{id}, the following considerations are needed.

  We have seen already that for the dispersion relation (10.27) there always is at least one breakaway point, namely $\Omega = -\sqrt{|r_{ia}|}$. The other breakaway points b_i of multiplicity μ (μ branches depart and μ branches arrive) are formally calculated [Willems 1970] as solutions of

$$\left[\frac{d^j}{d\Omega^j}\frac{N(\Omega)}{D(\Omega)}\right]_{b_i} = 0 \qquad \forall j = 1\ldots\mu-1, \tag{10.45}$$

that of course still obey

$$D(\Omega) + \nu_{id}N(\Omega) = 0. \tag{10.46}$$

Hence, breakaway points b_i of the dispersion relation (10.27) are solutions of the following cubic polynomial equation in Ω^2,

$$\begin{aligned} &\Omega^6 \ +(r_{ia}+r_{da}-3\Lambda)\Omega^4 + [\Lambda(r_{ia}+r_{da}) - 3r_{ia}r_{da}]\Omega^2 + r_{ia}r_{da}\Lambda \\ &\simeq \ \Omega^6 + r_{ia}\Omega^4 + r_{ia}(\Lambda - 3r_{da})\Omega^2 + r_{ia}r_{da}\Lambda \\ &= \ 0, \end{aligned} \tag{10.47}$$

with corresponding collision frequencies

$$\nu_{id} = -\frac{b_i^4 - b_i^2(r_{ia}+r_{da}) + r_{ia}r_{da}}{b_i(b_i^2 - \Lambda)}. \tag{10.48}$$

Table 10.1: Classification for different wavenumber regions

k	$\ldots$	k_Λ	$\ldots$	k_{cr}	$\ldots$
Λ	$+$	0	$-$	$-$	$-$
r_{da}	$+$	$+$	$+$	0	$-$
case	C		B		A

We recover the already familiar negative breakaway point

$$(b_1, \nu_{id}) \simeq (-\sqrt{-r_{ia}}, 2\sqrt{-r_{ia}}),$$

the approximation of which was established using the obvious inequalities $r_{da}, \Lambda \ll r_{ia}$. This is the only breakaway point for case A if $|\Lambda| < 9|r_{da}|$. Other possible breakaway points are b_2 and b_3, given through

$$\Omega = b_{2,3} = -\sqrt{\frac{1}{2}\left[3r_{da} - \Lambda \pm \sqrt{(\Lambda - r_{da})(\Lambda - 9r_{da})}\right]},$$

with corresponding real and positive collision frequencies

$$\nu_{id} \simeq -r_{ia}\frac{(r_{da} - b_{2,3}^2)}{b_{2,3}(b_{2,3}^2 - \Lambda)}.$$

For cases A (if $9|r_{da}| < |\Lambda|$), B and C is b_2 indeed a second breakaway point. Additionally, for the cases A ($9|r_{da}| < |\Lambda|$) and C, b_3 represents a third breakaway point.

10.3.2 Classification

We can make a classification for different dusty plasma configurations, depending on the signs of Λ and r_{da}. For every configuration, the poles $\pm i\sqrt{|r_{ia}|}$ are located on the imaginary axis and the origin is a zero. Furthermore, we note that a situation with positive Λ and negative r_{da} is impossible within the long wavelength assumption $k\lambda_D \ll 1$. After all, negative r_{da} requires $k > k_{cr}$, where k_{cr} is the critical wavenumber obtained in the collisionless limit, and thus $\omega_{Jd}/\omega_{pd} < k\lambda_D \ll 1$. Therefore a positive Λ demands $k < k_\Lambda$, but this is impossible since $k > k_{cr} > k_\Lambda$.

For dusty plasmas where the electromagnetic interactions are dominant *i.e.*

$$\left(1 + \frac{n_{i0}Z_i}{n_{d0}Z_d}\right)\omega_{pd} > \omega_{Jd} \tag{10.49}$$

there are three regions in wavenumber space, separated by k_Λ and k_{cr}, as displayed in Table 10.1. We repeat that $k_\Lambda < k_{cr}$, as proven earlier.

On the other hand, for dusty plasmas where self-gravitational interactions dominate *i.e.*

$$\left(1+\frac{n_{i0}Z_i}{n_{d0}Z_d}\right)\omega_{pd} < \omega_{Jd}, \tag{10.50}$$

the analysis is independent of the wavenumber and this configuration always falls in category C.

In the following section we will qualitatively describe how the magnitude of the dust-ion collision frequency affects the real frequencies and damping decrements of the Jeans and ion-acoustic modes, by plotting the loci of the roots of (10.27) in the possible configurations.

10.3.3 $\Lambda < 0$, $r_{da} < 0$

This situation corresponds to dusty plasmas for which self-gravitational interactions do not prevail, more specifically $(1+n_{i0}Z_i/n_{d0}Z_d)\,\omega_{pd} > \omega_{Jd}$ and for wavenumbers exceeding the critical wavenumber of the collisionless dispersion relation, namely $k > k_{cr} \simeq \omega_{Jd}/c_{da}$. The second condition is stronger than the first condition because if $\omega_{Jd}/\omega_{pd} < k\lambda_D \ll 1$, the first condition is automatically satisfied. We can conclude that this category is the category of dusty plasmas with negligible self-gravitational interactions, *i.e.* dusty plasmas for which $\omega_{Jd} \ll \omega_{pd}$ holds.

Now, we will derive in a systematical way some of the properties of the rootlocus plots for dusty plasmas in this category, a process which hardly requires calculations. For this category of dusty plasmas, all poles and zeros of equation (10.27) are located on the imaginary axis and alternate because here $|r_{da}| < |\Lambda| \ll |r_{ia}|$, as can be seen in equation (10.28). Since for any point on the negative real axis, the sum of the number of poles and zeros located to the left of the negative imaginary axis is odd ($p+q=7$), the entire imaginary axis is part of the rootlocus plot, as illustrated in Fig 10.2. We continue with the determination of the starting and ending angles and we recall that rootlocus plots are symmetrical with respect to the real axis, so that we only have to compute these angles in the upper half of the complex plane. The starting angles θ_s in the poles and the ending angles θ_e in the zeros, can be easily obtained from the expressions (10.43)-(10.44) as follows. We specify explicitly the origin of each term by means of the underbraces in order to clarify the procedure

$$\begin{aligned}
\theta_s(r_{ia}) &= \pi + \underbrace{\frac{3\pi}{2}}_{0,\Lambda,\overline{\Lambda}} - \underbrace{\frac{3\pi}{2}}_{\overline{r_{ia}},r_{da},\overline{r_{da}}} = \pi,\\
\theta_s(r_{da}) &= \pi + \underbrace{\frac{\pi}{2}}_{0} + \underbrace{\frac{\pi}{2}-\frac{\pi}{2}}_{\overline{\Lambda},\Lambda} - \underbrace{\frac{\pi}{2}}_{\overline{r_{da}}} - \underbrace{\left(\frac{\pi}{2}-\frac{\pi}{2}\right)}_{\overline{r_{ia}},r_{ia}} = \pi,\\
\theta_e(\Lambda) &= \pi + \underbrace{\pi}_{r_{da},\overline{r_{da}}} + \underbrace{\frac{\pi}{2}-\frac{\pi}{2}}_{\overline{r_{ia}},r_{ia}} - \underbrace{\pi}_{0,\overline{\Lambda}} = \pi.
\end{aligned}$$

Hence, the rootlocus plot leaves the imaginary axis from the poles r_{ia}, r_{da} and their complex conjugates in a straight angle and directed towards the left half of the complex plane. Equivalently, the rootlocus plot arrives in the zeros, perpendicular to the imaginary axis and coming from the left half of the complex plane. These starting/ending angles sketch the situation for $\nu_{id} \simeq 0$ and $\nu_{id} \to \infty$, as depicted in Fig. 10.2 below. We note that the former considerations for the angles can be checked independently, starting from the equations (10.29)-(10.32).

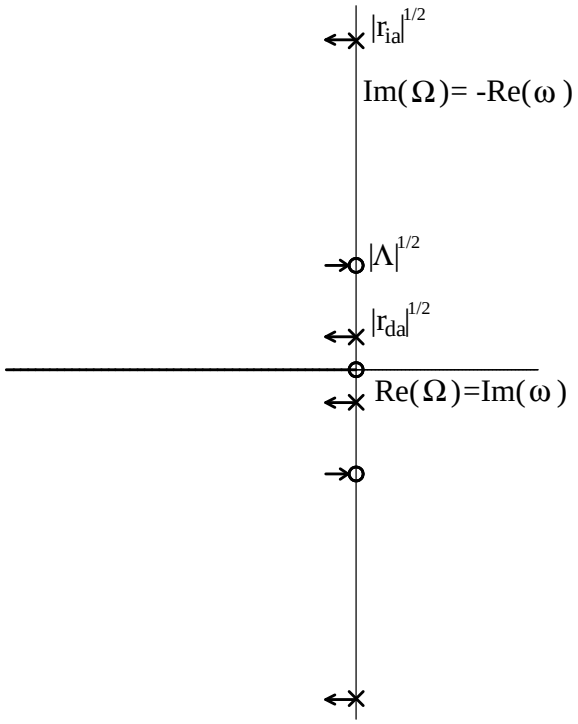

Fig 10.2: Asymptotical behaviour for $\nu_{id} \simeq 0$ and $\nu_{id} \to \infty$ in case of $\Lambda < 0$, $r_{da} < 0$

As stated earlier, the plot cannot cross the vertical axis except in the poles or zeros, therefore this configuration is always stable, since the rootlocus plot is entirely located in the left half of the complex plane. This confirms the results of D'Angelo [1998], albeit in a more general way.

We emphasize that statements about the stability of the system have been made with a minimal use of rootlocus theory and without the need of a plot. It is only for a qualitative determination of the real frequencies and damping decrements that a rootlocus plot has to be made. Qualitative and quantitative results can be found easily and rapidly for numerical examples, using existing routines, but analytical expressions can also be dealt with in a qualitative way, as is shown further on.

For being able to make an accurate rootlocus plot, one needs to determine the aforementioned breakaway points. These breakaway points are easily determined from the

expressions (10.47) and (10.48), for given values of r_{ia}, r_{da} and Λ, *i.e.* for given values of the dusty plasma parameters and for a fixed wavenumber. However, even without specifying the value of r_{ia}, r_{da} and Λ, some general statements concerning the breakaway points can be made.

For configurations with $|r_{da}| < |\Lambda| < 9|r_{da}|$, a general plot is not provided since the form of the rootlocus plot can have plural possibilities, depending on the precise magnitude of the parameters. For determining unambiguously the number of breakaway points and thus the form of the plot, one would need an additional specification of the magnitudes of r_{ia}, r_{da} and Λ.

On the other hand, for configurations $9|r_{da}| < |\Lambda|$, there are three breakaway points and the corresponding rootlocus plot is shown in Figure 10.3, wherein only $\sqrt{r_{da}}$, $\sqrt{|\Lambda|}$ and $\sqrt{r_{ia}}$ are labeled, the other poles and zeros are of course symmetrically located with respect to the origin. In this figure and in the following rootlocus plots, the arrows are directed towards larger collision frequencies.

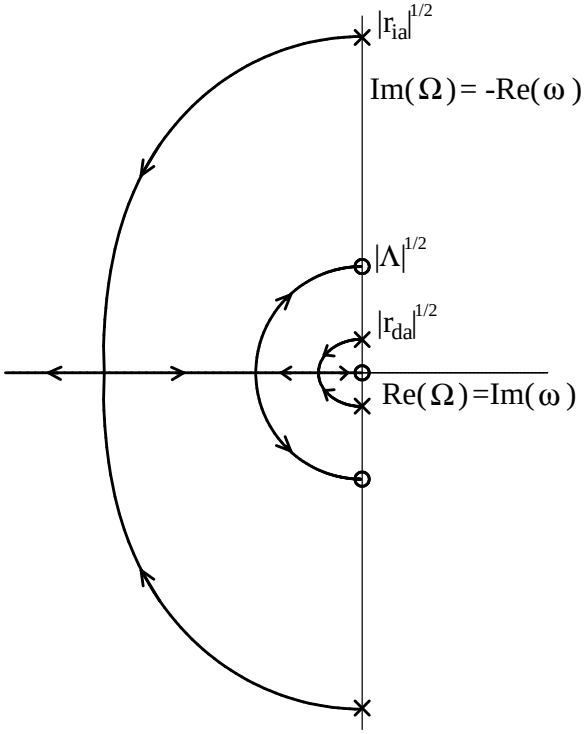

Fig 10.3: Rootlocus plot for wavenumbers $k > \omega_{Jd}/c_{da}$.

In Figure 10.3, the horizontal axis corresponds to imaginary values of the frequency ω and the vertical axis to real values of ω and it follows that dust-acoustic and ion-acoustic modes initially reduce in real frequency and become damped, when "turning on" the collisional frequency. As the collision frequency increases, the real frequency continues to

decrease and the modes become more strongly attenuated, until they become damped zero-frequency modes. Subsequently, the ion-acoustic and dust-acoustic mode remain of zero frequency and follow a horizontal path in Figure 10.3. It shows that one of the ion-acoustic modes becomes completely damped, while one of the dust-acoustic modes also vanishes as it becomes zero. For even larger collision frequencies, the remaining dust-acoustic and ion-acoustic mode begin to couple and leave the real axis again. We repeat that for the very high collision frequencies, the results are not physically meaningful anymore.

If one plots discrete points, corresponding to fixed collision frequencies, one can see that initially (for collision frequencies that are not too large) the modes do not deviate much from their respective collisionless limits.

10.3.4 $\Lambda < 0$, $r_{da} > 0$

This situation also corresponds to dusty plasmas for which self-gravitation is not having the upper hand, or equivalently

$$\left(1 + \frac{n_{i0}Z_i}{n_{d0}Z_d}\right)\omega_{pd} > \omega_{Jd}, \tag{10.51}$$

but now corresponds to the wavenumber region

$$k_\Lambda < k < k_{cr}. \tag{10.52}$$

In this configuration there are two poles ($\pm\sqrt{r_{da}}$), located on the real (=horizontal) axis, whereas the remaining two poles ($\pm i\sqrt{|r_{ia}|}$) are located on the imaginary axis. All the zeros, namely 0, and $\pm i\sqrt{|\Lambda|}$ are also located on the imaginary axis. Applying the familiar rule for finding the real solutions (in Ω), we find that the intervals $[-\infty, -\sqrt{r_{da}}]$ and $[0, \sqrt{r_{da}}]$ of the real axis are entirely part of the rootlocus plot. Obviously, this implies that this configuration $\Lambda < 0$, $r_{da} > 0$ is always unstable.

The initial and final situations are depicted in Fig 10.4 and are computed as follows. For obtaining $\theta_s(r_{ia})$, we first calculate explicitly the contribution of the complex conjugate roots r_{da} and $\overline{r_{da}}$, namely

$$\arg(r_{da} - r_{ia}) + \arg(\overline{r_{da}} - r_{ia}) = \pi, \tag{10.53}$$

which can be seen easily in figure 10.4. Hence the starting angle $\theta_s(r_{ia})$ for r_{ia} and the ending angle for Λ become, respectively

$$\begin{aligned}
\theta_s(r_{ia}) &= \pi + \underbrace{\frac{3\pi}{2}}_{0,\Lambda,\overline{\Lambda}} - \underbrace{\pi}_{r_{da},\overline{r_{da}}} - \underbrace{\frac{\pi}{2}}_{\overline{r_{ia}}} = \pi, \\
\theta_e(\Lambda) &= \pi + \underbrace{\pi}_{r_{da},\overline{r_{da}}} - \underbrace{\pi}_{0,\overline{\Lambda}} = \pi.
\end{aligned}$$

We conclude that just like in case A, the loci leave the poles $\pm i\sqrt{|r_{ia}|}$ in the left half of the complex plane and perpendicularly to the imaginary axis. Furthermore the loci of

the solutions of (10.27) also arrive perpendicularly with the imaginary axis in the zeros $\pm i\sqrt{|\Lambda|}$ and this in the left half of the complex plane.

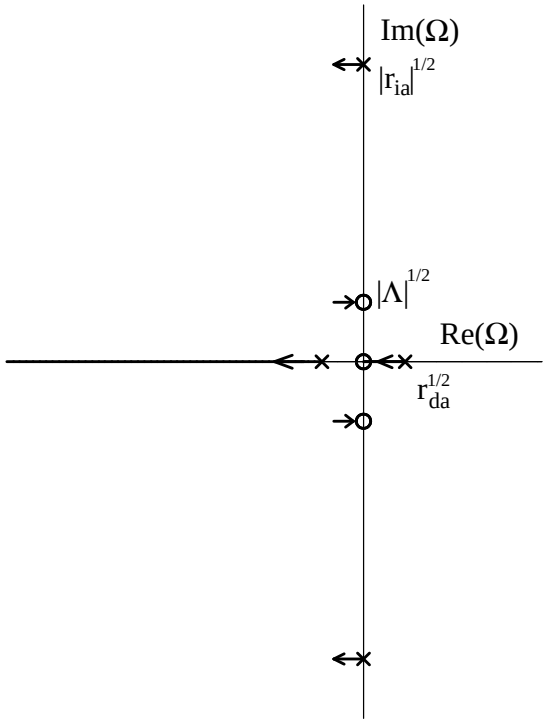

Fig 10.4: Asymptotical behaviour in case of $\Lambda < 0$ and $r_{da} > 0$

Since the branches of the rootlocus plot will not cross the vertical axis, the locus of the unstable Jeans mode, represented by r_{da} for $\nu_{id} = 0$, is already established. As the collision frequency ν_{id} increases, the unstable solution moves over the real axis towards the origin. Hence, the instability criterion for self-gravitational, collisionless dusty plasmas holds, but the growth rate of the Jeans instability will diminish as the dust-ion collision frequency increases.

The rootlocus plot of dusty plasmas in this category contains two breakaway points and has a qualitative form as shown in Figure 10.5. This figure shows that the damping decrements of the stable Jeans mode, represented by $\overline{r_{da}}$ for $\nu_{id} = 0$, and the ion-acoustic modes (related to r_{ia} and $\overline{r_{ia}}$) increase for small collision frequencies, whereas their real frequency diminishes. Here too, the ion-acoustic branches evolve towards zero-frequency modes for larger collision frequencies. Moreover, there is also a bifurcation on the real axis, as the dust-ion collision frequency ν_{id} increases, one of the ion-acoustic modes will become completely damped whereas the other couples with the stable dust-acoustic mode.

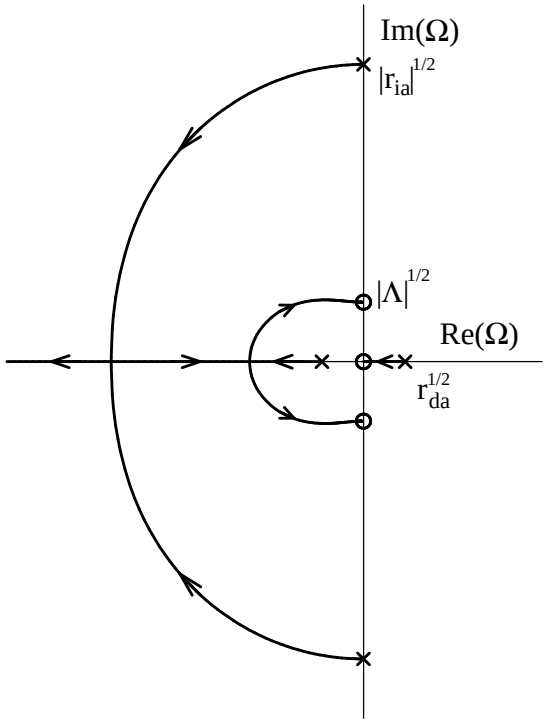

Fig 10.5: Rootlocus plot for dusty plasmas with $\omega_{pd} > \omega_{Jd}$ and corresponding to wavenumbers $k_\Lambda < k < k_{cr}$.

10.3.5 $\Lambda > 0$, $r_{da} > 0$

There are two different classes of dusty plasmas residing in this final category. On the one hand, dusty plasmas with relatively light dust species that obey

$$\left(1 + \frac{n_{i0}Z_i}{n_{d0}Z_d}\right)\omega_{pd} > \omega_{Jd}, \tag{10.54}$$

and in a situation

$$k < k_\Lambda. \tag{10.55}$$

On the other hand dusty plasmas where self-gravitation predominates *i.e.*

$$\left(1 + \frac{n_{i0}Z_i}{n_{d0}Z_d}\right)\omega_{pd} < \omega_{Jd}. \tag{10.56}$$

Indeed, for long wavelengths $k\lambda_D \ll 1$ the inequality $k < k_{cr} = \omega_{Jd}/(\omega_{pd}\lambda_D)$ will be always satisfied for this case. Note that the quantity k_Λ is meaningless in the latter situation as Λ is positive over the entire wavenumber range.

Both classes have qualitatively similar plots. The zeros are located on the real axis, as are the poles $\pm\sqrt{r_{da}}$. The poles are always larger (in absolute value) than the zeros since equation (10.28) demonstrates $\Lambda < |r_{ia}|, r_{da}$. The real intervals $[-\infty, -\sqrt{r_{da}}]$, $[-\sqrt{\Lambda}, 0]$ and $[\sqrt{\Lambda}, \sqrt{r_{da}}]$ belong to the rootlocus plot, rendering also this configuration unstable. The asymptotical behaviour is shown in Fig. 10.6, and for this we only need to compute $\theta_s(r_{ia})$ explicitly,

$$\theta_s(r_{ia}) = \pi + \underbrace{\frac{\pi}{2}}_{0} + \underbrace{\pi}_{\Lambda,\overline{\Lambda}} - \underbrace{\pi}_{r_{da},\overline{r_{da}}} - \underbrace{\frac{\pi}{2}}_{\overline{r_{ia}}} = \pi, \tag{10.57}$$

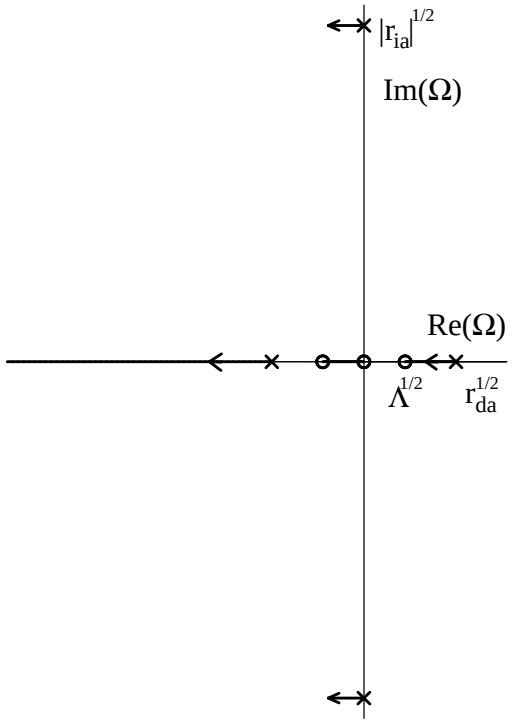

Fig 10.6: Asymptotical behaviour in case of $\Lambda > 0$ and $r_{da} > 0$

We have already seen that in case C, there will be three breakaway points, which yields a typical rootlocus plot as given in Fig. 10.7. The growth rate of the unstable Jeans mode will decrease until it reaches the pole $\sqrt{\Lambda}$, in this class of dusty plasmas the unstable mode will not vanish, even for infinitely large collision frequencies. Further, we notice that one of the ion-acoustic modes will also couple with the stable dust-acoustic mode while the other is wiped out. In effect, the only difference with the previous case (case B) is the evolution of the unstable root evolution for very large collision frequencies, the latter of which are not physically meaningful anyway.

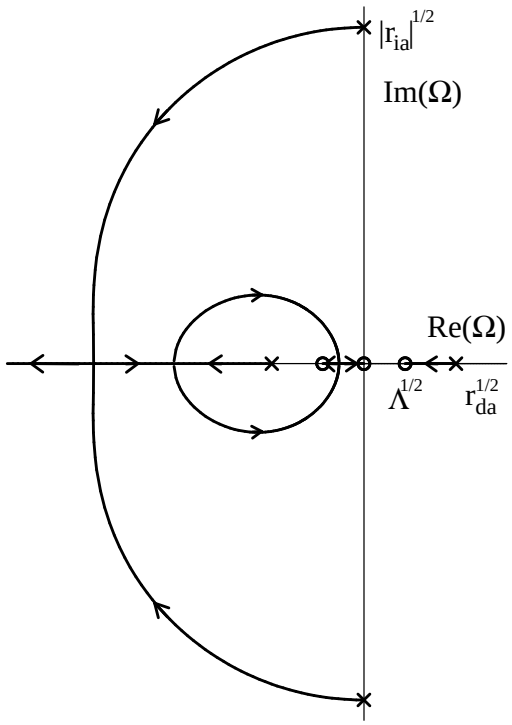

Fig 10.7: Rootlocus plot for dusty plasmas with $\Lambda > 0$ and $r_{da} > 0$

10.4 Summary

The stability of longitudinal disturbances in self-gravitating dusty plasmas has been investigated previously within a collisionless model. In this chapter, we studied the modifications of the Jeans instability criterion and low frequency modes in self-gravitating plasmas due to the inclusion of dust-ion collisions. Moreover, we illustrated qualitatively how the real frequency and damping decrement of the ion-acoustic and Jeans modes change over the spectrum of possible collision frequencies, using the semi-analytical rootlocus method. This method, often used in control engineering, proves to be an enlightening tool for the stability analysis of our dusty plasma model as it can produce physically meaningful graphs.

The most important conclusion is that dust-ion collisions reduce the growth rate of the unstable Jeans dust mode, but can never overturn the gravitational instability. In other words, the Jeans instability criterion remains unchanged when including dust-ion collisions in a dusty plasma that contains exclusively charged constituents, although a possible instability will develop more slowly.

Furthermore, the ion-acoustic modes are also damped and can become damped zero-frequency modes when the collision frequency exceeds a certain threshold. As the inclusion

of self-gravitational effects hardly modifies the ion-acoustic modes, the results of Ivlev et al. [1999] are partly reproduced and in some way generalized for the ion-acoustic branch.

Chapter 11

Conclusions

In this thesis, we focused on low-frequency waves and gravitational instabilities in large, astrophysical dusty plasmas. The most relevant low-frequency modes in dusty plasmas were reviewed in the fourth chapter and delineated clearly with respect to the different frequency regimes.

For the low-frequency perturbations under consideration in this thesis, the heavy dust grains are set in motion due to the electron and/or ion pressure. Because of the considerable mass of the dust grains, however the dust dynamics are strongly influenced by the self-gravitational interactions between the dust particles. In order to provide a sense of proportion, the fifth chapter started with a comparison of the magnitudes of the electrostatic and self-gravitational forces, acting on a single dust grain. Next, the concept of the infamous "Jeans swindle" was introduced and discussed in a one-dimensional model. The Jeans swindle provides an easy means of computing the conditions for a gravitational instability in a large, astrophysical medium. However, using the Jeans swindle in the derivation of the instability criterion, without giving a proper justification of the assessed homogeneity lengthscales, would somehow require a leap of faith and thus produce unreliable results. In this chapter, we analyzed the gravitational stability of a simplified, one-dimensional model and traced the weaknesses of the Jeans swindle. A corollary of this analysis is the proportionality of the Jeans length, obtained from the Jeans instability criterion, and the lengthscales over which the medium can be considered uniform. Because both quantities are of the same order of magnitude, deriving the "classic" instability criterion *i.e.* using the Jeans swindle, always provides valuable results. Indeed, even if the inspection *a posteriori* calls for overruling the Jeans swindle, the obtained critical Jeans length provides a good estimate of the inhomogeneity lengthscales.

In a wave description, the combination of Coulomb and gravitational forces acting on the dust particles results in the coupling of the different wave modes. This wave coupling was carefully explored for electrostatic waves in the sixth chapter. The impact of self-gravitation on the wave modes is interlaced with the distribution of dust sizes (masses), and the influence of a discrete dust distribution is explored. If the dust grains are exclusively charged, their presence enhances the gravitational stability of the plasma considerably. However, if neutral grains are also present, the impact on the critical Jeans lengths is

sweeping and the stabilizing role of the charged grains comes to nought. Provided neutrals are absent, the obtained critical Jeans lengths are in general of the form ω_{Jd}/V, with ω_{Jd} the Jeans frequency and with V some sort of average of the dust-acoustic velocities of the involved dust species. Finally, the streaming effects between dust species were also included, but in a relatively simple configuration, namely that of two oppositely streaming dust beams with equal parameters. The streaming between species can induce Buneman instabilities in the plasma. It has been investigated for which wavenumber regions and streaming velocities a Jeans and/or Buneman instability occurs.

Subsequently, the influence of self-gravitation on low-frequency electromagnetic modes was studied in chapter seven. For perpendicular propagation, the instability criterion is of the same form as for the electrostatic modes, but now the critical Jeans lengths are of the form ω_{Jd}/V_{ms}, with V_{ms} the magnetosonic velocity. It is found that the inclusion of a dust size distribution hardly changes the critical lengthscales for the perpendicular modes. Therefore, future investigations can be condensed by simplifying the model to a plasma with a single dust species with average properties because such a simplifications will hardly affect the accuracy. The study of the obliquely propagating modes starts within a model that is often referred to as the "classic" dusty plasma, namely a monodisperse model wherein the electrons and ions are assumed to be quasi-inertialess. For more general dusty plasmas, the dispersion law for obliquely propagating modes is of such complexity that an analytical approach would only yield unmanageably long expressions. Instead, we aimed specifically at the critical Jeans lengths and so curtailed the computations tremendously. Rather surprising, the outcome is that the critical Jeans lengths are exactly the same as for parallel propagation, except close to or at perpendicular propagation. Hence, the conditions for gravitational instability in dusty plasmas with isotropic pressures can be characterized by two lengthscales only. If neutrals are present, the conclusions already obtained in the study of the electrostatic modes holds. In this case, the critical lengthscales decrease to those obtained in neutral dust clouds and are typically of the form ω_{Jd}/c_{sd}, with c_{sd} a dust thermal speed.

For the sake of simplicity, a hydrodynamic description was used in all the previously discussed chapters. In the chapters 8 and 9 however, we refined the picture by reverting to a more general kinetic model. We deduced that within a kinetic model, the conditions for gravitational instability and the real frequencies of the investigated low-frequency waves are practically the same as in a fluid model. On the other hand, the growth rates are quite different in both models. Especially for wavenumbers, slightly larger than the critical wavenumber, the damping rates of the low-frequency waves can differ considerably in both descriptions, depending on the precise parameters of the self-gravitating dusty plasma. This is due to the "Landau damping", a collisionless damping mechanism, the physics of which is ignored completely in a fluid approach. We concluded that in self-gravitating plasmas, a single parameter determines whether the dust-acoustic wave can be excited for all wavenumbers or only for sufficiently large wavelengths.

The monodisperse kinetic model of chapter 8 was extended in chapter 9 to a kinetic model that comprises a continuous dust size distribution. For simplicity, the continuous size distribution was modelled as a decreasing power law, which is a good approximation

for astrophysical dust clouds. It was found that the precise value of the exponent of the power law will determine whether the smaller but numerous dust particles dominate the self-gravitational interactions or if this dominant role is rather played by the larger particles, which are less abundant. Furthermore, the influence of the shape of the power law on the Landau damping was investigated.

In the last chapter, we examined the influence of particle collisions on low-frequency modes in self-gravitating dusty plasmas which are void of neutrals. Because neutrals are assumed to be absent, the dust-ion collisions represent the major collision mechanism. The incorporation of dust-ion collisions does not alter the criterion for gravitational instability. Nevertheless, the dust-ion collisions perform some sort of stabilizing role since they decrease the growth rate of occurring Jeans instabilities. Furthermore, the influence of the magnitude of the dust-ion collision frequency on the real frequencies and damping decrements of the dust-acoustic and ion-acoustic mode was visualized in a qualitative way. For this, the rootlocus method has been used. This method provides a swift and easy means for getting a sense of proportion for the influence of the dust-ion collision frequency on the dust-acoustic and ion-acoustic modes.

Appendix A

Theorems of Sturm and Sonin-Polya

A.1 Theorems of Sturm

Sturm's separation theorem

If $y_1(x)$ and $y_2(x)$ are linearly independent solutions of the homogeneous, linear, second order differential equation

$$a_0(x)\frac{d^2y(x)}{dx^2} + a_1(x)\frac{dy(x)}{dx} + a_2(x)y(x) = 0, \tag{A.1}$$

then in each interval I wherein $a_0(x)$ does not become zero there will be a root of $y_2(x)$ between every two successive roots of $y_1(x)$ and vice versa. In other words, the roots of $y_1(x)$ and $y_2(x)$ will alternate.

Suppose that a and b are two successive roots of $y_1(x)$, so $y_1(a) = 0 = y_1(b)$.

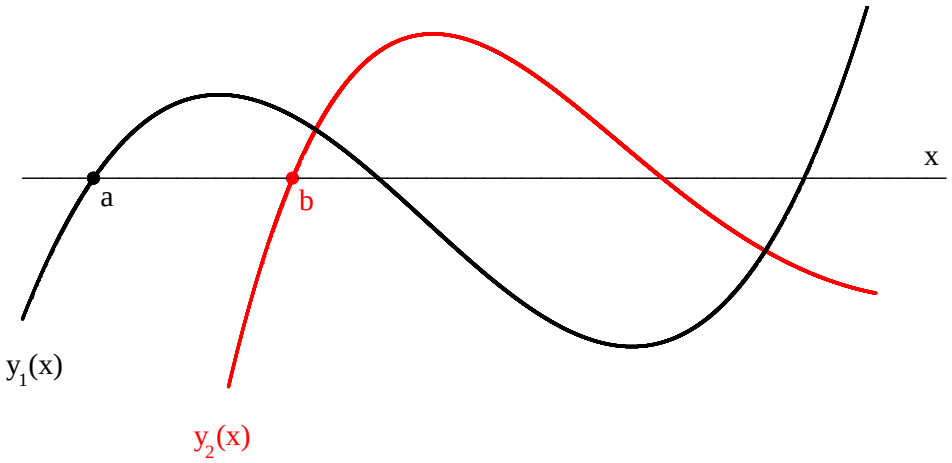

Fig A.1: Sturm's separation theorem

Since $y_1(x)$ and $y_2(x)$ are linearly independent in I, their Wronskian $W(x)$ differs everywhere from zero in I and thus has a fixed sign in I. We obtain the following expressions for the Wronskian

$$W(x) = y_1(x)\frac{dy_2(x)}{dx} - y_2(x)\frac{dy_1(x)}{dx}, \tag{A.2}$$

$$W(a) = -y_2(a)\left.\frac{dy_1(x)}{dx}\right|_{x=a}, \tag{A.3}$$

$$W(b) = -y_2(b)\left.\frac{dy_1(x)}{dx}\right|_{x=b}, \tag{A.4}$$

and since a and b are successive roots

$$\text{sign}\left[\left.\frac{dy_1(x)}{dx}\right|_{x=a}\right] = -\text{sign}\left[\left.\frac{dy_1(x)}{dx}\right|_{x=b}\right]. \tag{A.5}$$

Since $W(a)$ and $W(b)$ have the same sign ($W(x)$ is nonzero and continuous in I), $y_2(a)$ and $y_2(b)$ must have opposite signs, hence $y_2(x)$ must have at least one root in $[a, b]$. By exchanging the roles of $y_1(x)$ and $y_2(x)$, it can be proven that between two successive roots of $y_2(x)$, there is at least one root of $y_1(x)$.

Sturm's comparison theorem

Suppose $y_1(x)$ is a non-trivial solution of

$$\frac{d^2y_1(x)}{dx^2} + p_1(x)y_1(x) = 0 \tag{A.6}$$

and $y_2(x)$ a non-trivial solution of

$$\frac{d^2y_2(x)}{dx^2} + p_2(x)y_2(x) = 0 \tag{A.7}$$

in an interval I and suppose that $p_1(x) > p_2(x)$, $\forall x \in I$. Then there is at least one root of $y_1(x)$ between every two roots of $y_2(x)$ in I.

Suppose $x = a$ and $x = b$ are successive roots of $y_2(x)$ and that $y_1(x)$ has no roots in $[a, b]$. We assume that in $[a, b]$

$$\begin{aligned} &y_1(x) > 0, \\ &y_2(x) > 0. \end{aligned} \tag{A.8}$$

If this is not satisfied for $y_1(x)$ or $y_2(x)$ we change the sign of the concerned solution (this does not affect the location of the roots and is allowed for linear differential equations).

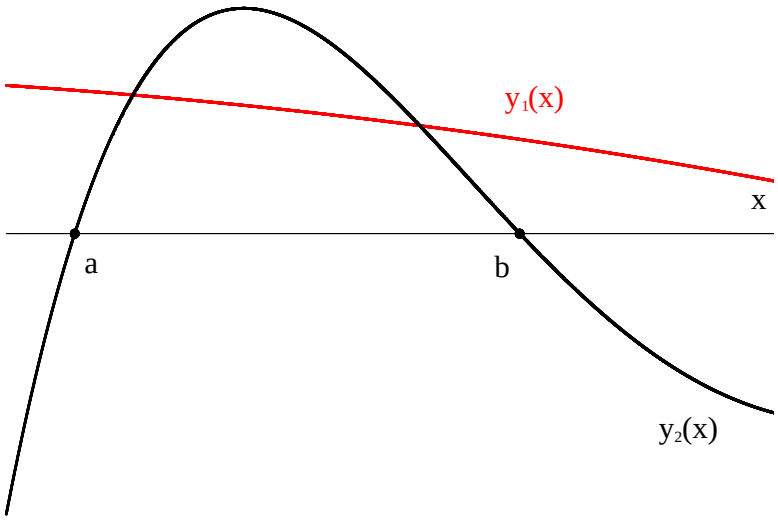

Fig A.2: Sturm's comparison theorem

Now

$$\begin{aligned} W(a) &= y_1(a)\left.\frac{dy_2(x)}{dx}\right|_{x=a}, \\ W(b) &= y_1(b)\left.\frac{dy_2(x)}{dx}\right|_{x=b}, \end{aligned} \tag{A.9}$$

and because

$$\left.\frac{dy_2(x)}{dx}\right|_{x=a} > 0 \text{ and } \left.\frac{dy_2(x)}{dx}\right|_{x=b} < 0 \tag{A.10}$$

we conclude

$$W(a) > 0 \text{ and } W(b) < 0, \tag{A.11}$$

Finally, we have in $[a, b]$

$$\begin{aligned} \frac{dW(x)}{dx} &= y_1(x)\frac{d^2y_2(x)}{dx^2} - y_2(x)\frac{d^2y_1(x)}{dx^2} \\ &= y_1(x)y_2(x)[p_1(x) - p_2(x)] > 0, \end{aligned} \tag{A.12}$$

meaning that $W(x)$ is an increasing function and contradicting (A.11). Consequently $y_1(x)$ must have at least one root in $[a, b]$.
This implies that every solution of

$$\frac{d^2y(x)}{dx^2} + p(x)y(x) = 0, \tag{A.13}$$

has maximum one root in every interval wherein $p(x) < 0$. Indeed, suppose the solution has two roots, namely a and b, then every solution of

$$\frac{d^2y(x)}{dx^2} = 0, \tag{A.14}$$

would have at least one root between a and b. Well then, $y = \text{cst} \neq 0$ does not have any root.

A.2 Theorem of Sonin-Polya

Suppose a second order differential equation is written in its self-adjoint form

$$\frac{d}{dx}\left[p(x)\frac{dy}{dx}\right] + q(x)y = 0. \tag{A.15}$$

If $p(x) > 0$ and $q(x) \neq 0$, with $p(x)$, $q(x)$ continuously differentiable in an interval I and $p(x) \cdot q(x)$ is non-increasing (non-decreasing) in I, then the absolute values of the relative extrema of every non-trivial solution of (A.15) form a non-decreasing (non-increasing) row if x increases.

Indeed, suppose $y(x)$ is a non-trivial solution of equation (A.15) and we define a function

$$F(x) = [y(x)]^2 + \frac{1}{p(x)q(x)}\left[p(x)\frac{dy(x)}{dx}\right]^2, \tag{A.16}$$

then differentiation of $F(x)$ leads to

$$F'(x) = 2yy' + \frac{2py'}{pq}(py')' - \frac{(pq)'}{(pq)^2}(py')^2, \tag{A.17}$$

when introducing the abbreviation $d\alpha(x)/dx = \alpha'$ for a function α. Since $(py')' = -qy$ we finally obtain

$$F'(x) = -\left(\frac{y'}{q}\right)^2 (pq)'. \tag{A.18}$$

Now suppose $p \cdot q$ is non-increasing, then $(pq)' \leqslant 0$ and consequently $F'(x) \geqslant 0$. We can conclude that $F(x)$ is a non-decreasing function. If we denote the points where $y(x)$ is extremal as x_i with $x_1 \leqslant x_2 \leqslant \ldots \leqslant x_n$, then $y'(x_i) = 0$ and substitution in (A.16) yields

$$[y(x_1)]^2 \leqslant [y(x_2)]^2 \leqslant \ldots \leqslant [y(x_n)]^2 \tag{A.19}$$

or

$$|y(x_1)| \leqslant |y(x_2)| \leqslant \ldots \leqslant |y(x_n)|\,. \tag{A.20}$$

The proof for non-decreasing pq is completely analogous.

For example, the theorem of Sonin-Polya can be applied to the well-known Bessel equation

$$x^2y'' + xy' + (x^2 - p^2)y = 0. \tag{A.21}$$

Rewriting the Bessel equation in its self-adjoint form gives

$$\frac{d}{dx}\left[x\frac{dy}{dx}\right] + \frac{x^2 - p^2}{x}y = 0. \tag{A.22}$$

For $x > 0$ we have $p(x) > 0$ and $p(x)q(x) = x^2 - p^2$ is increasing, consequently the absolute values of the extremal values indeed form a non-increasing row.

A.3 Rewriting differential equations

In order to rewrite second-order differential equations in a form so that the theorems of Sturm can be applied, the first derivative must be eliminated. Similarly for the application of the theorem of Sonin-Polya, the differential equation must be written in its self-adjoint form. The following sections show how this can be done.

A.3.1 Eliminating the $(n-1)$-th derivative

By changing the dependent variable, a differential equation of n-th order

$$a_n(x)\frac{d^n y(x)}{dx^n} + a_{n-1}(x)\frac{d^{n-1}y(x)}{dx^{n-1}} + \ldots + a_1(x)\frac{dy(x)}{dx} + a_0(x)y(x) = 0 \tag{A.23}$$

can be converted into a differential equation of order n, but wherein the $(n-1)$-th derivative is absent. This can be done by making a substitution

$$y(x) = u(x)F(x) \tag{A.24}$$

with

$$F(x) = \exp\left[-\frac{1}{n}\int \frac{a_{n-1}(x)}{a_n(x)}dx\right] \tag{A.25}$$

A.3.2 Self-adjoint form

Any second order differential equation can easily be written in its self adjoint form. First, the differential equation is divided by the coefficient of the highest derivative, so that we then have

$$\frac{d^2y(x)}{dx^2} + a_1(x)\frac{dy(x)}{dx} + a_0(x)y(x) = 0. \tag{A.26}$$

This can also be rewritten as

$$\frac{d}{dx}\left[p(x)\frac{dy}{dx}\right] + a_0(x)p(x)y = 0, \tag{A.27}$$

if $p(x)$ is the following positive function,

$$p(x) = \exp\left[\int a_1(x)dx\right]. \tag{A.28}$$

Bibliography

M. Abramowitz and I.A. Stegun, *Handbook of Mathematical Functions*, Dover, New York, 1972.

A.I. Akhiezer, I.A. Akhiezer, R.V. Polovin, A.G. Sitenko and K.N. Stepanov, *Plasma Electrodynamics. Volume 1: Linear Theory*, Pergamon Press, 1975.

H. Alfvén, On the existence of electromagnetic-hydrodynamic waves, *Arkiv. Mat. Astron. Fysik*, **29B(2)**, 1942.

H. Alfvén, *Cosmic Electrodynamics*, Oxford University Press, New York, 1950.

J.E. Allen, Probe theory – the orbital motion approach, *Phys. Scripta*, **45**, 497–503, 1992.

K. Avinash and P.K. Shukla, A purely growing instability in a gravitating dusty plasma, *Phys. Lett. A*, **189**, 470–472, 1994.

A. Barkan, R.L. Merlino and N. D'Angelo, Laboratory observation of the dust-acoustic wave mode, *Phys. Plasmas*, **2**, 3563–3565, 1995.

J. Binney and S. Tremaine, *Galactic Dynamics*, Princeton University Press, Princeton, New Jersey, 1987.

P. Bliokh, V. Sinitsin and V. Yaroshenko, *Dusty and Self-gravitational Plasmas in Space*, Kluwer Academic Publishers, 1995.

P. Bliokh and V. Yaroshenko, Damping of low-frequency electrostatic waves in dusty plasmas, *Plasma Phys. Rep.*, **22**, 411–416, 1996.

N.N. Bogoliubov, *Problems of a Dynamical Theory in Statistical Physics*, State Technical Press, Moscow, 1946.

M. Born and H.S. Green, *A General Kinetic Theory of Liquids*, Cambridge University Press, Cambridge, England, 1949.

A.P. Boss, Protostellar formation in rotating interstellar clouds. VI. nonuniform initial conditions, *Astrophys. J.*, **319**, 149–161, 1987.

A. Bouchoule, *Dusty plasmas. Physics, chemistry and technological impacts in plasma processing*, Wiley, Chichester, 1999.

A. Brattli, O. Havnes and F. Melandsø, The effect of a dust-size distribution on dust-acoustic waves, *J. Plasma Phys.*, **58**, 691–704, 1997.

O. Buneman, Instability, turbulence, and conductivity in current-carrying plasmas, *Phys. Res. Lett.*, **1**, 8–9, 1958.

O. Buneman, Dissipation of currents in ionized media, *Phys. Rev.*, **115**, 503–517, 1959.

V.M. Čadež, Applicability problem of Jeans criterion to a stationary self-gravitating cloud, *Astron. Astrophys.*, **235**, 242–244, 1990.

S. Chandrasekhar, The gravitational instability of an infinite homogeneous medium when Coriolis force is acting and a magnetic field is present, *Astrophys. J.*, **119**, 7–9, 1954.

S. Chandrasekhar, *Hydrodynamic and Hydromagnetic Stability*, Clarendon, Oxford, 1961.

V.W. Chow, D.A. Mendis and M. Rosenberg, Role of grain size and particle velocity distribution in secondary electron emission in space plasmas, *J. Geophys. Res.*, **98**, 19065–19076, 1993.

N. D'Angelo, Dusty plasma ionization instability with ion drag, *Phys. Plasmas*, **5**, 3155–3160, 1998.

U. De Angelis, The physics of dusty plasmas, *Phys. Scripta*, **45**, 465–474, 1992.

A. Evans, *The Dusty Universe*, Wiley, Chichester, 1994.

V.N. Faddeeva and N.M. Terentjev, *Tablitsy Znacheniy Integrala Veroyatnosty ot Kompleksnogo Argumenta (Tables of Integral Values of Probability of a Complex Argument)*, GITTL, Moscow (in Russian), 1954.

B. Farokhi, P.K. Shukla, N.L. Tsintsadze and D.D. Tskhakaya, Linear and nonlinear dust lattice waves in plasma crystals, *Phys. Lett. A*, **264**, 318–323, 1999.

A.M. Fridman and V.L. Polyachenko, *Physics of Gravitating Systems I*, Springer-Verlag, 1984.

B.D. Fried and S.D. Conte, *The Plasma Dispersion Function*, Academic Press, San Diego, 1961.

C.S. Gehman, C. Adams and R. Watkins, Linear gravitational instability of filamentary and sheetlike molecular clouds with magnetic fields, *Astrophys. J.*, **472**, 673–683, 1996.

C.K. Goertz, Dusty plasmas in the solar system, *Rev. Geophys.*, **27**, 271–292, 1989.

C.K. Goertz and W.H. Ip, Limitations of electrostatic charging of dust particles in a plasma, *Geophys. Res. Lett.*, **11**, 349–352, 1984.

D.A. Gurnett, E. Grun, D. Gallagher, W.S. Kurth and F.L. Scarf, Micron-sized particles detected near Saturn by Voyager plasma instrument, *Icarus*, **53**, 236–254, 1983.

O. Havnes, On the motion and destruction of grains in interstellar clouds, *Astron. Astrophys.*, **90**, 106–112, 1980.

O. Havnes, Charges on dust particles, *Adv. Space Res.*, **4**, (9)75–(9)83, 1984.

O. Havnes, A streaming instability interaction between the solar wind and cometary dust, *Astron. Astrophys.*, **193**, 309–312, 1988.

O. Havnes, T.K. Aanesen and F. Melandsø, On dust charges and plasma potentials in a dusty plasma with dust size distribution, *J. Geophys. Res.*, **95**, 6581–6585, 1990.

O. Havnes, T.K. Aslaksen, F. Melandsø and T. Nitter, Collisionless braking of dust particles in the electrostatic field of planetary dust rings, *Phys. Scripta*, **45**, 491–496, 1992.

O. Havnes, C.K. Goertz, G.E. Morfill, E. Grün and W. Ip, Dust charges, cloud potential, and instabilities in a dust cloud embedded in a plasma, *J. Geophys. Res.*, **92**, 2281–2287, 1987.

O. Havnes, G.E. Morfill and C.K. Goertz, Plasma potential and grain charges in a dust cloud embedded in a plasma, *J. Geophys. Res.*, **89**, 999–1003, 1984.

M. Horányi, Charged dust dynamics in the solar system, *Annu. Rev. Astron. Astrophys.*, **34**, 383–418, 1996.

H.L.F. Houpis and E.C. Whipple Jr., Electrostatic charge on a dust size distribution in a plasma, *J. Geophys. Res.*, **92**, 12057–12068, 1987.

O. Ishihara, Instability due to the dust-particulate–phonon interaction, *Phys. Rev. E*, **58**, 3733–3738, 1998.

S. Ishimaru, *Basic Principles of Plasma Physics*, Benjamin, Reading, Massachusetts, 1973.

A.V. Ivlev, D. Samsonov, J. Goree and G. Morfill, Acoustic modes in a collisional dusty plasma, *Phys. Plasmas*, **6**, 741–750, 1999.

G. Jacobs, F. Verheest, M.A. Hellberg and S.R. Pillay, Magnetosonic modes with dusty mass distributions, *Phys. Plasmas*, **7**, 4390–4395, 2000.

G. Jacobs, V. V. Yaroshenko and F. Verheest, Low-frequency electrostatic waves in self-gravitating dusty plasmas with dust-ion collisions, *Phys. Rev. E*, **66**, 026407, 2002.

J.H. Jeans, *Astronomy and Cosmogony*, Cambridge University Press, 1929.

J.G. Kirkwood, Statistical mechanical theory of transport processes I. General theory, *J. Chem. Phys.*, **14**, 180–201, 1946.

J.G. Kirkwood, The statistical mechanical theory of transport processes II. Transport in gases, *J. Chem. Phys.*, **15**, 72–76, 1947.

N.A. Krall and A.W. Trivelpiece, *Principles of Plasma Physics*, McGraw-Hill, New York, 1973.

L.D. Landau, On the vibrations of the electronic plasma, *J. Phys. (U.S.S.R.)*, **10**, 25–34, 1946.

I. Langmuir, *Proc. Nat. Acad. Sci.*, **14**, 627, 1926.

A.A. Mamun, M. Salahuddin and M. Salimullah, Ultra-low-frequency electrostatic waves in a self-gravitating magnetized and inhomogeneous dusty plasma, *Planet. Space Sci.*, **47**, 79–83, 1999.

J.S. Mathis, W. Rumpl and K.H. Nordsieck, The size distribution of interstellar grains, *Astrophys. J.*, **217**, 425–433, 1977.

J.A.M. McDonnell, W.M. Alexander, W.M. Burton, E. Bussoletti, G.C. Evans, S.T. Evans, J.G. Firth, R.J.L. Grard, S.F. Green, E. Grün, M.S. Hanner, D.W. Hughes, E. Igenbergs, J. Kissel, H. Kuczera, B.A. Lindblad, Y. Langevin, J.-C. Madeville, S. Nappo, G.S.A. Pankiewicz, C.H. Perry, G.H. Schwehm, Z. Sekanina, T.J. Stevenson, R.F. Turner, U. Weishaupt, M.K. Wallis and J.C. Zarnecki, The dust distribution within the inner coma of comet P/Halley 1982i: Encounter by Giotto's impact detector, *Astron. Astrophys.*, **187**, 719–741, 1987.

J.A.M. McDonnell, R. Beard, S.F. Green and G.H. Schwehn, Cometary and coma particulate modelling for the Rosetta mission aphelion rendezvous, *Ann. Geophys.*, **10**, 150–156, 1992.

F. Melandsø, Lattice waves in dust plasma crystals, *Phys. Plasmas*, **3**, 3890–3901, 1996.

F. Melandsø, T. Aslaksen and O. Havnes, A kinetic model for dust acoustic waves applied to planetary rings, *J. Geophys. Res.*, **98**, 13315–13323, 1993a.

F. Melandsø, T. Aslaksen and O. Havnes, A new damping effect for the dust-acoustic wave, *Planet. Space Sci.*, **41**, 321–325, 1993b.

D.A. Mendis and M. Rosenberg, Cosmic dusty plasma, *Annu. Rev. Astron. Astrophys.*, **32**, 419–463, 1994.

P. Meuris, *Wave Phenomena in Dusty Space Plasmas*, PhD thesis, Universiteit Gent, Belgium, 1998.

P. Meuris, F. Verheest and G.S. Lakhina, Influence of dust mass distributions on generalized Jeans-Buneman instabilities in dusty plasmas, *Planet. Space Sci.*, **45**, 449–454, 1997.

N. Meyer-Vernet, A. Lecacheux and B.M. Pedersen, Constraints on Saturn's E ring from the Voyager 1 radio astronomy instrument, *Icarus*, **123**, 113–128, 1996.

T. Nakano, Gravitational instability of magnetized gaseous disks, *Publ. Astron. Soc. Japan*, **40**, 593–604, 1988.

E.J. Öpik, Interplanetary dust and terrestrial accretion of meteoritic matter, *Irish Astron.*, **4**, 84–135, 1956.

K.N. Ostrikov, S.V. Vladimirov, M.Y. Yu and G.E. Morfill, Dust-acoustic wave instabilities in collisional plasmas, *Phys. Rev. E*, **61**, 4315–4321, 2000.

J.B. Pieper and J. Goree, Dispersion of plasma dust acoustic waves in the strong-coupling regime, *Phys. Res. Lett.*, **77**, 3137–3140, 1996.

S.R. Pillay, R. Bharuthram and F. Verheest, The Jeans-Buneman instability in the presence of an ion beam in a dusty plasma and the influence of dust-size distributions, *Phys. Scripta*, **61**, 112–118, 2000.

N. N. Rao and F. Verheest, Electrostatic dust modes in self-gravitating dense dusty plasmas with high fugacity, *Phys. Lett. A*, **268**, 390–394, 2000.

N.N. Rao, Magnetoacoustic modes in a magnetized dusty plasma, *Phys. Plasmas*, **53**, 317–334, 1995.

N.N. Rao, Dust-Coulomb waves in dense dusty plasmas, *Phys. Plasmas*, **6**, 4414, 1999.

N.N. Rao, Dust-Coulomb and dust-acoustic wave propagation in dense dusty plasmas with high fugacity, *Phys. Plasmas*, **7**, 795, 2000.

N.N. Rao, P.K. Shukla and M.Y. Yu, Dust-acoustic waves in dusty plasmas, *Planet. Space Sci.*, **38**, 543–546, 1990.

M. Rosenberg, Ion- and dust-acoustic instabilities in dusty plasmas, *Planet. Space Sci.*, **41**, 229–233, 1993.

M.R. Showalter and J.N. Cuzzi, Seeing ghosts: Photometry of Saturn's G-ring, *Icarus*, **103**, 124–143, 1993.

M.R. Showalter, J.B. Pollack, M.E. Ockert, L.R. Doyle and J.B. Dalton, A photometric study of Saturn's F-ring, *Icarus*, **100**, 394–411, 1992.

P.K. Shukla, Low-frequency modes in dusty plasmas, *Phys. Scripta*, **45**, 504–507, 1992.

P.K. Shukla, A survey of dusty plasma physics, *Phys. Plasmas*, **8**, 1791–1803, 2001.

P.K. Shukla, M.R. Amin and G.E. Morfill, Instability of dust-acoustic waves in partially ionized collisional dusty gases, *Phys. Scripta*, **59**, 389–390, 1999.

P.K. Shukla and A.A. Mamun, *Introduction to Dusty Plasma Physics*, Institute of Physics, Bristol, 2002.

P.K. Shukla and V.P. Silin, Dust ion-acoustic wave, *Phys. Scripta*, **45**, 508–508, 1992.

P.K. Shukla and F. Verheest, Jeans instability in collisional dusty plasmas, *Astrophys. Space Sci.*, **262**, 157–162, 1999.

L. Spitzer, *Physical Processes in the Interstellar Medium*, John Wiley & Sons, 1978.

T.H. Stix, *The Theory of Plasma Waves*, McGraw-Hill, New York, 1962.

T.H. Stix, *Waves in Plasmas*, American Institute of Physics, New York, 1992.

V.N. Tsytovich and U. De Angelis, Kinetic theory of dusty plasmas: I. General approach, *Phys. Plasmas*, **6**, 1093–1106, 1999.

V.N. Tsytovich and U. De Angelis, Kinetic theory of dusty plasmas II. Dust-plasma particle collision integrals, *Phys. Plasmas*, **7**, 554–563, 2000.

V.N. Tsytovich and U. De Angelis, Kinetic theory of dusty plasmas III. Dust-dust collision integrals, *Phys. Plasmas*, **8**, 1141–1153, 2001.

V.N. Tsytovich and U. De Angelis, Kinetic theory of dusty plasmas IV. Distribution and fluctuations of dust charges, *Phys. Plasmas*, **9**, 2497–2506, 2002.

R.K. Varma, Fluid equations for a dusty plasma with dust charge and mass distribution interacting with neutral dust through dust grain charging and secondary emission, *Phys. Plasmas*, **7**, 3885–3894, 2000.

F. Verheest, Waves and instabilities in dusty space plasmas, *Space Sci. Rev.*, **77**, 267–302, 1996.

F. Verheest, *Waves in Dusty Space Plasmas*, Kluwer Academic Publishers, 2000.

F. Verheest, V.M. Čadež and G. Jacobs, Janus faces of Jeans instabilities, *AIP Conference Proceedings*, **537**, 91–98, 2000a.

F. Verheest, M.A. Hellberg and R.L. Mace, Self-gravitational magnetosonic modes in dusty plasmas with quasi-inertialess constituents, *Phys. Plasmas*, **6**, 279–284, 1999.

F. Verheest, G. Jacobs and M.A. Hellberg, Transition from Langmuir-Jeans to Alfvén-Jeans modes in dusty plasmas, *Phys. Scripta*, **T84**, 171–174, 2000b.

F. Verheest, G. Jacobs and V. Yaroshenko, Gravitational collapse in dusty plasmas with dust mass distributions and neutral gas, *Phys. Plasmas*, **7**, 3004–3008, 2000c.

F. Verheest and P. Meuris, Whistler-like instabilities due to charge fluctuations in dusty plasmas, *Phys. Lett. A*, **198**, 228–232, 1995.

F. Verheest, P. Meuris, R.L. Mace and M.A. Hellberg, Alfvén-Jeans and magnetosonic modes in multispecies self-gravitating dusty plasmas, *Astrophys. Space Sci.*, **254**, 253–267, 1997.

F. Verheest, Victoria V. Yaroshenko and Manfred A. Hellberg, Electrostatic modes in (self-gravitating) dusty plasmas with charge and mass distributions, *Phys. Plasmas*, **9**, 2479–2485, 2002.

F. Verheest, V.V. Yaroshenko, G. Jacobs and P. Meuris, Charge and mass fluctuations in dusty plasmas revisited, *Phys. Scripta*, **64**, 494–500, 2001.

A. A. Vlasov, On the kinetic theory of an assembly of particles with collective interactions, *J. Phys. (U.S.S.R.)*, **9**, 25–40, 1945.

J. Vranješ and V.M. Čadež, Gravitational instability of a homogeneous gas cloud with radiation, *Astrophys. Space Sci.*, **235**, 242–244, 1990.

J.C. Weingartner and B.T. Draine, Dust grain size distributions and extinction in the Milky Way, Large Magellanic Cloud and Small Magellanic Cloud, *Astrophys. J.*, **548**, 296–309, 2001.

E.C. Whipple, T.G. Northrop and D.A. Mendis, The electrostatics of a dusty plasma, *J. Geophys. Res.*, **90**, 7405–7413, 1985.

E.C. Whipple Jr., Potentials of surfaces in space, *Rep. Prog. Phys.*, **44**, 1197–1250, 1981.

D.C.B. Whittet, *Dust in the Galactic Environment*, Institute of Physics Publishing, 1992.

J. Willems, *Stability Theory of Dynamical Systems*, Nelson and Sons, London, 1970.

D. Winske and M. Rosenberg, Nonlinear development of the dust acoustic instability in a collisional dusty plasma, *IEEE Trans. Plasma Sci.*, **26**, 92–99, 1998.

W.J. Xu, N. D'Angelo and R.L. Merlino, Dusty plasmas: The effect of closely packed grains, *J. Geophys. Res.*, **98**, 7843–7847, 1993.

V.V. Yaroshenko, G. Jacobs and F. Verheest, Dust-acoustic modes in self-gravitating plasmas with dust size distributions, *Phys. Rev. E*, **64**, 036401, 2001a.

V.V. Yaroshenko, G. Jacobs and F. Verheest, Kinetic approach to low-frequency waves in dusty self-gravitating plasmas, *Phys. Rev. E*, **63**, 066406, 2001b.

J. Yvon, *La Théorie des Fluides et l'Equation d'Etat*, Hermann et Cie, Paris, 1935.